

Fall 2005

Microcapsule biosensors based on competitive binding and fluorescence resonance energy transfer assays

Swetha Chinnayelka
Louisiana Tech University

Follow this and additional works at: <https://digitalcommons.latech.edu/dissertations>

 Part of the [Analytical Chemistry Commons](#), and the [Biochemistry Commons](#)

Recommended Citation

Chinnayelka, Swetha, "" (2005). *Dissertation*. 584.
<https://digitalcommons.latech.edu/dissertations/584>

This Dissertation is brought to you for free and open access by the Graduate School at Louisiana Tech Digital Commons. It has been accepted for inclusion in Doctoral Dissertations by an authorized administrator of Louisiana Tech Digital Commons. For more information, please contact digitalcommons@latech.edu.

NOTE TO USERS

This reproduction is the best copy available.

UMI[®]

MICROCAPSULE BIOSENSORS BASED ON COMPETITIVE
BINDING AND FLUORESCENCE RESONANCE ENERGY
TRANSFER ASSAYS

by

Swetha Chinnayelka, MS

A Dissertation Presented in Partial Fulfillment
of the Requirements for the Degree
Doctor of Philosophy

COLLEGE OF ENGINEERING AND SCIENCE
LOUISIANA TECH UNIVERSITY

November 2005

UMI Number: 3192318

INFORMATION TO USERS

The quality of this reproduction is dependent upon the quality of the copy submitted. Broken or indistinct print, colored or poor quality illustrations and photographs, print bleed-through, substandard margins, and improper alignment can adversely affect reproduction.

In the unlikely event that the author did not send a complete manuscript and there are missing pages, these will be noted. Also, if unauthorized copyright material had to be removed, a note will indicate the deletion.

UMI[®]

UMI Microform 3192318

Copyright 2006 by ProQuest Information and Learning Company.

All rights reserved. This microform edition is protected against unauthorized copying under Title 17, United States Code.

ProQuest Information and Learning Company
300 North Zeeb Road
P.O. Box 1346
Ann Arbor, MI 48106-1346

LOUISIANA TECH UNIVERSITY
THE GRADUATE SCHOOL

10/27/2005
Date

We hereby recommend that the dissertation prepared under our supervision by **Swetha Chinnavelka** entitled "**Microcapsule Biosensors Based on Competitive Binding and Fluorescence Resonance Energy Transfer Assays**" be accepted in partial fulfillment of the requirements for the Degree of Doctor of Philosophy.



Supervisor of Dissertation Research

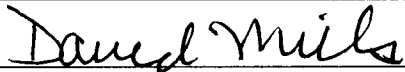
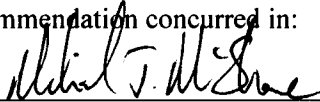


Head of Department

Ph.D. in Engineering

Department

Recommendation concurred in:



Advisory Committee

Approved:

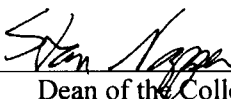


Director of Graduate Studies

Approved:



Dean of the Graduate School



Dean of the College

ABSTRACT

Fluorescent sensing systems offer the potential for minimally invasive monitoring with implantable devices, but they require carrier technologies that provide suitable immobilization, accessibility, and biocompatibility while maintaining adequate response characteristics. Towards the development of this goal, a general design of a biosensor with the capability of detecting different metabolites was investigated. The approach is based on the encapsulation of a competitive binding assay in microcapsules and monitoring the changes in fluorescence resonance energy transfer (FRET) in the presence of analyte. To experimentally demonstrate this type of sensing system, glucose was chosen as the model target analyte. The design, fabrication, and characterization of several embodiments of a non-consuming fluorescence affinity glucose sensor are described in this dissertation. The novel feature of this system used through out the work is the employment of microcapsules for entrapping the sensing assay, which allows for the free movement of sensing elements while maintaining their constant concentrations with continuously-varying analyte concentration.

Initially, a FRET based glucose sensor was demonstrated by encapsulating multi-layers of Concanavalin A (Con A)/dextran in microcapsules. Even though microcapsules comprised of Con A/dextran complexes showed reasonable glucose sensitivity, there are some significant obstacles to practical use of this system due to toxicity, aggregation, and irreversible binding. Therefore, to overcome the limitations of Con A, an improved FRET

assay was developed by replacing Con A with apo-glucose oxidase (apo-GOx). Apo-GOx is highly specific toward β -D-glucose, reduces the concern over aggregation as it can only bind to one glucose molecule (whereas, Con A binds to four glucose molecules), and also could be more biocompatible than Con A by recombinant production.

The first attempt at the apo-GOx/dextran assay encapsulated in microcapsules used a blue-light-excited FRET pair (FITC/TRITC). The assay elements were encapsulated in microcapsules using photosensitive polymers (poly(styrene sulfonate) and diazoresin) in the shell structure. The results of glucose sensitivity experiments showed a controllable and reversible sensor response with sensitivity in the range of 2 – 6 % /mM over the range of 0 – 40 mM glucose. In spite of the advantages of this system, it is not ideal for *in vivo* studies, as the short-wavelength dyes will be difficult to interrogate transdermally due to high tissue scattering. Additionally, diazoresin contains formaldehyde groups that could prove to be toxic.

To reduce the interference of tissue scattering, the sensor operating region was extended into the longer and near infrared (NIR) wavelength regions by choosing appropriate donor (Alexa FluorTM 647)-acceptor (QSY21) pair and reference dye (Alexa FluorTM 750). The competitive binding assay operating in red/near infrared region was loaded into organo/inorgano microcapsules using glycidyl-silane as the crosslinking element. These microcapsules exhibited glucose sensitivity of ~2-5%/mM over the range of 0-30mM, which is comparable to the assay operating in the visible region. Thus, this assay is superior to the apo-GOx/dextran based assays operating in visible region, because it has the advantages of excellent sensitivity, and a significant increase in the detected signal levels due to the use of NIR dyes (during *in vivo* measurements), and the

use of silane simplifies the encapsulation procedure and also makes this system more biocompatible. Based on the sensitivity, specificity, and reversible response in the region of interest (0-30mM), this sensing system can potentially be used for glucose monitoring in diabetic patients.

These findings demonstrate the feasibility of designing different biosensors using apo-enzymes as specific molecular recognition elements in competitive binding assays. The concept of the encapsulation of a competitive binding assay in microcapsules is advantageous, as it allows for the stable entrapment of the sensing assay elements and free movement of the analyte molecules. Thus, the concept of sensing that is demonstrated in this dissertation can potentially be used to develop a wide variety of biosensors by choosing corresponding apo-enzyme and ligand molecules.

APPROVAL FOR SCHOLARLY DISSEMINATION

The author grants to the Prescott Memorial Library of Louisiana Tech University the right to reproduce, by appropriate methods, upon request, any or all portions of this Dissertation. It is understood that "proper request" consists of the agreement, on the part of the requesting party, that said reproduction is for his personal use and that subsequent reproduction will not occur without written approval of the author of this Dissertation. Further, any portions of the Dissertation used in books, papers, and other works must be appropriately referenced to this Dissertation.

Finally, the author of this Dissertation reserves the right to publish freely, in the literature, at any time, any or all portions of this Dissertation.

Author C. Swetha

Date 11/10/2005

TABLE OF CONTENTS

ABSTRACT.....	iii
TABLE OF CONTENTS.....	vii
LIST OF TABLES.....	x
LIST OF FIGURES.....	xi
ACKNOWLEDGMENTS.....	xvi
CHAPTER 1 INTRODUCTION.....	1
1.1 Implantable Glucose Sensors – Under Research.....	3
1.2 Objectives and Novel Aspects.....	5
1.3 Organization of Chapters.....	6
CHAPTER 2 LITERATURE REVIEW.....	8
2.1 Types of Glucose Sensors.....	8
2.1.1 Enzymatic Sensors.....	11
2.2 Competitive Binding (CB) – Based Glucose Sensors.....	16
2.2.1 Viscosity Measurements – CB Assay.....	18
2.2.2 Mass/Thickness Measurements – CB Assay.....	19
2.2.3 Surface Plasmon Resonance Based Glucose Sensors.....	20
2.2.4 CB Based Fluorescence Affinity Glucose Sensors.....	23
2.2.5 CB and FRET Based Glucose Sensors.....	24
2.2.6 Transdermal Glucose Sensing.....	29
2.3 Glucose sensors Based on Apo-Enzymes.....	33
2.3.1 Apo-Glucose Oxidase.....	33
2.3.2 Apo-Glucose Dehydrogenase (apo-GD).....	35
2.3.3 Glucokinase Based Sensor.....	36
2.4 Glucose Binding Proteins.....	38
2.5 Boronic Acid Based Sensors.....	42
CHAPTER 3 THEORY.....	46
3.1 Fluorescence Resonance Energy Transfer (FRET) Phenomenon.....	46
3.1.1 FRET Theory.....	48
3.2 Competitive Binding Process.....	51
3.2.1 Competitive Binding Theory.....	52
3.3 Combination of FRET and Competitive Binding Techniques.....	61

3.3.1	Theory – Combination of FRET and CB techniques.....	62
CHAPTER 4 LECETIN/SACCHARIDE BASED GLUCOSE SENSOR.....		64
4.1	Sensor Design.....	65
4.2	Experimental Section.....	66
4.3	Methods.....	67
4.3.1	Assembly on QCM Resonator.....	67
4.3.2	Assembly on Microspheres.....	68
4.3.3	Glucose Effect on Con A/Dextran Coated MF Particles.....	69
4.3.4	Encapsulation and Hollow Capsule Formation.....	70
4.3.5	Glucose Effect on Capsules Containing Con A/Dextran Multilayers.....	71
4.4	Results and Discussion.....	72
4.4.1	QCM Results.....	72
4.4.2	Microparticle Coating Results.....	74
4.4.3	Polymer-Coated Microcapsules.....	78
4.5	Conclusion.....	82
CHAPTER 5 FLOURESCENT GLUCOSE SENSORS OPERATING IN VISIBLE REGION.....		84
5.1	Sensor Design.....	85
5.2	Experimental Section.....	86
5.3	Methods.....	87
5.3.1	Preparation of Apo-GOx.....	87
5.3.2	Assessment of FAD Cofactor Removal.....	87
5.3.3	Solution Phase Experiments.....	88
5.3.4	Fabrication of Diazo-resin-Based Hollow Microcapsules.....	89
5.3.5	Encapsulation of Sensing Chemistry in DAR-Based Microcapsules.....	90
5.3.6	Estimation of the Encapsulation Efficiency.....	91
5.3.7	Stability of Encapsulation.....	92
5.3.8	Sensor Response in Microcapsules.....	93
5.3.9	Reversibility.....	93
5.4	Results and Discussion.....	94
5.4.1	Assessment of FAD Co-factor Removal.....	94
5.4.2	Energy Transfer Experiments.....	95
5.4.3	Effect of Concentration on Sensor Response.....	99
5.4.4	Specificity.....	102
5.4.5	Encapsulation of FD/TAG Complexes in Microcapsules.....	103
5.4.6	Leaching of Encapsulated Molecules from Microcapsules.....	107
5.4.7	Sensor Response to Glucose Addition in Microcapsules.....	109
5.4.8	Effect of Capsule Concentration on Sensor Response.....	111
5.4.9	Reversibility of the Glucose Sensors.....	114
5.5	Conclusion.....	116
CHAPTER 6 FLOURESCENT GLUCOSE SENSORS OPERATING IN ORANGE/RED REGION.....		118
6.1	Sensor Design.....	118

6.2	Experimental Section.....	119
6.3	Methods	120
6.3.1	Solution Phase Experiments	120
6.3.2	Formation of Hollow Microcapsules	121
6.3.3	Encapsulation of Sensing Elements	121
6.3.4	Sensor Response to Random Glucose Concentrations in Microcapsules... ..	122
6.4	Results and Discussion	123
6.4.1	Solution Phase Glucose Response Tests.....	123
6.4.2	Sensor Specificity	125
6.4.3	Encapsulation of Sensing Chemistry in Microcapsules.....	125
6.4.4	Demonstration of Reversible Sensor Response	126
6.5	Conclusion.....	129
CHAPTER 7 FLUORESCENT NEAR INFRARED GLUCOSE SENSORS		130
7.1	Sensor Design	130
7.2	Experimental Section.....	132
7.3	Methods	132
7.3.1	Solution Phase Experiments	132
7.3.2	Fabrication of Silane-Based Organo/Inorgano Microcapsules	134
7.3.3	Encapsulation of Sensing Chemistry in Organo/Inorgano Hybrid Microcapsules	136
7.3.4	Sensor Response in Microcapsules.....	137
7.4	Results and Discussion	138
7.4.1	Solution Phase Experiments	138
7.4.2	Encapsulation of AF-AG/QSY-dex Complexes in Microcapsules.....	142
7.4.3	Sensor Response to Glucose Addition in Microcapsules	143
7.4.4	Demonstration of Reversible Sensor Response	145
7.4.5	Photobleaching Effect.....	147
7.5	Conclusion.....	148
CHAPTER 8 SUMMARY AND FUTURE WORK		150
8.1	Summary.....	150
8.2	Future Work.....	154
REFERENCES		156

LIST OF TABLES

Table 3.1. Parameters used to study the effect of total assay concentration on sensor response.....	56
Table 5.1. Encapsulation efficiency parameters for FITC-dextran of two different molecular weights.	107
Table 5.2. Details of the sample used for testing sensor response in microcapsules.....	110
Table 5.3. Change in sensitivity and dissociation constant with varying capsule concentration.	113
Table 7.1. Change in sensitivity and dissociation constant with varying capsule concentration.	145
Table 8.1. Sensor response characteristics of different variations of competitive binding assays.	151

LIST OF FIGURES

Figure 1.1.	(a) Skin cross-section showing the implanted sensors between dermis and epidermis, (b) Subcutaneous implantation of microspheres loaded with sensing assay elements and interrogation of sensors by (c) exciting the fluorescent assay elements and (d) collecting the emitted light. ²⁸	4
Figure 2.1.	(a) Confocal microscopy image of spheres used for glucose sensitivity experiments; (b) Plot of experimentally and theoretically obtained fractional fluorescence peak ratio values at different glucose concentrations. ⁵¹	13
Figure 2.2.	(a) Intrinsic fluorescence of hexokinase in solution with increasing glucose concentration, in (●) PBS; (□) serum; (▲) low-molecular weight fraction of serum; (b) Change in intrinsic fluorescence of sol-gel immobilized hexokinase in (■) PBS or (●) serum. ⁶³	15
Figure 2.3.	Different types of non-consuming glucose sensors.....	16
Figure 2.4.	Illustration of Competitive binding technique: (a) donor molecules, (b) Mixture of donor and acceptor molecules, and (c) glucose competes with dextran to occupy binding sites on Con A, and displaces dextran from Con A.	17
Figure 2.5.	Binding affinity of various sugars to Concanavalin A. ⁸⁶	17
Figure 2.6.	Changes in Viscosity (η) of dextran and Con A (10 gm/L) dispersions. Dextran concentrations were, (○) 190 gm/L, (▼) 120 gm/L, (▲) 80 gm/L, (●) 40 gm/L. ⁶⁷	18
Figure 2.7.	(a) Layer-by-Layer assembly of Con A/glycogen multilayers using two modes of interactions; (b) Disintegration of the Con A-glycogen multilayer film (10 bilayers) in the presence of 10 mM (a) D-galactose, (b) D-glucose, (c) D-mannose, (d) Methyl- α -D-glucopyranoside, and (e) Methyl- α -D-mannopyranoside at pH 7.4. ⁷⁵	20
Figure 2.8.	Change in SPR angle of Con A:dextran-solutions at various glucose concentrations. ⁷⁸	22
Figure 2.9.	Competitive binding and SPR based glucose sensing mechanism: the dissociation of Con A-aggregated dextran-coated gold nanoparticles. ⁸¹	22
Figure 2.10.	Heterogeneous fluorescence affinity sensor. ⁸⁶	24
Figure 2.11.	(a) Schematic of homogeneous FRET based glucose sensor; Changes in FITC fluorescence with the addition of (b) Rh-Con A to FD, and (c) glucose to FD/Rh-Con A complexes. ⁸⁶	25
Figure 2.12.	Excited state decay of Cy5-Con A with the addition of (a) MIMG, and (b) glucose. ⁹¹	28

Figure 2.13. Changes in FRET between APC-Con A and MG dextran in the presence of (a) PBS, Serum and BSA; (b) PBS, serum passed through 10kDa and 30kDa filters, and unfiltered serum. ⁹⁶	29
Figure 2.14. Fluorescence affinity glucose sensor, (a) In the absence of glucose, AF 488 labeled Con A is bound to fixed glucose residues inside porous beads, (b) In the presence of glucose, Con A is displaced from the beads and diffuses out of them, and (c) Changes in fluorescence of AF 488-Con A with the addition of glucose. ⁹⁷	31
Figure 2.15. Fluorescence emission spectra from the fiber (comprised of QSY-Con A and AF 647 dextran) during its exposure to different glucose concentrations. ⁹⁹	32
Figure 2.16. (a) Emission spectra, and (b) Average lifetime of apo-glucose oxidase-1,8-ANS in the presence of varying glucose concentrations. ²³	34
Figure 2.17. Polarization spectra of ANS-labeled GD in the presence of 3% acetone, and at different concentrations of glucose. ¹⁰³	36
Figure 2.18. Effect of ONPG and glucose on the emission intensity of BSGK.....	37
Figure 2.19. (a) Tertiary structure of GBP ^{21,93} ; Change in fluorescence intensity due to the binding of glucose to (b) L255C-acrylodan (c) and H152C-IANBD glucose binding protein conjugates. ¹⁰⁵	39
Figure 2.20. (a) Emission spectra of ANS-Q26 GGBP in the presence of glucose, (b) Modulation at 2.1MHz with the addition of glucose to ANS-Q26 GGBP. ⁹³	39
Figure 2.21. (a) Emission spectra, and (b) Modulation at 1.58Hz with the addition of glucose to Ru-GBP-Acrylodan. ²¹	40
Figure 2.22. Design of a (a) glucose indicator protein for glucose sensing based on FRET between two green fluorescent proteins, (b) glucose sensor by incorporating Figure 2-15(a) in a hollow-fiber. ¹⁰⁷	41
Figure 2.23. Fluorescence intensity (average of 3 measurements) at 527 nm (YFP emission) with increasing glucose concentration. ¹⁰⁷	41
Figure 2.24. Change in fluorescence spectra of DSTBA and CSTBA in solution-phase (a,b) and when doped in contact lens. ^{109,107}	43
Figure 3.1. Fluorescence excitation and emission spectra of (a) donor and (b) acceptor molecules. ¹¹⁹	47
Figure 3.2. A simplified Jablonski diagram showing the coupled energy transfer transitions between the donor and acceptor molecules during the FRET process. ¹¹⁷	47
Figure 3.3. Effect of the distance between donor and acceptor molecules (r) on the energy transfer efficiency (E); where R_0 is the Förster distance.	50
Figure 3.4. Schematic representation of the combination of FRET and competitive binding techniques: (a) FITC-dextran/TRITC-Con A complexes, and (b) displacement of dextran from Con A in the presence of glucose; (c) strong donor and acceptor peaks (d) strong donor peak relative to acceptor peak in the presence of glucose.	52
Figure 3.5. Effect of dimensionless analyte concentration and the total ligand/receptor (L_t/R_t) ratio on the response of competitive binding based assay. ¹³⁴	55

Figure 3.6.	Effect of the total assay concentration on sensor response.	57
Figure 3.7.	Effect of (a) parameter a, with constant b=100 and c=1.01; (b) parameter b, with constant a=1 and c=1.01; (c) parameter c, with constant a=1 and b=100; on the calibration curves obtained from the theoretical model (Equation 3.19). Values of the variable parameters are given in the corresponding graph. ¹³⁰	60
Figure 3.8.	Effect of dimensionless analyte concentration and FRET efficiency on the relative fluorescence when the total ligand/receptor ratio is (a) 0.01, and (b) 0.1. ¹³³	63
Figure 4.1.	Fabrication process flow diagram (LbL assembly) of the biosensor (a) Microparticle as positively-charged substrate (b) Deposition of dextran (anionic) and Con A layers alternatively (c) Adsorption of the polymer multilayers (d) Dissolution of core to yield capsules (e) Titration of glucose to displace dextran from Con A.	66
Figure 4.2.	Mass deposited and released during adsorption of polyelectrolytes, FITC-dextran, and succinyl-Con A on the QCM resonator, and exposure of multilayer films to glucose.	72
Figure 4.3.	Normalized absorbance spectra of FITC-dextran, succinyl-Con A, and glucose solutions used for assembling on QCM resonator, and testing their glucose sensitivity (scaled up with factors of 12.5X, 25X, and 1000X, respectively).	74
Figure 4.4.	Mean and standard deviation values for zeta potential measurements of coated MF particles. Film architecture: {(FITC-Dextran/TRITC-Con A) ₃ /FITC-Dextran/(PAH/PSS) ₅ }	75
Figure 4.5.	(a) Normalized fluorescence spectra of particle suspension after depositing fluorescent materials FITC-dextran (FD) and TRITC-Con A (TC); (b) FITC:TRITC peak intensity ratios after adsorbing each layer on MF particles.....	76
Figure 4.6.	Fluorescence spectra of MF particle suspension coated with {(FITC-dextran/TRITC-Con A) ₃ /FITC-dextran}, along with supernatant a) prior to addition of glucose, and b) after glucose titration.	78
Figure 4.7.	Confocal microscope images of capsules with {(FITC-dextran/TRITC-Con A) ₄ /FITC-dextran/(PAH/PSS) ₄ /PAH} as shell structure, and corresponding intensity line scans of capsules, showing FITC (left) and TRITC (right) intensities	79
Figure 4.8.	Effect of glucose titration into suspension of capsules comprising {(FITC-dextran/TRITC-Con A) ₄ /FITC-dextran/(PAH/PSS) ₄ /PAH} as shell layers	80
Figure 5.1.	Schematic of a glucose assay based on competitive binding between dextran and glucose for binding sites on apo-GOx.	85
Figure 5.2.	Fabrication of microcapsules and encapsulation of FD/TAG complexes.	90
Figure 5.3.	(a) Absorbance of GOx and apo-GOx. (b) GOx, apo-GOx, and TRITC-apo-GOx activities with respect to time.	95
Figure 5.4.	Normalized fluorescence spectra with the addition of (a) TRITC-apo-GOx (TAG) to FD-500kDa; (b) β -D-glucose added to the	

	sample containing FD/TAG complexes. (c) Change in the FITC:TRITC intensity peak ratio with the addition of glucose.	96
Figure 5.5.	FITC:TRITC peak intensity ratio with the addition of glucose to FD/TAG complexes. Error bars show one standard deviation of three replicate measurements.	98
Figure 5.6.	Percentage change in FITC:TRITC peak ratio with the addition of glucose into different FD/TAG complex concentrations. Lines are regression curves used only to clearly indicate the trend for each set of measurements. Error bars show one standard deviation of three replicate measurements.	100
Figure 5.7.	Relationship of sensitivity (%/mM) and dissociation constant (k_d) to concentration of assay components (constant mole ratio).	101
Figure 5.8.	Percentage change in the normalized FITC:TRITC peak ratio values with the addition of different sugars. Error bars denote one standard deviation of three replicate measurements.	103
Figure 5.9	Confocal images of the microcapsules (a) & (b) in FD-500KDa/TAG complex loading solution; (c) & (d) after UV exposure and rinsing in DI water; (e) phase transmission image of the loaded microcapsules; (f) overlay of FITC, TRITC fluorescence and transmission mode image. Fluorescence line scan of the capsules (g) during loading process (from a and b) and (h) after encapsulation process (from c and d).	105
Figure 5.10.	Percentage of the initially encapsulated FD and TAG in the microcapsules lost to the supernatant; (500K-FD and 500K-TAG) and (2M-FD and 2M-TAG) indicate the FD and TAG moles in the supernatant corresponding to the capsules loaded with (FD-500kDa/TAG) and (FD-2MDa/TAG) complexes, respectively.	108
Figure 5.11.	Percentage change in the normalized FITC:TRITC peak ratio with the addition of glucose to the microcapsules loaded with FD-500kDa/TAG and FD-2MDa/TAG complexes. Error bars show one standard deviation of three replicate measurements.	110
Figure 5.12.	Effect of capsule concentration on the change in FITC:TRITC peak ratio with the addition of glucose solution. Error bars show one standard deviation of three replicate measurements.	112
Figure 5.13.	Percentage change in the normalized FITC:TRITC peak ratio with the addition of random glucose concentrations to the microcapsules loaded with FD-500kDa/TAG complexes. Error bars show one standard deviation of three replicate measurements.	114
Figure 6.1.	Schematic of the microcapsules loaded with dextran/apo-GOx complexes.	122
Figure 6.2.	(a) Normalized fluorescence spectra with the addition of β -D-glucose to TD/CAG complexes in PBS buffer, (b) Percentage change in TRITC: Cy5 peak ratio with the addition of β -D-glucose, β -D-glucose, and mannose solutions. Error bars show one standard deviation of three replicate measurements.	124

Figure 6.3.	Confocal fluorescence images of typical microcapsules loaded with TRITC-dextran and Cy5-apo-GOx; (a) TRITC and (b) Cy5 fluorescence; (c) Overlay of the TRITC and Cy5 fluorescence.....	126
Figure 6.4.	Percentage in TRITC: Cy5 peak ratio with the addition of random β -D-glucose concentrations to the TD/CAG loaded microcapsules. Error bars show one standard deviation of three replicate measurements.	126
Figure 7.1.	Schematic of the RET quenching system for glucose monitoring based on the competitive binding between dextran and glucose for binding sites on apo-GOx.....	131
Figure 7.2.	Chemical crosslinking of PAH and silane (step 1); Hydrolysis and condensation of silane in the presence of water (step 2).....	135
Figure 7.3.	Fabrication of organic/inorganic hybrid microcapsules (a – c); encapsulation of AF647-AG/QSY-dextran into hollow microcapsules (d – f); and (g) incorporation of reference dye (AF-750).....	136
Figure 7.4.	Quenching of AF647-AG due to increasing concentrations of QSY21-dextran.....	139
Figure 7.5.	Normalized (a) Fluorescence spectra and (b) Percentage change in AF647:/AF750 peak ratio with the addition of glucose into AF-AG/QSY-dex complexes with different dextran concentrations. Lines are regression curves used only to clearly indicate the trend for each set of measurements. Error bars show one standard deviation of three replicate measurements.	140
Figure 7.6.	(a) Surface potential values obtained after coating each layer on $MnCO_3$ particles. Error bars show one standard deviation of three replicate measurements; (b) Confocal fluorescence images of microcapsules loaded with AF647-apo-GOx, QSY21-dextran and AF750-PAH with AF647 fluorescence.	142
Figure 7.7.	Fluorescence spectra of the microcapsules loaded with sensing assay and reference dye (AF750) with the addition of glucose solution. All the spectra are normalized to the reference peak at 776nm.	144
Figure 7.8.	Effect of capsule concentration on the change in AF647:AF750 peak ratio with the addition of glucose solution. Error bars show one standard deviation of three replicate measurements.....	144
Figure 7.9.	Percentage change in AF647:AF750 peak ratio with the addition of random β -D-glucose concentrations to the AF-AG/QSY-dex loaded microcapsules. Error bars show one standard deviation of three replicate measurements.	146
Figure 7.10.	Photobleaching of the AF647-AG/QSY-dex and AF750 loaded microcapsules by continuously exciting at 640nm (a) with and without glucose, and (b) Change in the peak ratio with respect to time, with and without glucose..	148

ACKNOWLEDGMENTS

I would like to take this opportunity to thank my advisor, Dr. Michael J. McShane, who supported me during all these years. I would like to thank Drs. Huiguang Zhu, Quincy Brown, and Patrick Grant for their collaborations and helpful discussions. Also, I would like to thank entire BioMINDS lab for their day-to-day support. I would like to thank my parents, Mr. C. Krishna Reddy and Mrs. C. Vanitha Reddy, my brother, C. Nishanth Reddy for supporting me and helping me in reaching my goal. At last, but the most important I would like to thank my husband Mr. Dinesh Kommirredy, without whom this would not have been possible.

I would like to dedicate this dissertation to my family.

CHAPTER 1

INTRODUCTION

In recent years, interest towards developing biosensors for continuous monitoring with high specificity has increased, mainly because of the potential of avoiding the long-term side effects of many diseases, by taking appropriate measures when the disease is in its early stage. Several variations of biosensors were previously reported for various applications.¹⁻⁴ Some of the molecular recognition techniques used in developing biosensors are based on antigen/antibody, enzyme/substrate, and affinity (competitive binding) interactions. One of the sensing mechanisms that has been extensively explored in the past, is the competitive binding process, which is based on the variations in the binding affinities of two molecules towards the substrate. The main goal of this dissertation is to develop a generic design for biosensors, based on the combination of competitive binding and fluorescence spectroscopic techniques. This design must also be applicable to the detection of a wide variety of analytes.

In order to demonstrate the working principle of this sensing system, glucose is chosen as the model analyte molecule, because of its importance and need in the biosensor industry. Biosensors for monitoring blood glucose are of special interest, because the incidence of diabetes mellitus is increasing uncontrollably worldwide, and is

one of the leading causes of death by disease, with over 170 million diabetics worldwide.⁵⁻⁷ Diabetes is a disease affecting the body's ability to produce or use insulin and thus resulting in large fluctuations in blood glucose levels, unless proper treatment is provided in time.⁸⁻¹⁰ When left untreated or improperly managed, diabetes can increase the risk of heart disease, adult blindness, kidney disease, and erectile dysfunction.¹¹ Therefore, most diabetics are required to measure the blood glucose concentrations several times a day.⁸⁻¹² In spite of the enormous advantages in monitoring glucose level several times a day, and the availability of about 40 types of glucose meters in the market place (which are based on the finger-prick method), frequent monitoring is not widely practiced due to a number of reasons such as, painful testing procedures or ignorance of the advantages, difficulty in understanding the readings, tediousness, etc.^{10,13,14} Therefore, there is an urgent need for the development of a simple and painless monitoring system to help improve the lives and longevity of diabetic patients.

In an attempt to advance glucose sensing technology, a variety of minimally invasive continuous glucose monitoring systems (e.g. implantable needle-type amperometric electrode), have been introduced into the market.^{8,10,15,16} However, these instruments are not yet completely reliable, as they have problems associated with unpredictable drift, stability, lifetime, repeated calibration (~4 times a day), a long warm up time, etc.^{17,18} In spite of enormous efforts to develop implantable glucose monitoring systems, there are many parameters that need to be improved. In order to be frequently used by the diabetic patients, sensors should be less cumbersome, require fewer calibrations, have a biocompatible surface, offer long sensor lifetime, and understandable read-out technology.⁶ Other parameters that are necessary include repeatable sensor

fabrication, specificity, linear response in the region of interest, accuracy, and rapid response time. In order to meet all the requirements for the production of glucose sensors, different sensing approaches are being continuously explored. Among these, fluorescence spectroscopy is receiving significant attention because of its high sensitivity and suitability for fast and non- or minimally-invasive measurements.

Currently, fluorescence techniques are widely used as a read-out technology for various biosensors based on different working principles. Several variations of enzymatic activity and affinity based glucose sensors based on using fluorescence intensity and lifetime measurements have been previously reported in the literature¹⁹⁻²³ and are proposed for *in vivo* use. However, a practical design for their use under *in vivo* conditions was not reported. Thus, there remains a need to develop an implantable glucose monitoring system permitting frequent monitoring of glucose level.

1.1 Implantable Glucose Sensors **– Under Research**

In order to develop a subcutaneously implantable glucose sensor, the sensing assay chemistry must be encapsulated into a microcontainer, which can allow the analyte molecules to diffuse in, while holding the assay elements without leaching. The assay loaded microcontainers can then be implanted subcutaneously and interrogated remotely by exciting the fluorescent molecules in the microcontainers and collecting the emitted light coming out of the skin, the so called “smart tattoo” approach,²⁴⁻²⁷ as shown in Figure 1.1. This technology has significant advantages over other mechanisms, because there is no need for inserting any kind of probes, and it can also prevent some of the cytotoxicity problems without allowing the leaching of free assay elements.

The first sensor designed to function similar to the above-mentioned “smart tattoo” technology, was based on the encapsulation of lectin/dextran in poly(ethylene glycol) hydrogel spheres.²⁶ However, the prototype of the fabricated sensors showed substantial leaching of assay components from the hydrogel spheres. The millimeter size of the spheres is also not appropriate for implantation, as the body mounts a substantial host response. There were also difficulties in the production of monodispersed and uniformly loaded spheres. These sensors showed sensitivity in the range of 0-600mg/dL. Although it was mentioned that the sensor response was 90% reversible, results were not shown.

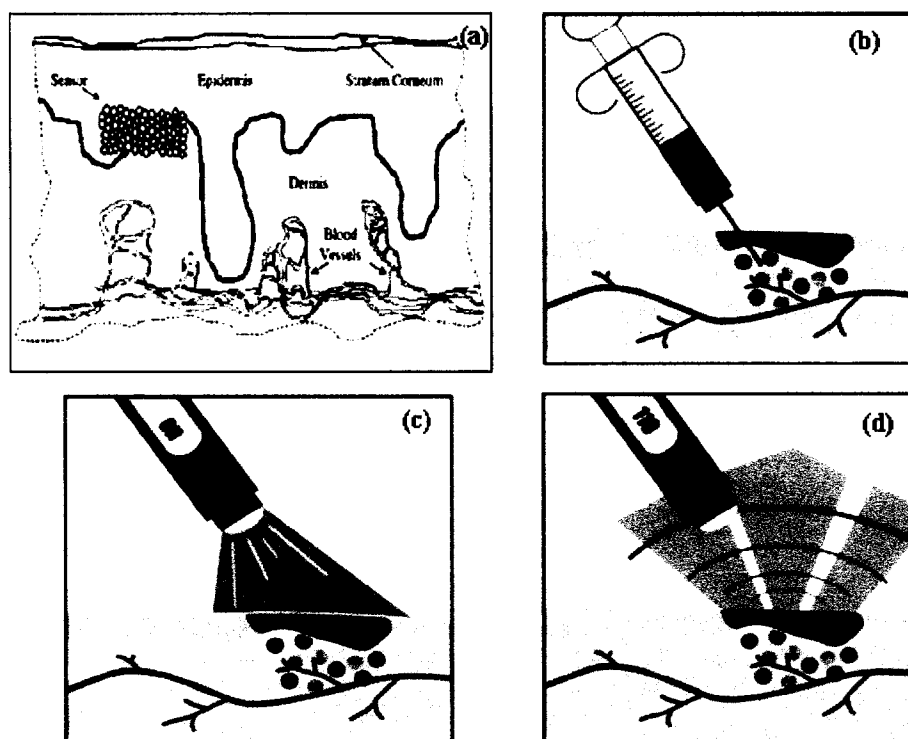


Figure 1.1. (a) Skin cross-section showing the implanted sensors between dermis and epidermis, (b) Subcutaneous implantation of microparticles loaded with sensing assay elements and interrogation of sensors by (c) exciting the fluorescent assay elements and (d) collecting the emitted light.²⁸

1.2 Objectives and Novel Aspects

Due to the severe limitations of existing smart tattoo systems, this dissertation work is focused on developing smart tattoo based non-consuming glucose sensors by overcoming the problems associated with previously reported sensing systems. The sensing mechanism in this new system is based on the competitive displacement of ligand by target-analyte, in order to occupy a binding site on the receptor molecule. These changes in the distance between ligand and receptor are monitored using fluorescence spectroscopic techniques. The significant advancement in this design is the packaging of competitive binding assay in microscale containers. In fact, as the microcapsules are about 5 μ m in diameter they can also be used as implantable sensors for frequent or continuous monitoring.

The novelty of this work is the demonstration of a general design of a new approach to the fluorescent affinity glucose sensing system based on a competitive binding assay. It is believed that this system can be extended to the detection of a wide variety of analytes other than glucose. The uniqueness in the competitive binding assay is the use of apo-enzyme (deactivated enzyme) as the receptor molecule whereby the apo-enzyme results in high specificity and does not exhibit the problems of aggregation and toxicity, which were seen with lectins. This design can potentially be used as a platform technology for detecting different analytes simply by selecting the appropriate enzyme and competitive ligand molecules.

In comparison to previously reported sensors, a significant achievement in this study is the efficient and stable encapsulation of sensing assay elements in microcapsules, without any loss in sensitivity which makes them more appropriate for use in the smart-

tattoo system. Also, this work demonstrates step-by-step development of the fluorescent affinity sensors operating in visible (green/orange, orange/red), and near-infrared (NIR) regions. Another notable feature is that even after extending the operating region from visible to NIR, there is no loss in sensitivity, which makes it more suitable for *in vivo* use, because there will be a significant increase in signal to noise ratio in NIR regions compared to shorter wavelengths. The important features of this sensing system are (1) non-toxic, which was the major disadvantage of all the lectin-based sensors, (2) efficient encapsulation of sensing assay elements in microcapsules, and (3) excellent sensor response of microcapsules comprised of sensing elements. The major objectives of this work are to design, fabricate glucose sensors and characterize its functional properties and response. Chapter Four to Chapter Seven will demonstrate various designs for developing glucose sensors, which have the potential to be used in minimally invasive systems based on the smart tattoo approach.

1.3 Organization of Chapters

The chapters in this dissertation are organized as follows. Chapter Two reviews various non-consuming fluorescence glucose monitoring techniques reported by different researchers and addresses the disadvantages in these systems and the need for improvements. Chapter Three explains the theory involved for the sensing mechanisms employed in this work. Chapter Four demonstrates for the first time a fluorescence glucose sensor based on the encapsulation of a Con A/dextran competitive binding assay into microcapsules. This work has been published in a peer reviewed journal, in a special issue on glucose sensing (*Journal of Fluorescence*, 14 (5), 585-595, 2004). Chapter Five demonstrates the apo-glucose oxidase (apo-GOx)/dextran based glucose assay,

encapsulated in microcapsules. This is believed to be superior to the Con A/dextran approach, due to the reduced toxicity and higher specificity to β -D-glucose. This work was divided into two parts and was published in two peer reviewed journals, (apo-enzyme competitive binding assay in *Biomacromolecules*, 5(5), 1657-1661, 2004; microcapsule system for glucose sensing in *Analytical Chemistry*, 77(17), 5501-5511, 2005). Chapter Six demonstrates the extension of apo-GOx/dextran based glucose sensor into the long wavelength (orange/red) visible light region. This work on the extension of the operating region of apo-GOx/dextran assay into longer wavelength regions was also submitted to a peer reviewed journal, *Diabetes Technology and Therapeutics*. Chapter Seven demonstrates a novel glucose sensor based on the quenching mechanism using the apo-GOx/dextran assay, operating in the NIR region. Also, this assay is encapsulated into organo/inorgano microcapsules using glycidyl-silane as the crosslinking element to entrap the loading assay elements. As this assay operates in the NIR region, it is superior to all the sensors demonstrated in the previous chapters. The successful demonstration of the competitive binding assay into NIR region indicates that the assay can be modified to meet the requirements of the application. Finally, Chapter Eight summarizes the major findings of this work and discusses possibilities of further experiments.

CHAPTER 2

LITERATURE REVIEW

The main goal of this research is to develop a minimally invasive approach for glucose monitoring by designing subcutaneously implantable microcarriers comprising glucose sensitive materials. These microcarriers can be excited from outside the body using harmless visible or near infrared (NIR) light and the fluorescence light coming out of the skin can be collected using suitable detectors — the so-called “smart tattoo” concept. This chapter reports on the previous work on non-consuming fluorescent glucose sensors for the application as implantable systems. This discussion starts with a brief description of the types of glucose sensors (enzymatic and affinity), and then focuses more on the different types of affinity (non-consuming) based glucose sensors.

2.1 Types of Glucose Sensors

Frequently used transduction mechanisms in glucose sensors reported to-date, can be classified into two groups, electrochemical and optical techniques.^{1-4,6} Electrochemical sensors are the glucose sensors which include one of the following devices: amperometric, potentiometric, and conductometric devices, which are based on monitoring the electric current associated with the electrons involved in the redox processes, concentration of selective ions using ion selective electrodes, and conductance

changes due to changes in the overall ionic environment, respectively.^{6,29} In spite of good *in vitro* results, long term *in vivo* glucose monitoring with amperometric sensors has not been completely successful due to a gradual loss of sensor function, which indicates that the surrounding environment plays an important role in the sensor's behavior. These sensors faced challenges in preventing the biofouling of enzyme-containing membranes, frequent replacement of the sensor, insufficient selectivity, and only allowing for retrospective data analysis.³⁰ The influences of wound healing, host response to the implant, and blood supply in the surrounding tissue on sensor performance need to be addressed. Also, more insight is needed in the physiological processes at the sensor-tissue interface.³¹ The sensors based on reverse-iontophoresis have most of the defects found in amperometric sensors such as, the need of calibration on a daily-basis. Sensors based on optical measurements are an attractive alternative, as they may transduce chemical concentration information into an optical signal which may be analyzed spectroscopically.³² Among all the available techniques, fluorescence measurements are considered to be superior; the reasons for which, are described below.

Need for fluorescence measurements

Fluorescence spectroscopy is one of the widely used techniques in biomedical research. Its sensitivity, which is a thousand times greater than absorption spectroscopy, is a major asset of this technique. The high sensitivity is due to the emission intensities measured with a lower background level. This technique allows the research at very low concentrations, which is very economical when working with expensive reagents.³³⁻³⁵ Fluorescence measurements cause no damage to the body, as long as sub UV frequencies are not used in excitation. As NIR light can pass through several centimeters in tissue, by

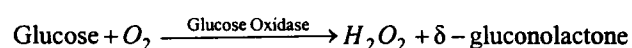
selecting suitable NIR dyes, the sensors can be efficiently interrogated from outside the body by sending light in and then collecting the light coming out of the skin. Thus, this technique opens the door for minimally-invasive monitoring.

By using different fluorescent dyes, analyte-sensitive structural and micro-environment changes in a molecule can be monitored in real-time. For example, fluorescence intensity of anilino-naphthalenesulfonic acid (ANS) conjugated to glucose binding protein decreases with the addition of glucose, as it is exposed to a high polarity environment.²³ Also, fluorescence resonance energy transfer (FRET), which is described in detail in Chapter Three, is widely used for monitoring the glucose-sensitive distance changes (~ few angstroms) between two molecules.²²

In the enzymatic sensors (e.g. glucose oxidase, GOx), GOx catalyzes the conversion of β -D-glucose and oxygen to D-glucono-1,5-lactone and hydrogen peroxide.^{36,37} In these sensors, fluorescent dyes are incorporated in the sensing assay in order to indicate the changes in the concentration of the resultant by-products, such as change in pH due to the production of acid, and change in oxygen levels during the reaction between glucose and GOx. Thus, the fluorescence techniques are widely used all over the world for developing glucose sensors and various biomedical applications. The fluorescence glucose sensors can be broadly divided into two categories (a) Enzymatic sensors, and (b) Affinity sensors. The following section provides a brief description of enzymatic sensors, with detailed discussion on affinity sensors, which is the research topic of this dissertation.

2.1.1 Enzymatic Sensors

Most of the currently available glucose sensors are based on a flavo-enzyme, GOx. GOx is a homo-dimer, which catalyses the oxidation of β -D-glucose, in a two step process.³⁸ In the first step, two protons and electrons are transferred from glucose to GOx, resulting in the oxidation of β -D-glucose to δ -gluconolactone, and reduction of GOx to GOxH₂. In the second step GOxH₂ is oxidized to GOx by molecular oxygen, releasing hydrogen peroxide (H₂O₂); and δ -gluconolactone is hydrolyzed non-enzymatically into gluconic acid.³⁹ The overall reaction is written as,



All together, there are three ingredients (O₂ consumption, H₂O₂, and acid production) of the glucose oxidation catalyzed by GOx, which can be monitored to estimate the changes in glucose concentration. Thus, different fluorescent glucose sensors can be designed by incorporating an oxygen-sensitive or pH sensitive fluorophore to indicate the changes in glucose, and a reference fluorophore, which is insensitive to glucose concentrations, in a sensing chamber. Different variations of GOx based fluorescent glucose sensors will be discussed below.

Kopelman et al., proposed ratiometric sensors for real-time biochemical monitoring, which are also known as polyacrylamide PEBBLES (Probes Encapsulated By Biologically Localized Embedding).^{40 - 42} They proposed a glucose sensor, by incorporating all the sensing elements: the enzyme, GOx, oxygen sensitive fluorescent indicator, ruthenium (Ru), and an oxygen insensitive fluorescent dye, Oregon Green 488-dextran or Texas Red-dextran, as a reference dye for conducting ratiometric measurements, in nanospheres prepared using microemulsion polymerization process.⁴⁰

The enzymatic oxidation of glucose to gluconic acid results in the decrease in oxygen levels, which is measured by the oxygen sensitive dye, Ru.⁴⁰ The nanosensors showed a linear range of 0.3-5 mM glucose with a response time of 150 seconds. PEBBLEs were also used in developing intracellular sensors for pH and calcium,⁴³ oxygen,^{44, 45} potassium,⁴⁶ magnesium,⁴⁷ zinc,⁴⁸ chloride,⁴⁹ glucose,⁴⁰ and iron.⁵⁰ However there are some significant disadvantages, such as, the uniformity cannot be maintained from sensor to sensor within the same batch and from batch to batch, due to the nature of the emulsion process, and the leaching of encapsulated chemistry over time. Since PEBBLEs are typically less than 200 nm in diameter, they are not suitable for dermal implantation since they are likely to be phagocytosed by macrophages.

Brown et al., proposed a glucose sensor based on the incorporation of enzyme, analyte indicator and reference dyes in a microcontainer, which has the potential for application as an implantable glucose sensor – so called “smart tattoo” concept.^{51,52} In this work, calcium alginate microspheres coated with polyelectrolyte multilayers (PEM's) were used as microcarriers for holding GOx, and entrapping an oxygen-quenched Ru-compound. A reference dye, Alexa Fluor 488 (AF488), was incorporated in the multilayer nanofilms on the surface of the microspheres, which can also stabilize enzyme entrapment and control glucose diffusion. The confocal microscope image shown in Figure 2.1(a) for the completed sensor, shows the indicator dye (red) in the sphere interior and reference dye (green) on the sphere walls. The changes in fluorescence spectra with varying glucose concentrations are represented in Figure 2.1(b) as a change in peak ratio. R_{sat} is the intensity ratio of Ru to AF488 in O₂-saturated buffer, and R_g is the intensity ratio at each glucose concentration. These sensors have a more suitable size

range (20-30 μm) as compared to above-mentioned PEBBLE sensors. Also, these sensors were made much more sensitive and stable through several advances in modeling and fabrication approaches.^{51, 53 - 56} However, major limitations in these enzymatic based sensors are glucose consumption and high dependence of the measurements on local oxygen levels.

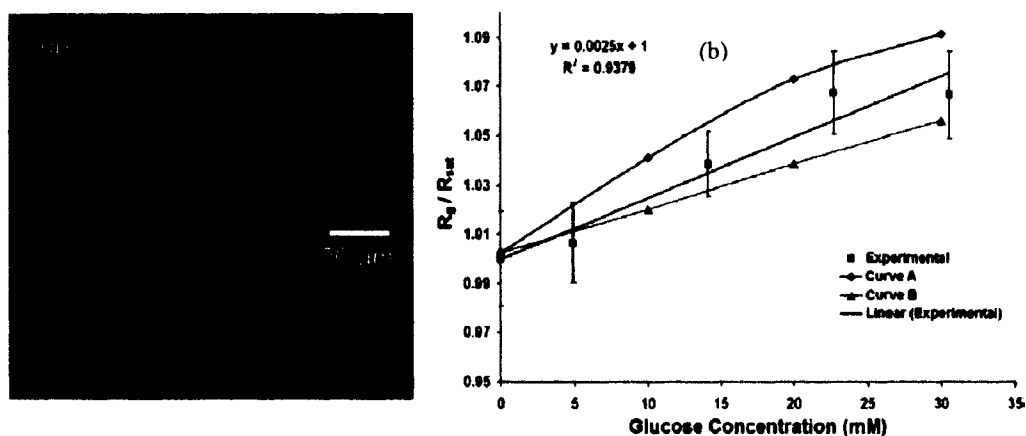
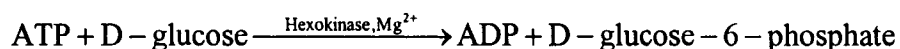


Figure 2.1. (a) Confocal microscopy image of spheres used for glucose sensitivity experiments; (b) Plot of experimentally and theoretically obtained fractional fluorescence peak ratio values at different glucose concentrations.⁵¹

In recent years, there have been several variations of biosensors based on nanotubes and their surface modification.⁵⁷⁻⁶¹ Strano and co-workers reported a single walled nanotube (SWNT) based near infrared glucose sensor.⁶¹ They showed that the surfactant used to suspend the nanotubes can be exchanged with GOx to obtain a single layer of GOx on the surface of SWNTs. Ferricyanide, which reduces the inherent fluorescence (in NIR region) of nanotubes was irreversibly absorbed onto the nanotube sidewall. In the presence of β -D-glucose, hydrogen peroxide is produced due to the reaction between glucose and GOx, which then reduces ferricyanide. This reduction transfers electrons back into the nanotube, thereby increasing the fluorescence. Therefore,

by monitoring the changes in fluorescence, glucose concentration can be estimated. In order to use biosensors based on SWNTs, the surface of the nanotube must be functionalized with ligand specificity. This step of surface modification is very complex and hard to achieve as the covalent sidewall functionalization of SWNTs diminishes their optical properties owing to the disruption of the one-dimensional electronic structure. Therefore, non-covalent binding is required for optical SWNT biosensors. In addition, the SWNTs must be maintained as individual molecules, otherwise the aggregation may result in loss of fluorescence.^{61,62}

Hexokinases, in comparison to GOx, have been less explored as glucose receptors for fluorescence-based sensing. These enzymes catalyze the transfer of the γ -phosphoryl group of ATP to the hydroxyl group at position C6 of glucose:



Pickup et al., proposed a glucose sensor based on the glucose sensitive changes of the intrinsic fluorescence from hexokinase.⁶³ In solution, there was about a 23% (Figure 2.2(a)) change in fluorescence of hexokinase (at 320nm) with the addition of 1 mM glucose solution. However, it was observed that the glucose sensitive changes in hexokinase were abolished in the presence of serum, as shown in Figure 2.2(a). To overcome this problem, hexokinase was immobilized in tetramethylorthosilicate-derived sol-gel. With the entrapment in sol-gel, hexokinase showed 25% change in intrinsic fluorescence and the signal saturation was extended to 50 mM glucose (Figure 2.2(b)). The linear range was further increased to 110 mM by covering the sol-gel with a polymethacrylate membrane. The effect of serum on the sensitivity was very minimal when hexokinase was entrapped in sol-gel, with or without covering membrane, opening

the doors for *in vivo* monitoring. However, a major disadvantage of this system is the use of UV light for excitation, which requires complex or bulky light sources, and also there will be interference from various proteins in the biological samples.

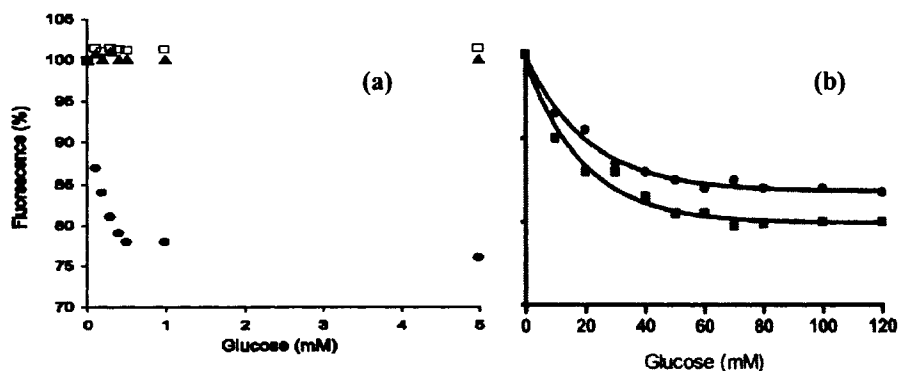


Figure 2.2. (a) Intrinsic fluorescence of hexokinase in solution with increasing glucose concentration, in (●) PBS; (□) serum; (▲) low-molecular weight fraction of serum; (b) Change in intrinsic fluorescence of sol-gel immobilized hexokinase in (■) PBS or (●) serum.⁶³

2.1.2 Affinity Sensors

Affinity biosensors are analytical devices comprising a recognition element such as an antibody, receptor protein, biomimetic material, or DNA interfaced with a signal transduction mechanism to convert the analyte concentration to a measurable signal. Several variations of affinity glucose sensors are discussed in the following section.²⁰⁻²³ Unlike enzymatic sensors, for the case of affinity based glucose sensors, glucose is not consumed during the receptor and glucose binding and, therefore, no by-products are produced; thus the name “non-consuming” glucose sensors. Also, the measurements are more direct, as they are not affected by oxygen and pH variations.

There are different types of glucose sensors that fall into this category, as depicted in Figure 2.3. Among all these sensors, competitive-binding based glucose sensing has been extensively explored for the last two decades. This concept is discussed in more detail in the following sections of this chapter.

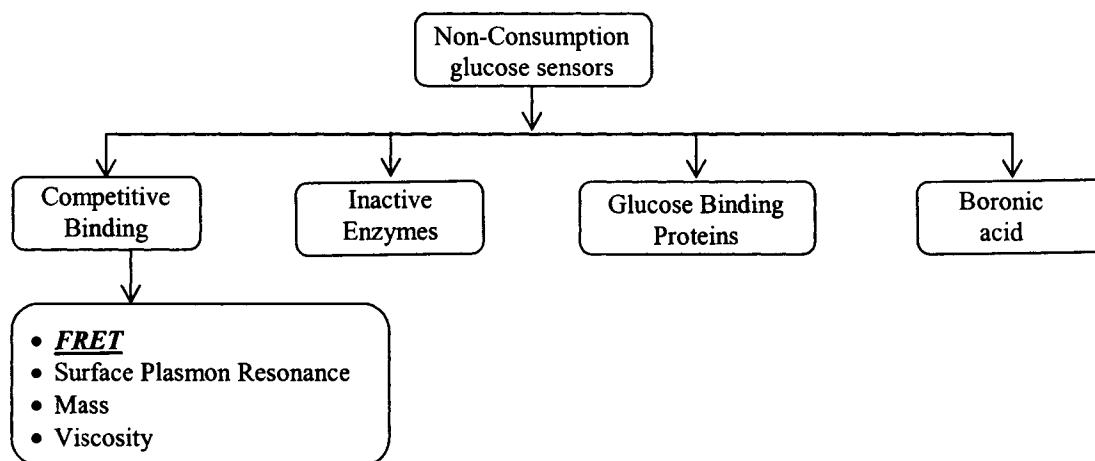


Figure 2.3. Different types of non-consuming glucose sensors.

2.2 Competitive Binding (CB) -Based Glucose Sensors

A competitive binding (CB) based glucose sensing scheme, as depicted in Figure 2.4, involves three components, (i) receptor/substrate (e.g. Con A), (ii) ligand/analyte-analog (e.g. dextran), and (iii) analyte (e.g. glucose). The CB mechanism for glucose is based on the fact that the receptor has different binding affinities for various sugars (Figure 2.5). When receptor is exposed to ligand and analyte they will compete to occupy the binding sites on receptor. As receptor has greater affinity toward analyte over ligand, analyte displaces ligand from receptor. This process generates more free-ligand and receptor/glucose complexes (Figure 2.4(c)). Generally, free-ligand concentration or the distance between receptor/ligand is monitored to estimate glucose concentrations. This process is called CB technique, which is generally used in conjunction with several other techniques, such as FRET, QCM, SPR, and viscosity to estimate glucose concentration. Concanavalin A (Con A) and dextran are widely used as the model receptor and ligand molecules during the demonstration of CB process. The structure of Con A and its interaction with dextran, will play a significant role in the sensing process.

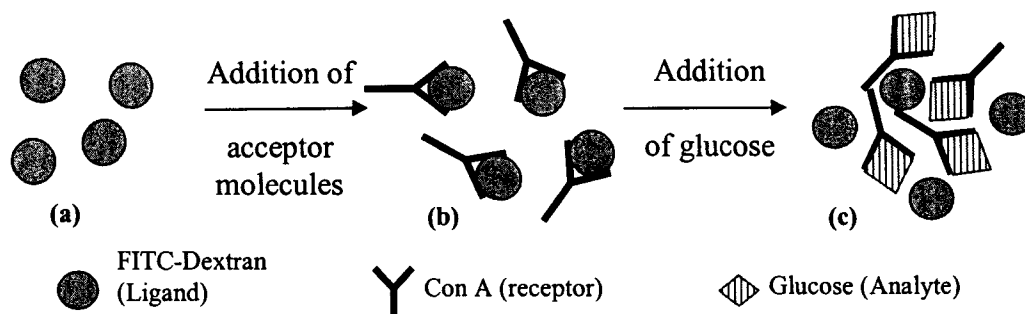


Figure 2.4. Illustration of Competitive binding technique: (a) donor molecules, (b) Mixture of donor and acceptor molecules, and (c) glucose competes with dextran to occupy binding sites on Con A, and displaces dextran from Con A.

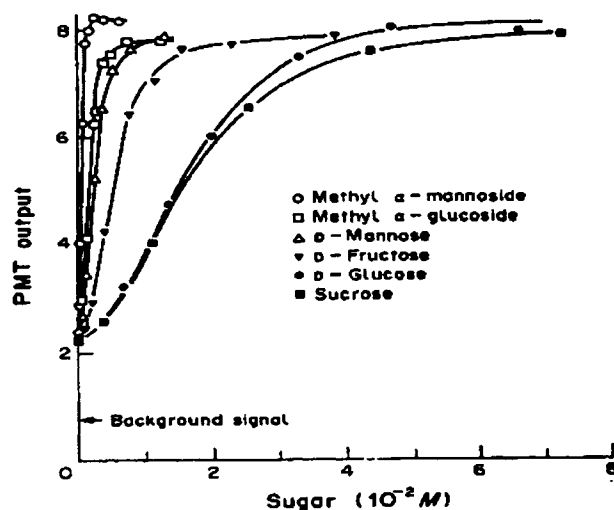


Figure 2.5. Binding affinity of various sugars to Concanavalin A.⁸⁶

Con A belongs to a group of proteins called lectins, which are known for binding to specific sugar molecules. Con A has specific binding sites for α -D-glucose. Native Con A is comprised of four subunits each having a molecular weight of 26kDa and one sugar binding site. Also, Con A contains bound calcium and manganese ions per subunit, which are essential for the occurrence of sugar binding. Depending on the solution characteristics and properties, Con A can exist in dimeric, tetrameric, and higher order forms.⁶⁴ It has been observed that Con A recognizes terminal as well as internal

saccharide residues.⁶⁴ Because of the sugar specificity of Con A, it has been successfully employed in glucose sensors.⁶⁵ Previously reported Con A based affinity sensors in conjunction with different transduction mechanisms are discussed in detail below.

2.2.1 Viscosity Measurements – CB Assay

Viscosity is the measure of a fluid's resistance to flow. A fluid with large viscosity moves slowly, because it experiences a large amount of internal friction, and a fluid with low viscosity flows easily because it experiences very little friction when it is in motion. Ehwald et al., showed that there are significant changes in the viscosity values of the dextran/Con A complexes with the addition of glucose due to the competitive displacement of dextran from Con A, as shown in Figure 2.6.^{66,67}

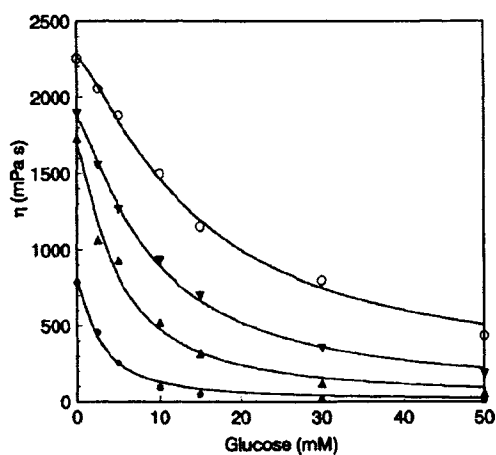


Figure 2.6. Changes in Viscosity (η) of dextran and Con A (10 gm/L) dispersions. Dextran concentrations were, (○) 190 gm/L, (▼) 120 gm/L, (▲) 80 gm/L, (●) 40 gm/L.⁶⁷

It can be observed from Figure 2.6 that with the increase in glucose concentration, there is a decrease in viscosity value, because of the decrease in large complexes of Con A/dextran. Also, viscosity values were observed to vary with the change in dextran concentration and molecular weight.⁶⁸

2.2.2 Mass/Thickness Measurements – CB Assay

Sugar specificity of Con A based on mass/thickness measurements was demonstrated in 1991, using layer-by-layer (LbL) assembly process.⁶⁹ LbL self assembly is well known for its simplicity in constructing multilayer thin films of various macromolecules. In most cases, this process involves the construction of thin films of oppositely charged molecules on a substrate based on electrostatic forces of attraction.⁷⁰ However, in the present case, multilayers of Con A/glycogen thin films were coated on a flat substrate based on the binding affinity between the two molecules. The Con A/glycogen assembly process was monitored by measuring frequency changes in a quartz crystal microbalance (QCM) resonator. It was observed that the binding constants can be varied by controlling the glycolipid concentrations.⁷¹ Lvov et al., further demonstrated the multilayer assembly of Con A in two modes of interactions, as a polyion and a biospecific agent, as shown in Figure 2.7(a).⁷² This was demonstrated by constructing the thin films of Con A (anionic)/poly(ethyleneimine) (PEI, polycation), and Con A/glycogen on a QCM resonator in the neutral pH region (Figure 2.7(a)). It was observed that there are linear frequency shifts in two modes of assembly. The multireceptor sites of Con A are very important in building multilayers of Con A and glycogen.⁷² The sugar specific nature of Con A was further utilized to build a multilayer of Con A/glycoproteins⁷³ (GOx, HRP) and Con A/avidin.⁷⁴ UV-Vis absorption spectroscopy⁷⁴ and QCM^{73,74} measurements were used to monitor the LbL assembly process. This research was further developed by Anzai's group to demonstrate the glucose sensitivity of the Con A/glycogen multilayers. It was shown that the Con A/glycogen multilayers can be completely disintegrated (Figure 2.7(b)) upon exposure to sugars (D-glucose, D-

mannose) in the aqueous solution at neutral pH.⁷⁵ This behavior is observed because of the competition between the sugar and glycogen to occupy the binding sites on Con A, and since the sugar has greater affinity toward Con A compared to glycogen, glycogen is displaced from Con A, thus disintegrating the con A/glycogen multilayers.⁷⁵ Also, the variation in the sensor response with different sugars is shown in Figure 2.7(b).

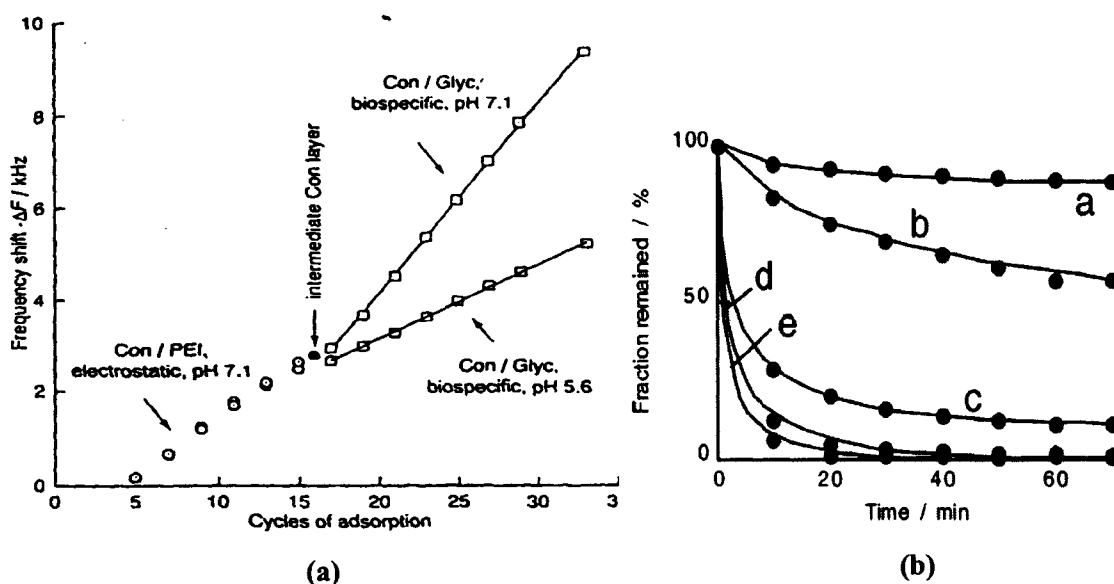


Figure 2.7. (a) Layer-by-Layer assembly of Con A/glycogen multilayers using two modes of interactions; (b) Disintegration of the Con A-glycogen multilayer film (10 bilayers) in the presence of 10 mM (a) D-galactose, (b) D-glucose, (c) D-mannose, (d) Methyl- α -D-glucopyranoside, and (e) Methyl- α -D-mannopyranoside at pH 7.4.⁷⁵

2.2.3 Surface Plasmon Resonance Based Glucose Sensors

Surface plasmon resonance (SPR) is a relatively new technique. It is a powerful tool for studying the interactions between high molecular weight molecules, e.g. antibody-antigen and nucleic acid interactions. The detection capability of SPR is extended to low molecular weight compounds, such as pesticides,⁷⁶ saccharides,⁷⁷ etc., using indirect or CB approaches. The SPR detection principle relies on the change in refractive index and the corresponding shift in the SPR angle that occurs on binding of

the target-analytes to the immobilized receptor/recognition molecules. Thus, the glucose-sensitive dissociation of Con A and dextran was demonstrated using SPR techniques.⁷⁶⁻⁸³

Ballerstadt et al., were the first to demonstrate a glucose sensor based on SPR and CB techniques. A glucose sensing SPR-probe was constructed by placing a thin layer of Con A/dextran (high viscosity) dispersion on the gold surface of an SPR-probe.⁷⁸ The changes in viscosity were monitored when the Con A/dextran SPR-probe came in contact with different glucose concentrations. By monitoring the shift in SPR angle, as shown in Figure 2.8, it can be observed that with the increase in glucose concentration there is a decrease in resonance angle due to the separation of dextran and Con A.

A novel technique for glucose monitoring was developed by Geddes et al., based on the changes in SPR peak due to the aggregation of dextran coated-gold nanoparticles in the presence of Con A and disassociation in the presence of glucose.⁸¹⁻⁸³ Due to the binding affinity between Con A and dextran, dextran coated-gold particles form large aggregates in the presence of Con A (Figure 2.9), resulting in a significant shift and broadening of gold plasmon absorption. As Con A has greater affinity towards glucose over dextran in the presence of glucose, dextran coated-gold particles are displaced from Con A, which results in the segregation of gold particles (Figure 2.9). This reduction in gold particle aggregation will be indicated as a shift in SPR angle. These sensors were also optimized in regard to stability, pH effects and dynamic range of glucose sensing.^{81,82} A similar sensor was developed using silver nanoparticles.⁸³

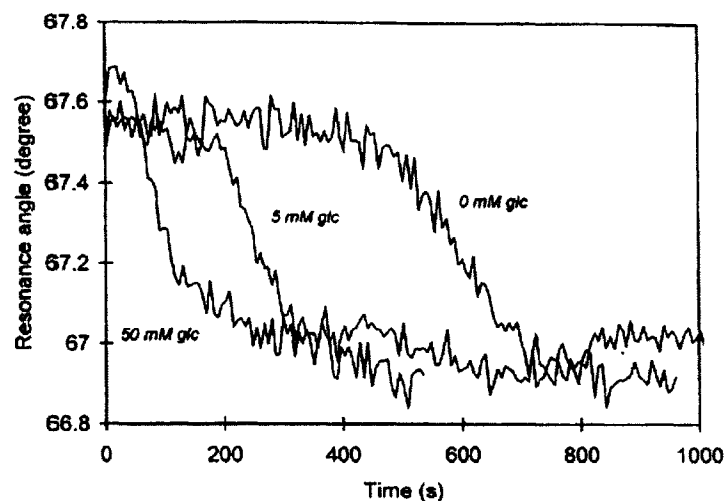


Figure 2.8. Change in SPR angle of Con A:dextran-solutions at various glucose concentrations.⁷⁸

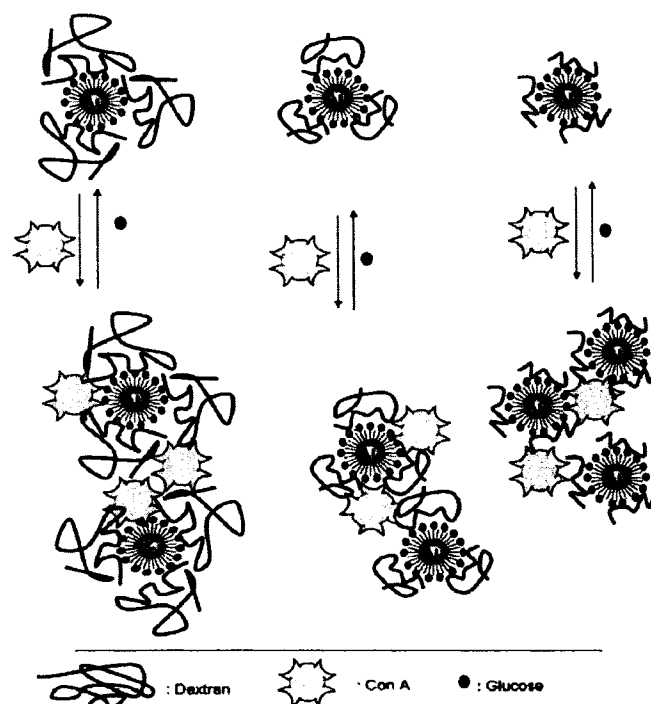


Figure 2.9. Competitive binding and SPR based glucose sensing mechanism: the dissociation of Con A-aggregated dextran-coated gold nanoparticles.⁸¹

All of the above mentioned Con A-based glucose sensors using viscosity, frequency, and SPR techniques were successfully demonstrated. There are some disadvantages, such as low sensitivity and need to realize the final goal, which is an

implantable continuous glucose monitoring system. For reaching the final goal fluorescence sensors are more practical, because of the high sensitivity and the possibility of remote interrogation of the implanted sensors.

2.2.4 CB Based Fluorescence Affinity Glucose Sensors

The combination of CB and fluorescence techniques for glucose sensing is very popular because of its simplicity and reliability. This sensing mechanism attracted many researchers, because of the non-consumption property and the employment of highly sensitive fluorescence measurement techniques. The advantages of fluorescence techniques, specifically FRET are discussed in detail in the sections that follow.

Schultz et al., developed the first affinity glucose sensor in 1979, based on the binding specificity between Con A and saccharides.^{84, 85} This transduction mechanism employs the CB based Con A/dextran system.⁸⁵ Dextran was conjugated to fluorescein-isothiocyanate (FITC) in order to use fluorescence techniques to measure free-dextran. The sensing system was fabricated by immobilizing Con A on the inner surface of the dialysis fiber and filling the interior with freely floating FITC-dextran (FD). Finally, one end of the fiber was sealed and an optical fiber was inserted into the other end (Figure 2.10).⁸⁵ The molecular weight of the dextran and porosity of the membrane were selected such that the fiber can retain dextran in the interior while glucose can move freely. In the absence of glucose, certain fraction of FD was bound to the Con A immobilized on the fiber. Exposure of the fiber to glucose results in the displacement of FD from Con A. This competitive displacement of FD in the presence of glucose will result in the increase in number of free-FD molecules. Thus, glucose concentration was estimated by measuring free-FD concentration using fluorescence measurements.

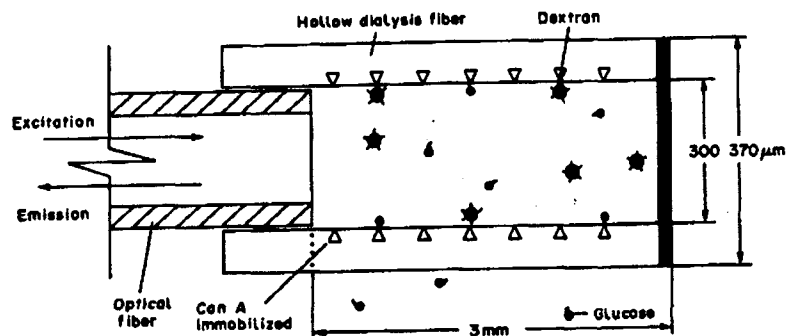


Figure 2.10. Heterogeneous fluorescence affinity sensor.⁸⁶

In spite of the novelty of this technique there were some disadvantages such as, the repeatability of the Con A immobilization on the fiber and the alignment of the optical and mechanical fibers.²² Sensor properties were affected by the quenching effects on FITC or alterations in the Con A binding activity. The change in fluorescence signal due to concentration and instrumental drift, cannot be corrected because of the absence of a reference fluorophore. In order to overcome these limitations, the above mentioned design was improved using FRET techniques.

2.2.5 CB and FRET Based Glucose Sensors

FRET is a phenomenon between two fluorescent molecules, which involves non-radiative energy transfer from one fluorophore (donor) to another (acceptor) when the two fluorophores are in close proximity. As the distance between the two fluorophores increases, there is a decrease in energy transfer. Thus, the glucose concentrations can be monitored by observing the changes in energy transfer. The FRET phenomenon is discussed in detail in Chapter Three.

Glucose Sensors Based on Intensity Measurements. The Schultz group demonstrated a FRET based homogeneous glucose sensor as shown in Figure 2.11, by eliminating the Con A immobilization step from the above-demonstrated heterogeneous

system. FITC and Rhodamine (Rh) were used as the donor and acceptor fluorophores, conjugated to ligand (dextran) and receptor (Con A), respectively.⁸⁶

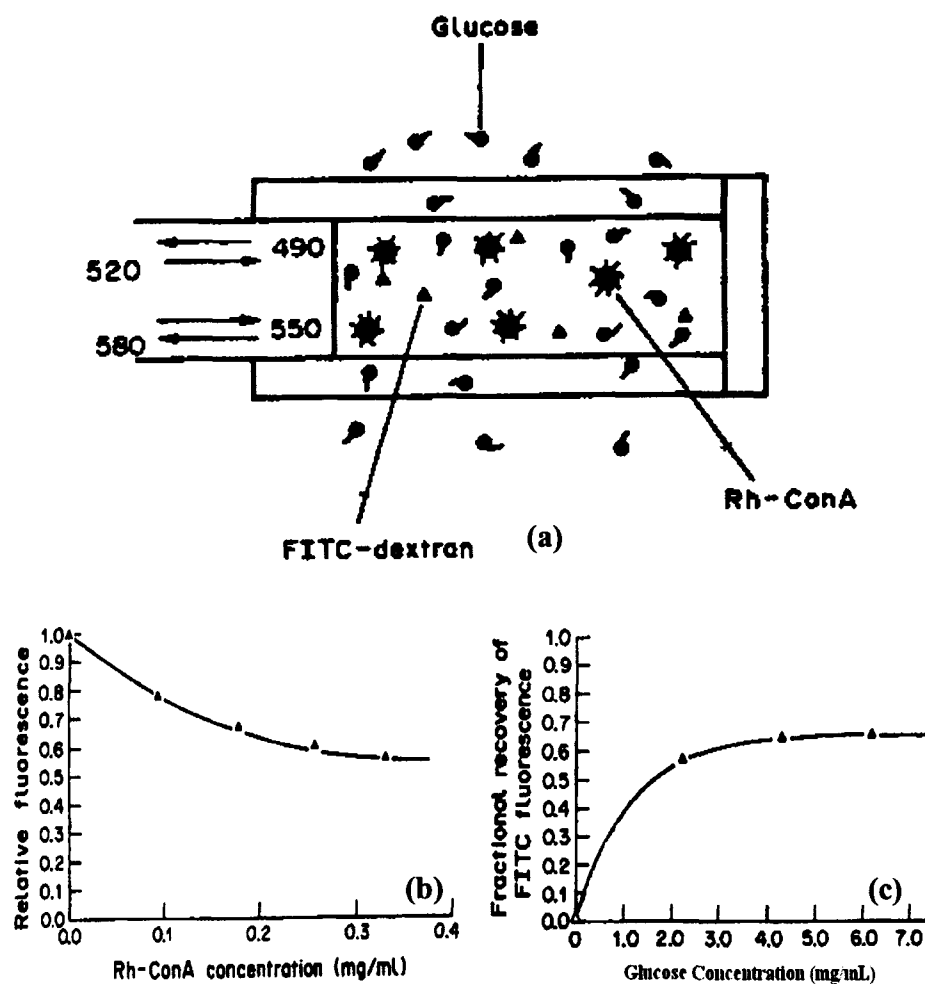


Figure 2.11. (a) Schematic of homogeneous FRET based glucose sensor; Changes in FITC fluorescence with the addition of (b) Rh-Con A to FD, and (c) glucose to FD/Rh-Con A complexes.⁸⁶

When FD/Rh-Con A complex was excited at the FITC-excitation wavelength (488 nm), energy is transferred non-radiatively from FITC to Rh, which results in the Rh emission. It was observed that with the addition of glucose, FD and Rh-Con A were dissociated, increasing the distance between them, which in turn resulted in the decrease in energy transfer from FITC to Rh, and was indicated as an increase in FITC emission

peak relative to Rh (Figure 2.11). Thus, the level of FITC fluorescence was used to determine the glucose concentrations.⁸⁶

It is well known that aggregation is one of the main problems associated with Con A, mostly when it is bound to dextran. While it is also known that the aggregation can be prevented by maintaining optimal pH (6 to 7) and temperature (< 40°C), this is not always possible, especially for *in vivo* measurements. To overcome this problem, the Schultz group proposed the idea of replacing Con A with succinyl (succ)-Con A, which will not aggregate at high temperatures and pH.^{87,88}

Succ-Con A is prepared by reacting lysine residues on Con A with succinic anhydride, which results in the conversion of the positively charged lysine side chains into negative charges. These changes in the charge distribution of the Con A and the sterical interactions will result in two identical dimers from one tetramer that do not re-aggregate into the tetramers even at high temperatures.⁸⁸ Dextran and succ-Con A were labeled with FITC and TRITC respectively. This assay is similar to the above-mentioned system,⁸⁶ with the variation in the type of Con A and acceptor fluorophore. Glucose concentrations of up to 1600mg/dL could be detected with a time response of ~10min.^{87,88}

In all of the above described sensing mechanisms, Con A must be either chemically modified or otherwise labeled with a fluorophore, which is time consuming. In addition, these procedures on Con A could affect the binding activity between ligand/analyte. In order to overcome these concerns, Schultz lab proposed the idea of fluorescence quenching of ligands held in close proximity by a multivalent receptor.⁸⁹ In order to reduce this idea into practice, some fraction of the ligand (dextran) molecules

was labeled with FITC (donor) and the rest was labeled with RITC (acceptor). In the absence of any Con A-specific sugars (e.g. α -D-glucose), Con A binds to FITC and RITC labeled dextrans bringing them into close proximity, which results in the energy transfer from FITC to RITC. With the addition of glucose, two dextran molecules are displaced resulting in the increase in FITC fluorescence due to the decrease in RET.⁸⁹

In all the above demonstrated sensing systems, changes in fluorescence intensities were measured to estimate the changes in glucose concentration. Even though this method is highly sensitive, allowing one to work at very low concentrations, there are some disadvantages when the issue of non-invasive monitoring is considered. There will be significant loss in intensities when the measurements are performed in a scattering media (skin). To avoid these problems, lifetime measurements were proposed by Lakowicz et al., using the same transduction mechanism. Also, the lifetime measurements are not affected by the concentration and optical properties of the sample.⁹⁰ Several variations of lifetime measurements based glucose sensors are discussed below.

Glucose Sensors Based on Lifetime Measurements. Based on the same CB and FRET transduction principle, several methods for glucose sensing were demonstrated using fluorescence lifetime measurements.⁹⁰⁻⁹⁵ In one of the sensor designs, Con A was labeled to Ru (donor), and malachite green (MG, acceptor) was labeled to insulin and maltose (MIMG) to provide binding affinity for Con A. With the addition of Ru-Con A to MIMG, there was a decrease in the fluorescence intensity and decay time of Ru, due to the energy transfer from Ru to MG. However, with the addition of glucose, MIMG was displaced from Ru-Con A, resulting in the increased intensity and decay time of Ru.⁹⁰

Another sensor design was reported on similar grounds by replacing Ru with Cy5, as shown in Figure 2.12.⁹¹ By comparing the results from Ru-Con A and Cy5-Con A, it was observed that the reversibility was significantly improved in the case of Cy5-Con A. It is noteworthy that Cy5 has a smaller Stokes shift and lifetime, but relatively high quantum yield. Also, the use of Cy5 allows excitation with red laser diodes.

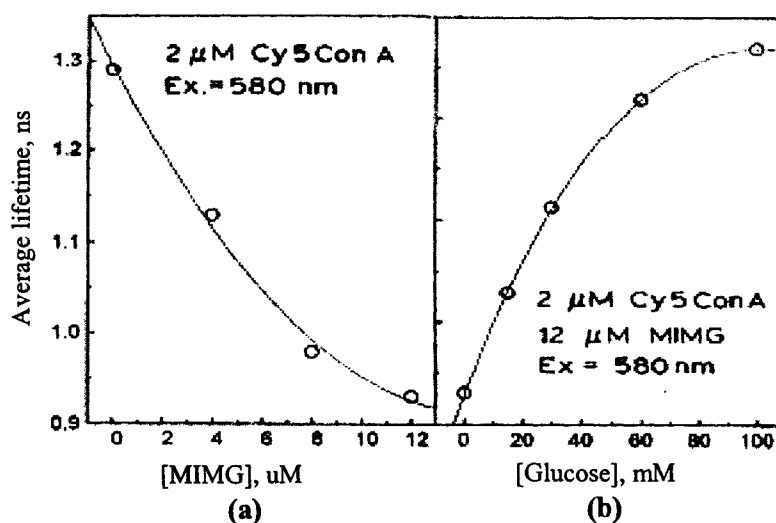


Figure 2.12. Excited state decay of Cy5-Con A with the addition of (a) MIMG, and (b) glucose.⁹¹

Another FRET based glucose sensor operating in the NIR region was developed using allophycocyanin (APC, donor) labeled Con A and MG (acceptor) labeled dextran.⁹⁶ As glucose competitively displaces MG-dextran, there was a reduction in FRET as shown in (Figure 2.13), which was assessed by fluorescence lifetime measurements. This assay showed significant changes in the range of 2.5–30 mM glucose levels. It was observed that albumin and serum inhibit FRET significantly (Figure 2.13(a)), but the interference was prevented by removing high molecular weight substances using filters, as shown in Figure 2.13(b). Thus, APC showed promise for use in a glucose sensor, which can be interrogated remotely.⁹⁶

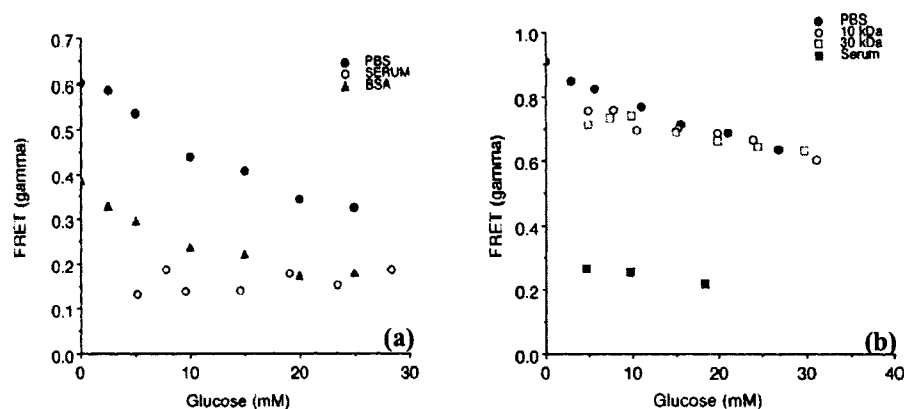


Figure 2.13. Changes in FRET between APC-Con A and MG dextran in the presence of (a) PBS, Serum and BSA; (b) PBS, serum passed through 10kDa and 30kDa filters, and unfiltered serum.⁹⁶

Most of the above-mentioned intensity and lifetime measurements based sensing systems were successfully demonstrated in solution. The potential disadvantage of these fiber-based approaches is the risk of infection at the site of optical fiber intrusion into the skin. However, in order to implement these sensors for non-invasive monitoring, the sensing elements must be encapsulated in a microcarrier, e.g. microcapsules, microspheres, etc., which have the ability to display changes in fluorescence for varying glucose concentrations. The following section will discuss all the previously reported fluorescence affinity sensing systems for transdermal monitoring.

2.2.6 Transdermal Glucose Sensing

PEG hydrogel based glucose sensor. To overcome the difficulties with currently available non-invasive monitoring systems, a novel system based on the “smart tattoo” concept was proposed, which could be implanted in the skin and interrogated remotely using harmless visible or NIR light excitation.^{26,27} The feasibility of this concept has been demonstrated for the short wavelengths of the FITC-TRITC RET pair, by modeling and experimental studies of tissue.²⁴⁻²⁷ Prototypes consisting of poly(ethylene glycol) (PEG) hydrogel microspheres with covalently-immobilized TRITC-Con A molecules and

physically entrapped FD in the gel matrix were constructed, and the glucose response for the system was further controlled by varying the Con A:dextran ratio inside the hydrogel. *In vitro* experiments of hydrogel spheres showed an optimum fluorescent intensity change between 0-800mg/dL with a linear response up to 600mg/dL.²⁷ Despite the encapsulation of Con A/dextran assay into microspheres, there still remain some critical problems in maintaining the stability of the response and the production of uniform and strongly responsive glucose-sensitive microspheres.

Sephadex bead based affinity glucose sensor. The Schultz group proposed a minimally-invasive approach for glucose monitoring based on the implantation of the semi-permeable membrane chamber containing glucose-sensitive assay elements.⁹⁷ In this sensing system, AF 488-Con A molecules were bound to the glucose residues on the interior of the sephadex beads (Figure 2.14(a)), which were made up of dextran tagged to an absorption dye. The excitation light cannot excite AF 488-Con A molecules residing inside the beads as the absorption spectrum of the dye conjugated to dextran overlaps with the fluorescence excitation spectrum of the fluorophore labeled to Con A. But, with the addition of glucose, the AF 488-Con A is displaced from the dextran matrix, and diffuses out of the colored beads into the outside space (Figure 2.14(b)) where it is exposed to light, thus resulting in a fluorescence increase corresponding to AF 488 peak, as shown in Figure 2.14(c). This sensor featured a glucose detection range extending from 0.15 to 100 mM, exhibiting the strongest dynamic signal change from 0.2 to 30 mM. It showed a reasonably fast response time of 4-5 min.⁹⁷ In order to use the affinity sensor *in vivo*, it is desirable to replace the visible range fluorescent dyes with NIR fluorophores to compensate for the high tissue scattering losses.

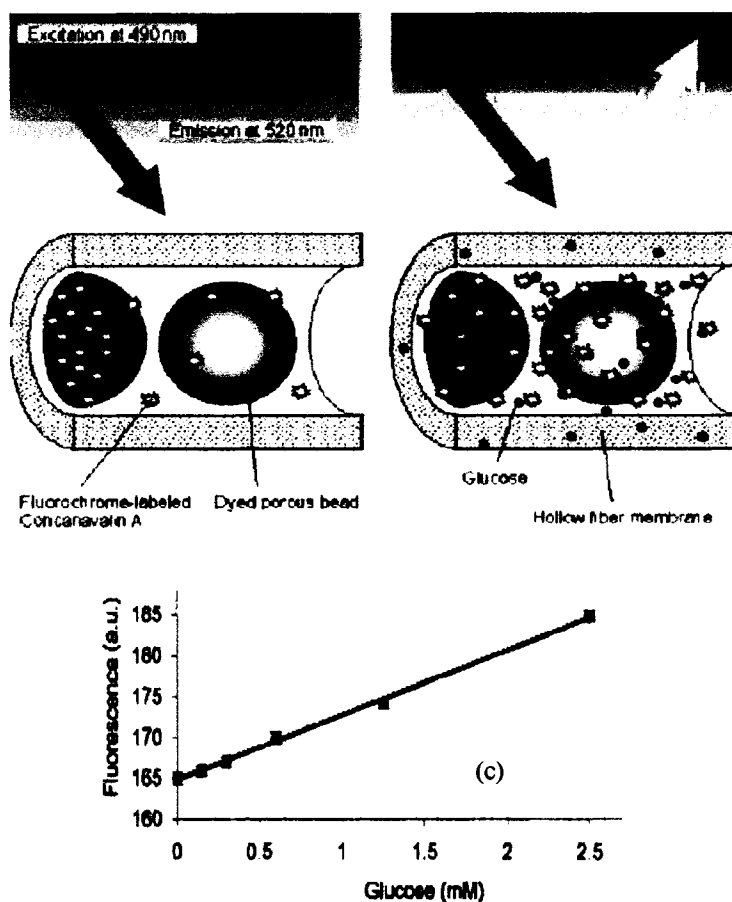


Figure 2.14. Fluorescence affinity glucose sensor, (a) In the absence of glucose, AF 488 labeled Con A is bound to fixed glucose residues inside porous beads, (b) In the presence of glucose, Con A is displaced from the beads and diffuses out of them, and (c) Changes in Fluorescent intensity of AF 488-Con A with the addition of glucose.⁹⁷

The above mentioned sephadex bead based affinity sensor system was further extended into the NIR region by conjugating Con A with AF647 dye.⁹⁸ From the long term performance studies conducted on this system, it was observed that the signal levels were dropping after 3-4 weeks, due to the leakage of Con A through the sealed membrane.⁹⁸ Thus, there are some issues to be resolved in this design.

Glucose sensor based on quenching mechanism. Ballerstadt et al., proposed another design for a glucose sensor operating in the NIR region. In this system, Con A and dextran were linked to NIR dyes, such as QSY21TM, Alexa Fluor[®] 647 (AF647), and

LD800, which were used as acceptor/quencher, donor and reference dyes, respectively.⁹⁹ QSY21 quenches AF647 when they are in close proximity, but it will not fluoresce, resulting in the non-ratiometric measurements. Therefore a glucose-insensitive dye (reference dye), LD800 was incorporated in the sensing system for correcting varying concentrations, instrumentation drifts, etc. The sensor system was fabricated by making a hollow fiber-based capsule using regenerated cellulose, which is comprised of three fibers filled with QSY21™ ConA-Sepharose and AF 647-dextran, and two fibers containing the reference dye LD800. The size of the completed sensor was estimated to be 2mm in diameter and 6mm in length. In the absence of glucose, AF-dextran and QSY-Con A are closely spaced, which results in low donor fluorescence due to acceptor quenching. However, the quenching is reversed by competitive displacement of dextran from Con A by glucose. It can be observed that the quenching is reduced with the addition of glucose, which is indicated as an increase in the AF647 peak normalized to the LD800 reference peak, as shown in Figure 2.15.⁹⁹ Thus, a glucose sensor operating in the NIR region is successfully demonstrated.

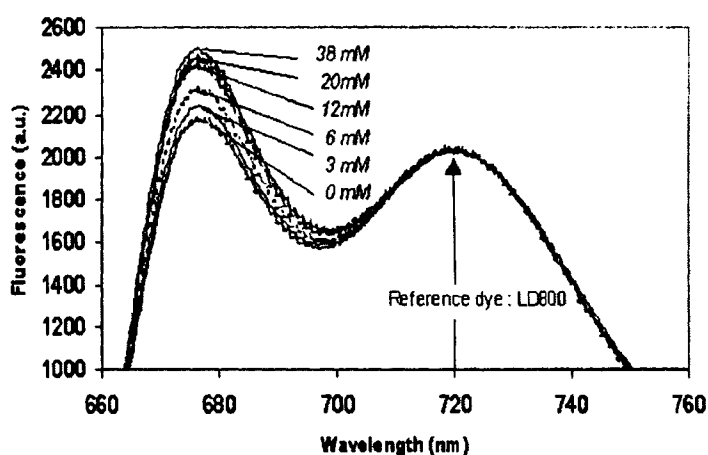


Figure 2.15. Fluorescence emission spectra from the fiber (comprised of QSY-Con A and AF 647 dextran) during its exposure to different glucose concentrations.⁹⁹

However, it is important to note that all of the above mentioned Con A/dextran based affinity sensing systems carry the disadvantages of Con A, such as toxicity, aggregation, and non-specific binding. Therefore, it is necessary to find a replacement for Con A. One such molecule, is apo-glucose oxidase (apo-GOx), which was previously used as a biosensor based on its ability to reconstitute into a holoenzyme with the addition of semi-artificial cofactors.^{20,21} In order to overcome the limitations of Con A, D'Auria et al., proposed the idea of using a deactivated enzyme, which retains the binding ability towards glucose without any catalytic activity and shows a decrease in intrinsic fluorescence upon binding to glucose, thus acting as a sensor by itself. The details of these sensors based on deactivated enzymes are given below.

2.3 Glucose sensors Based on Apo-Enzymes

2.3.1 Apo-Glucose Oxidase

Glucose oxidase (GOx) is an oxidoreductase enzyme, highly specific for β -D-glucose. GOx catalyzes the conversion of β -D-glucose and oxygen to D-glucono-1,5-lactone and hydrogen peroxide. GOx is a flavoprotein which is widely used for the estimation of glucose concentration in blood or urine samples and is based on the production of hydrogen peroxide in the reaction.³⁶ To overcome the problems associated with the consumption of glucose in GOx based sensors, such as production of by-products, instability, and irreversibility, a glucose sensor was proposed based on the intrinsic fluorescence changes in apo-GOx with the addition of glucose. Apo-GOx is produced by completely deactivating the native enzyme, GOx, by removing the FAD cofactor. The intrinsic fluorescence peak of apo-GOx at 340 nm is the characteristic of

partially shielded tryptophan residues. Although apo-GOx showed an 18% decrease in the fluorescence at 340 nm with the addition of 20 mM glucose, indicating retention of its ability to bind β -D-glucose, there is no indication of catalytic reaction.^{23,100,101}

The intrinsic fluorescence from proteins cannot be used for realistic clinical applications because of the huge background signal from the biological samples and the need for complex or bulky light sources. To overcome this problem, a visible dye (ANS) is linked to apo-GOx. ANS is known as a polarity-sensitive fluorophore, and displays an increasing quantum yield in low polarity environments. It was observed that the addition of apo-GOx to an ANS solution resulted in an approximate 30-fold increase in the ANS intensity, suggesting that it is exposed to a lower polarity environment. However, this effect was reversed, as apo-GOx showed a decrease in intensity upon glucose addition, indicating that ANS is being exposed to an increasing polar environment with glucose addition, as shown in Figure 2.16(a).²³

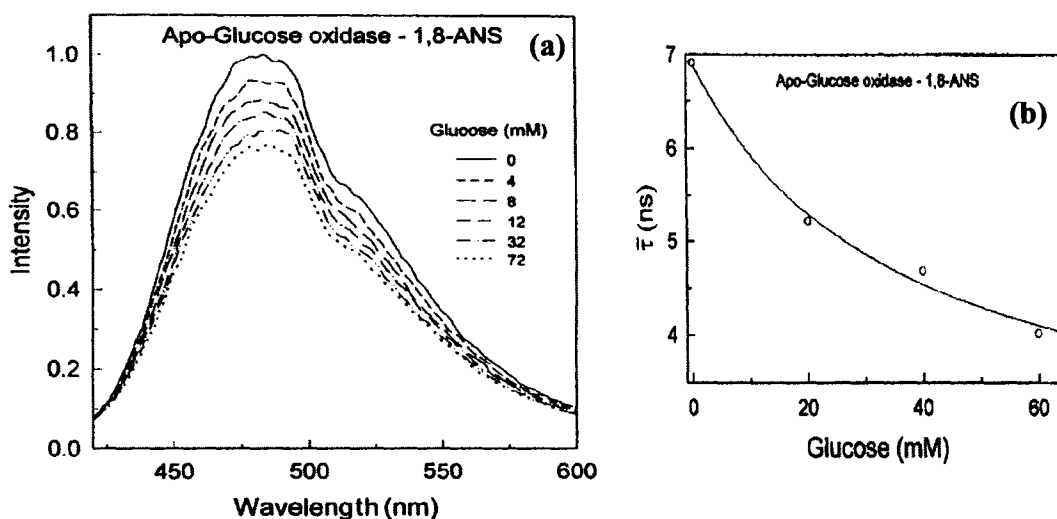


Figure 2.16. (a) Emission spectra, and (b) Average lifetime of apo-glucose oxidase-1,8-ANS in the presence of varying glucose concentrations.²³

Fluorescence lifetime studies of ANS-labeled apo-GOx showed that the addition of glucose shifts the frequency response to higher frequencies due to a decreased ANS lifetime. The shorter lifetime of ANS in the presence of glucose is consistent with the suggestion that glucose displaces the ANS in a more polar environment. There was over a 40% decrease in mean lifetime upon glucose addition, as shown in Figure 2.16(b).²³

The apo-GOx based glucose sensor described above showed positive results, but the binding ability of GOx can be easily hindered by its low stability to heat, pH changes, and organic solvents. To overcome these problems, enzymes isolated from thermophilic sources were used, which are very stable and active at higher temperatures. A sensor based on the enzyme from a thermophilic source is demonstrated below.

2.3.2 Apo-Glucose Dehydrogenase (apo-GD)

Glucose dehydrogenase (GD) from the thermoacidophilic archaeon *Thermoplasma acidophilum*, is used as the glucose binding protein in this sensing system. GD is a tetramer (160 kDa) composed of four similar subunits of about 40 kDa each. GD shows full activity at 55°C after 9 hrs and at 75°C the half-life is approximately 3 hrs. Also, the incubation of enzyme with 50% (v/v) methanol, acetone or ethanol for up to 6 hrs, at room temperature showed no appreciable loss of activity.¹⁰²

The transduction mechanism in apo-GD is similar to the above-demonstrated apo-GOx sensor.¹⁰³ As the thermophilic proteins show increased activity at higher temperatures and in the presence of non-polar solvents, all the experiments were conducted in the presence of 3% acetone. A drastic increase in ANS intensity values was observed with the addition of apo-GD. Also, with the addition of glucose, ANS showed a 25% decrease in the intensity values.¹⁰³ The lifetime studies showed modest changes.

Therefore, glucose induced changes were more carefully studied using polarization techniques, which indicated that the ANS-apo-GD system can sense glucose concentrations up to 20 mM with an accuracy of ± 2.5 mM (Figure 2.17).¹⁰³ The dissociation constant was observed to be 10 mM. In spite of its robustness, apo-GD based sensors respond better in the presence of acetone, which is not the ideal case for implantable glucose sensors.

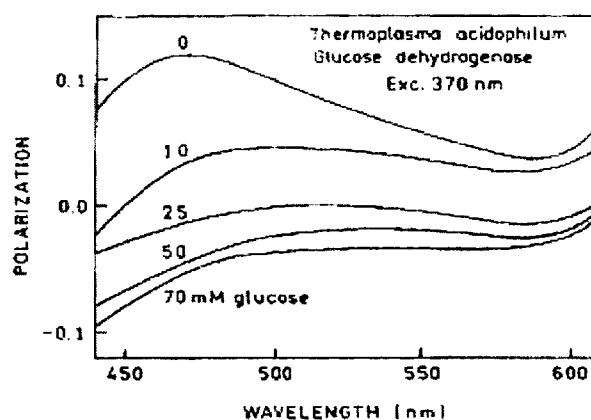
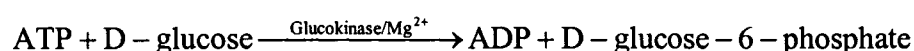


Figure 2.17. Polarization spectra of ANS-labeled GD in the presence of 3% acetone, and at different concentrations of glucose.¹⁰³

2.3.3 Glucokinase Based Sensor

As a further development to the above described sensing mechanisms, D' Auria et al., proposed a glucose sensor using glucokinase from the thermophilic microorganism *Bacillus stearotherophilus*.¹⁰⁴ This system has the advantages of CB and FRET mechanisms in addition to apo-enzyme based sensors (e.g. specificity, non-consuming). These enzymes catalyze the reaction shown below. However, in the absence of ATP, glucokinase will not consume any glucose, thus phosphorylation will not occur.



Using the idea of carrying on the above reaction in the absence of ATP, a glucose sensor based on CB and RET was proposed. The intrinsic fluorescence from glucokinase and *o*-Nitrophenyl- β -D-glucopyranoside (ONPG) were used as donor-receptor and acceptor-ligand molecules. It was observed that ONPG quenched the intrinsic fluorescence from tryptophan residues on glucokinase. This effect was reversed with the addition of glucose (Figure 2.18), as glucose has higher affinity towards glucokinase over ONPG. The changes in polarization with the addition of glucose to the above described glucokinase based sensor system were also reported.¹⁰⁴

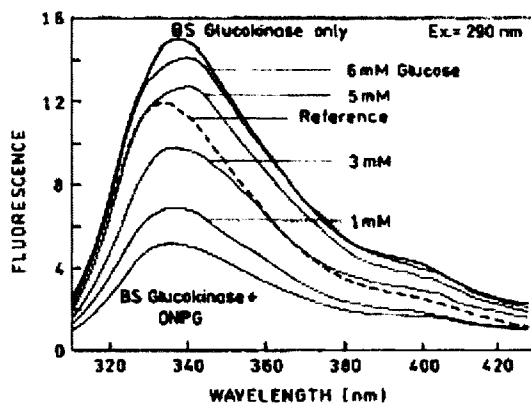


Figure 2.18. Effect of ONPG and glucose on the emission intensity of BSGK.¹⁰⁴

The wide variety of biosensing schemes that are demonstrated in the previous sections are highly-specific towards the analyte, but they are not attractive for practical purposes, e.g. noninvasive detection due to the lack of an intrinsic sensing mechanism. For example, a variety of well characterized glucose binding proteins (GBPs), do not show any change in optical signal with glucose binding which renders them unattractive for noninvasive monitoring. Many researchers are working towards the development of a transduction mechanism to monitor the binding events in GBPs. The next section will focus on the mechanism developed to monitor glucose levels using GBPs.

2.4 Glucose Binding Proteins

Hellinga et al., were the first to propose protein engineering techniques to develop a transduction mechanism to detect glucose using GBPs.^{105,106} An optical transduction mechanism was designed by incorporating environmental sensitive fluorophores into GBPs (Figure 2.19(a)). This technique involved the prediction of potential fluorescent allosteric signal transduction (FAST) sites in the periplasmic GBP of *Escherichia coli* (*E. coli*), and creation of single cysteine mutations at these FAST sites.

To observe the responses of different sites, acrylodan, and (((2-(iodoacetoxy)ethyl)methyl)amino)-7-nitrobenz-2-oxa-1,3-diazole (IANBD) were selected, based on their environmental sensitive behavior, as the indicator dyes to be covalently coupled to the L255 and H152 cysteine residues, respectively. The glucose sensitivity of GBPs coupled with acrylodan and IANBD, in Figure 2.19(b-c), shows that with the addition of glucose both samples are showing significant changes in fluorescence intensity.¹⁰⁵ This technique of introducing FAST sites into analyte-indicator proteins was further used by several groups to develop biosensors using proteins from *E. Coli*.

Based on this approach of introducing sensing elements into GBPs, a simple design for glucose sensing was proposed by Tolosa et al., based on a mutant glucose/galactose binding protein (GGBP) from *E. Coli* and phase modulation fluoremetry.⁹³ The glutamine 26 in GGBP (Figure 2.19(a)) was mutated to contain a single cysteine residue and was conjugated with a sulfhydryl-reactive probe 2-(4'-iodoacetamidoanilino)naphthalene-6-sulfonic acid (I-ANS). The labeled protein displayed a twofold decrease in intensity in response to glucose, with dissociation constant near 1 μ M glucose (Figure 2.20(a)), but displayed modest lifetime changes.

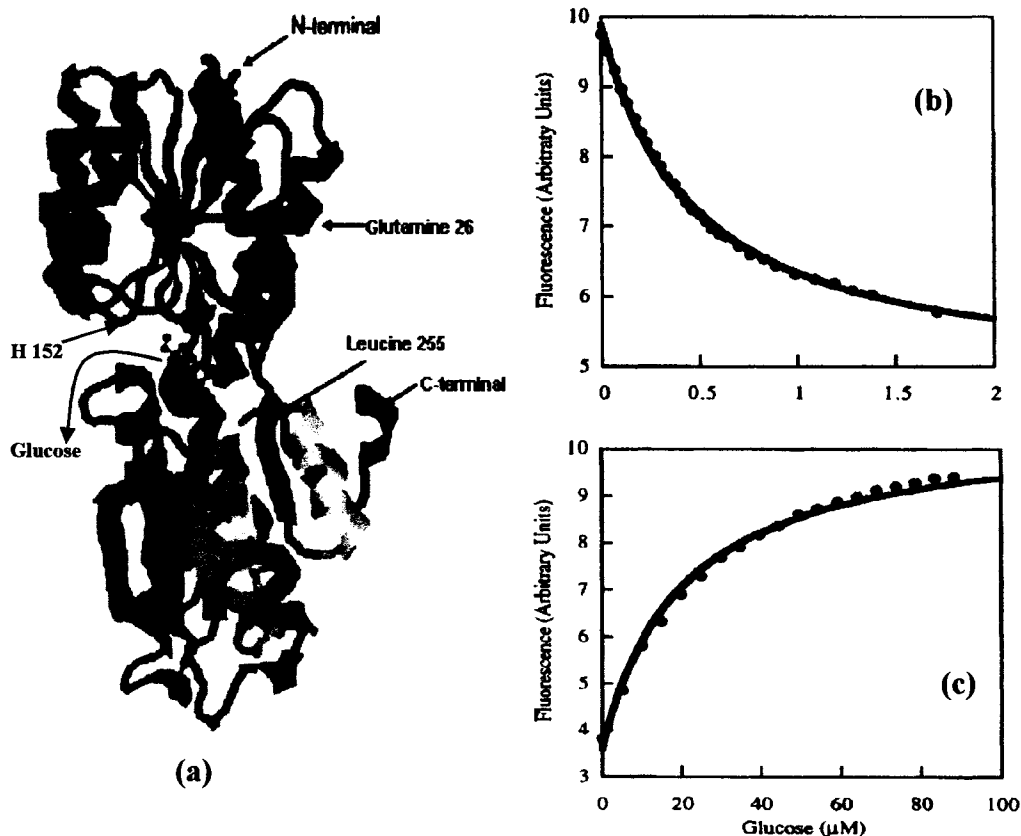


Figure 2.19. (a) Tertiary structure of GBP^{21,93}; Change in fluorescence intensity due to the binding of glucose to (b) L255C-acrylodan (c) and H152C-IANBD glucose binding protein conjugates.¹⁰⁵

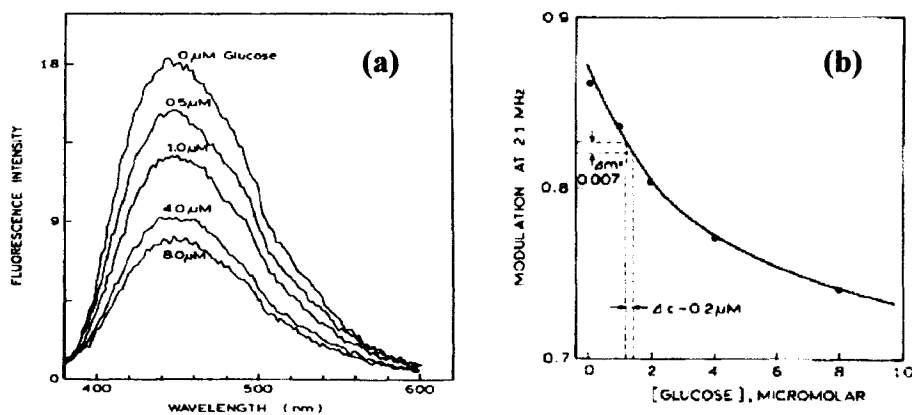


Figure 2.20. (a) Emission spectra of ANS-Q26 GGBP in the presence of glucose, (b) Modulation at 2.1MHz with the addition of glucose to ANS-Q26 GGBP.⁹³

In order to overcome this problem, a sensor was created by combining ANS-GGBP with Ru metal-ligand complex on the surface of the cuvette. With the addition of

glucose, there were significant changes in the relative intensity of the ANS26-GGBP and Ru complex resulting in a dramatic change in modulation at a low frequency of 2.1 MHz, as shown in Figure 2.20(b). Modulation measurements at 2.1 MHz were shown to accurately determine the glucose concentration.⁹³

Rao et al., further developed this sensor to overcome the problems associated with lifetime measurements. They used an *E. coli* GBP labeled with two fluorophores, acrylodan (environment-sensitive) and metal ligand complex of Ru at the cysteine (Leucine 255) mutation and N-terminal, respectively (Figure 2.19(a)). The acrylodan emission is quenched in the presence of glucose while the Ru emission remained constant, thereby serving as a reference, as shown in Figure 2.21(a). In addition to ratiometric measurements, the presence of the long-lived Ru metal-ligand complex allows for low-cost modulation-based sensing.²¹ It can be observed from Figure 2.21(b) that there is significant change in modulation with the addition of glucose.

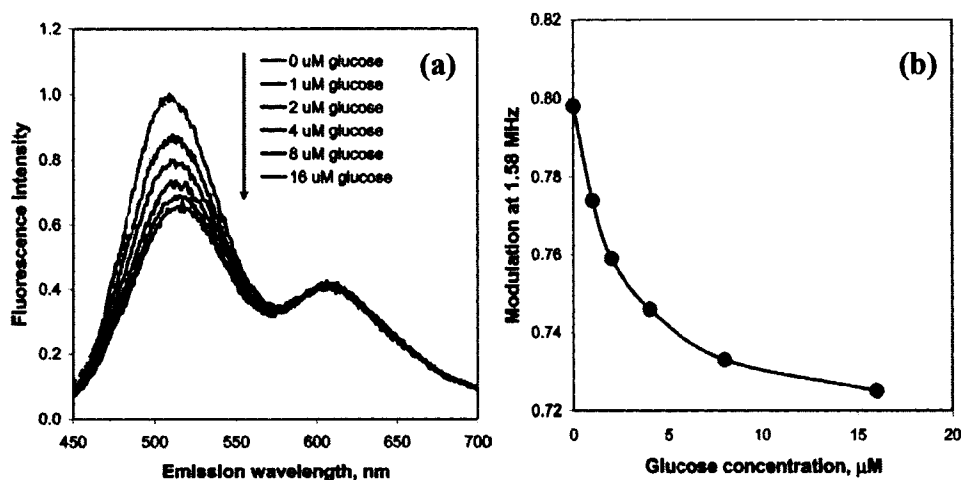


Figure 2.21. (a) Emission spectra, and (b) Modulation at 1.58Hz with the addition of glucose to Ru-GBP-Acrylodan.²¹

Schultz et al., proposed another variation of a biosensor based on a glucose indicator protein (GIP), which was created by conjugating two fluorescent reporter

proteins to each end of the *E. coli* GBP, as shown in Figure 2.22(a). In this method, the distance between the two fluorescent proteins changes with the addition of glucose (Figure 2.22(a)), which can be monitored by measuring the changes in FRET.¹⁰⁷ The GBP adopts an “open” form in the presence of the glucose, which triggers a conformational change, causing GFP and YFP to move apart from the center line of GBP leading to the change in FRET, as shown in Figure 2.22(a).

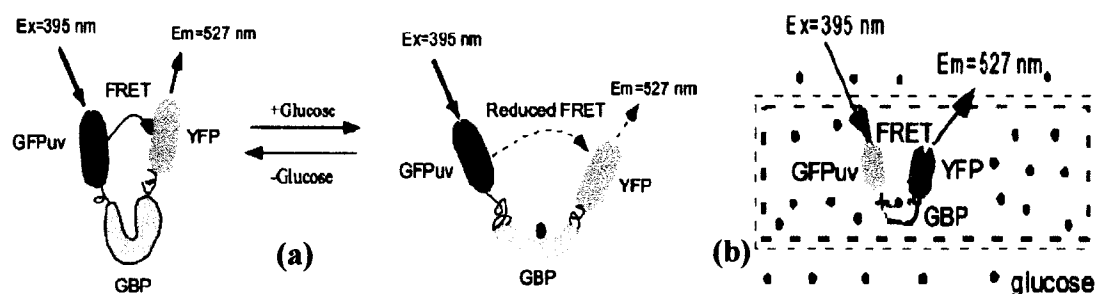


Figure 2.22. Design of a (a) glucose indicator protein for glucose sensing based on FRET between two green fluorescent proteins, (b) glucose sensor by incorporating Figure 2-15(a) in a hollow-fiber.¹⁰⁷

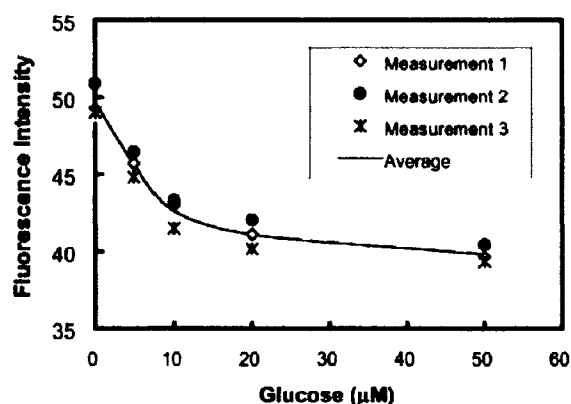


Figure 2.23. Fluorescence intensity (average of 3 measurements) at 527 nm (YFP emission) with increasing glucose concentration.¹⁰⁷

Green (GFP_{uv}) and yellow (YFP) fluorescent proteins were used as donor and acceptor molecules, respectively, in the FRET phenomenon. GIP is created by conjugating GFP_{uv} and YFP to C terminus and N terminus of GBP, respectively, as

shown in Figure 2.19. A glucose microsensor was fabricated as shown in Figure 2.22(b), by entrapping GIP into the hollow fiber which is accomplished by placing one end of a hollow fiber in a GIP solution and sealing the other end. When glucose binds to a GBP, there is change in the protein conformation, resulting in the increase in separation between GFP_{uv} and YFP and thus producing a reduction in FRET. This sensing system showed a response time within 100sec and an optional range of 10 μ M of glucose (Figure 2.23).¹⁰⁷ The main disadvantage of the GBP based glucose sensors is the low dissociation constant, because of which it cannot be used for glucose monitoring in diabetics.

2.5 Boronic Acid Based Sensors

Boronic acids (BAs) are known to have high affinity for carbohydrates, based on which several variations of glucose sensors have been reported by Lakowicz,¹⁰⁸⁻¹¹⁴ Shinkai,¹⁹ and Wang.¹¹⁵ BAs are weak Lewis acids, consisting of one boron (electron-deficient) atom and two hydroxyl groups. These acids have the tendency to form anionic borate by reacting with strong bases (OH⁻), with a pK_a of ~9. BAs coupled with esters to form BA diester groups show a pK_a of ~6.¹⁰⁹

In the last decade, BA containing fluorophores were used to monitor changes in sugar concentration by observing the changes in spectral properties of the fluorophores due to a charge transfer (CT) mechanism. CT occurs when there is high concentration of fluorophores containing BA and electron donor groups on the same fluorophore. For this mechanism, BA group (in the absence of sugar) acts as an electron withdrawing group, but, in the presence of sugar, BA takes on its anionic form as [-B(OH)(sugar)]⁻ and is no longer an electron withdrawing group. Hence, many fluorescent dyes with BA group can be used for glucose sensing by monitoring spectral (intensity, peak wavelength) shifts.¹⁰⁹

Lakowicz et al., proposed the idea of non-invasive glucose monitoring by using a contact lens as the substrate to dope these glucose-sensitive fluorophores containing BA groups.¹⁰⁹ 4'-Dimethylaminostilbene-4-boronic acid (DSTBA), 4'-cyanostilbene-4-boronic acid (CSTBA), 1-(p-boronophenyl)-4-(p-dimethyl-aminophenyl)buta-1,2-diene (DDPBBA), chalc1, and chalc 2 were used as the glucose sensitive BA containing fluorophores, among which the results corresponding to DSTBA and CSTBA are demonstrated below. Fluorescence spectra corresponding to DSTBA and CSTBA, with the addition of glucose, are shown in Figure 2.24(a-b). It can be observed in the case of DSTBA that there is a decrease in the intensity and a blue-shift in the peak wavelength with the increase in glucose concentration. Whereas in the case of CSTBA, there is also a decrease in intensity but with a red-shift in the peak wavelength.

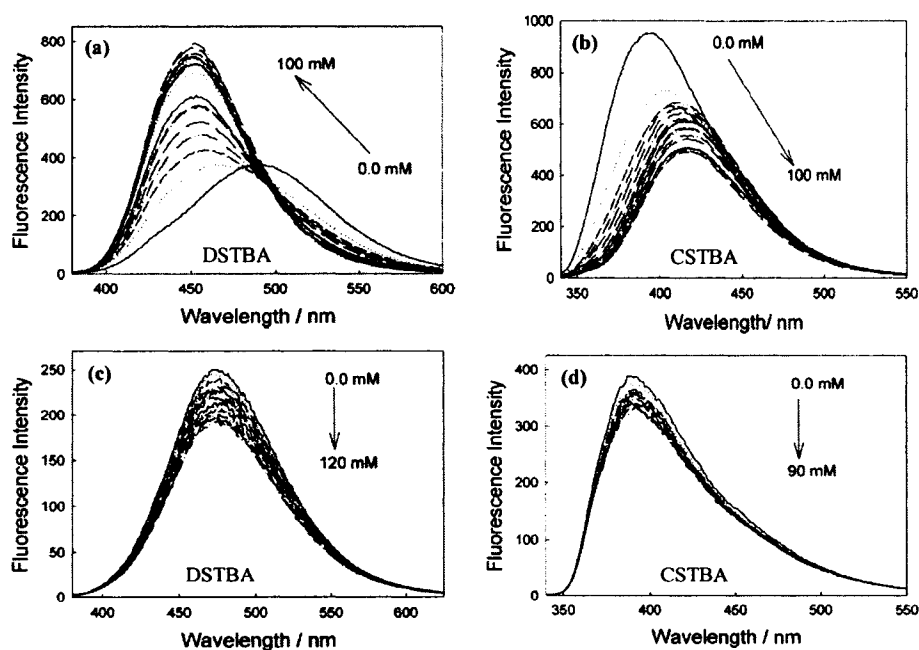


Figure 2.24. Change in fluorescence spectra of DSTBA and CSTBA in solution-phase (a,b) and when doped in contact lens (c,d).¹⁰⁹

The changes in fluorescence spectra of DSTBA and CSTBA doped contact lenses are monitored with the increase in glucose concentrations, as shown in Figure 2.24(c-d). By comparing solution phase and contact lens doped results, it can be observed that there is a significant decrease in the linear range and sensitivity. It is also noteworthy that these fluorophores showed more affinity towards fructose over glucose. Also, there is the significant effect of leaching, i.e. ~ 10 – 12 % of the fluorophore concentration is leached out in 45min.¹⁰⁹ Using similar principles, BA-fluorophores were designed to measure the tear glucose levels in hyperglycaemia patients.¹⁰⁸ A mono-BA based fluorescent sensor was designed using 3-nitronaphthalic anhydride and 3-aminophenylboronic acid. This novel saccharide probe exhibited dual emission, enabling ratiometric sensing, and displayed a remarkable sensitivity for glucose relative to fructose and galactose.¹¹¹ In spite of the successful demonstration of BA-based glucose sensors, there are unsolved problems due to the specificity^{109,110,115} and leaching that occurs overtime.

In conclusion, this chapter has provided a broad background of previously reported literature on glucose sensors. It was noted from these previous studies that many researchers have proposed the idea of developing an implantable fluorescence affinity glucose sensor, but there have been limited research articles (~5) where the idea has been demonstrated. These sensors were based on Con A, glucose binding proteins, and boronic acids, which have major disadvantages such as toxicity, low dissociation constant, and very low specificity, respectively. Also, all these systems lack an efficient encapsulation technique.

This dissertation work is focused on developing biosensors by encapsulating competitive binding based fluorescence sensing assay in microcontainers. The work is

novel based on the encapsulation of sensing assay into hollow containers where the assay molecules are free to move. This kind of free movement is restricted in previously demonstrated PEG hydrogel spheres. Due to the toxic nature of Con A, we proposed a novel idea of replacing Con A with apo-GOx, which has been previously used as a glucose sensor by itself. Using apo-GOx, the problems associated with Con A, such as toxicity, low specificity, and aggregation can be eliminated. Thus, this work on the incorporation of apo-GOx into a competitive binding assay and the encapsulation of sensing assay into hollow microcontainers is unique and is not being pursued anywhere else in the world. As described in the following chapters, it has been possible to demonstrate (a) the glucose sensitivity of apo-GOx/dextran complexes in solution phase, (b) the formation of several embodiments of hollow containers used for the encapsulation of sensing assay, and (c) the glucose sensitivity of microcontainers loaded with sensing assays from the visible to near-infrared operating region.

CHAPTER 3

THEORY

One of the most important and extensively explored fluorescence sensing techniques is fluorescence resonance energy transfer (FRET). FRET has been employed in spectroscopy and microscopy techniques for detecting and imaging various biomolecular interactions. Glucose sensors based on FRET in conjunction with the competitive binding process, are being continuously explored and are highly promising, as detailed in Chapter Two. This chapter discusses the theory behind glucose sensing mechanisms, such as FRET, and competitive binding processes. Modeling of the affinity sensors, which illustrates the influence of various parameters, e.g. receptor and ligand concentrations, dissociation constants, etc., on sensor response, is discussed in detail. These modeling results assist in estimating assay concentrations to obtain certain sensor parameters. Also, the effect of changing various parameters can assist in speculating the sensor response characteristics, thus helping in designing a customized sensing system.

3.1 Fluorescence Resonance Energy Transfer (FRET) Phenomenon

FRET is the non-radiative energy transfer of excited state energy from the excited state fluorophore (donor, D) to another (acceptor, A). FRET occurs when, (i) the fluorophores are in close proximity, (ii) the emission spectrum of donor overlaps with the

excitation spectrum of the acceptor (Figure 3.1), and (iii) the dipoles are properly oriented.¹¹⁶ This phenomenon is a non-radiative transition i.e., it does not occur via photon emission from excited-state-D and its re-absorption by A. When the donor fluorophore is excited at an appropriate wavelength, its electrons jump from the ground state (S_0) to higher vibrational level (S_1, S_2, S_3). Within picoseconds these electrons decay to the lowest of these vibrational levels (S_1) and then decay more slowly (nsec) to one of the S_0 states and a photon is emitted with wavelength longer than the exciting wavelength (Figure 3.2). FRET can be regarded as the interaction of transition dipoles of donor and acceptor groups; thus, the name fluorescence resonance energy transfer (FRET).^{117,118}

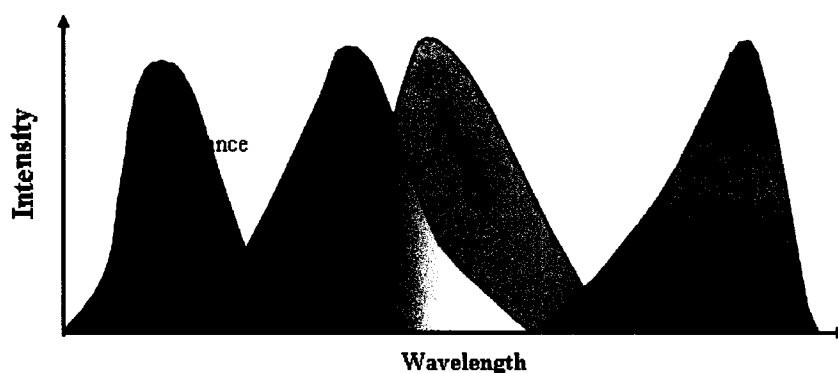


Figure 3.1. Fluorescence excitation and emission spectra of (a) donor and (b) acceptor molecules.¹¹⁹

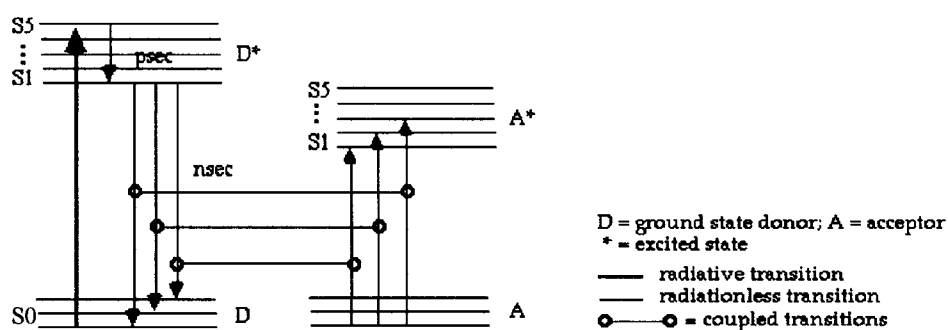


Figure 3.2. A simplified Jablonski diagram showing the coupled energy transfer transitions between the donor and acceptor molecules during the FRET process.¹¹⁷

3.1.1 FRET Theory

The FRET phenomenon is a very complex process.¹²⁰⁻¹²² A simplified theory of FRET that is sufficient to describe the affinity sensors of this work is described as follows. Assuming a single D–A pair is separated by a distance r , the rate of energy transfer, k_T , from a donor to acceptor molecule is given by:

$$k_T = \frac{1}{\tau_D} \left(\frac{R_0}{r} \right)^6 \quad (3.1)$$

where, τ_D is the fluorescence lifetime of the donor in the absence of the acceptor, and R_0 is the Förster distance, i.e, the distance at which half the donor molecules are quenched by the acceptor molecules. R_0 is proportional to several parameters, according to

$$R_0 = K \sqrt[6]{\kappa^2 n^{-4} \phi_D J[\lambda]} \quad (3.2)$$

In this Equation 3.2, K is a numerical constant, which depends on the units used. The term κ^2 refers to the relative spatial orientation of the dipoles of D and A. Based on the relative orientation of donor and acceptor, κ^2 value can range from 0 to 4. For collinear and parallel transitional dipoles $\kappa^2=4$, and for parallel dipoles $\kappa^2=1$. As the sixth root of κ^2 is considered in the Equation 3.2, the variation of κ^2 from 1 to 4 results in 26% error in r (in Equation 3.1) value. For the random orientation case (as is usually assumed, especially for solution phase measurements), κ^2 value is taken as 2/3. Though this value is debatable, it was previously reported that the uncertainty in intra-molecular distance as determined using FRET is only 10%¹¹⁸. The remaining terms, n , ϕ_D , and $J[\lambda]$ correspond to the solvent refractive index, quantum yield of D in the absence of A, and the overlap integral, which measures the degree of overlap between the emission spectrum of D and the absorption spectrum of A, respectively. A key point from this

discussion is that there must be significant spectral overlap for the dipoles to interact and for the proper excitation of A by D. Also, the energy transfer efficiency is directly proportional to the spectral overlap, and this also directly effects the Förster distance of a particular D-A pair. Figure 3.1 shows the D and A excitation and emission spectra in an ideal energy transfer system, wherein D and A have very distinct excitation spectra (so that A can only be excited by energy transfer, and not by direct photon absorption at the wavelengths used to excite D); the D emission and A excitation spectra overlap strongly; and the D and A emission maxima are well separated, so that the quenching of D fluorescence and the enhancement of A fluorescence can be individually measured.^{121,122}

In Practice, R_0 values vary significantly for different D-A FRET pairs, ranging from 40-80 Å. This distance must be comparable to the size of the proteins or other biomacromolecules being used for efficient energy transfer from D to A. The energy transfer (E) is given as the fraction of photons absorbed by D that are transferred to A and, therefore, is given as the ratio of transfer rate to the total decay rate of the donor,

$$E = \frac{k_T}{\tau_D^{-1} + k_T} \quad (3.3)$$

From Equations 3.1 and 3.3, we have, $E = \frac{R_0^6}{R_0^6 + r^6}$ (3.4)

It should be clear from the above Equation 3.4 that when D and A are separated by Förster distance (R_0), the FRET is 50% efficient. However, another noticeable property is that the FRET efficiency is highly dependent on the distance between D and A molecules, which is shown graphically in Figure 3.3. The notable feature is that FRET efficiency decreases rapidly when the distance between D and A molecules is greater

than the Förster distance, because FRET is inversely proportional to the sixth power of the distance between D and A molecules (Equation 3.4).

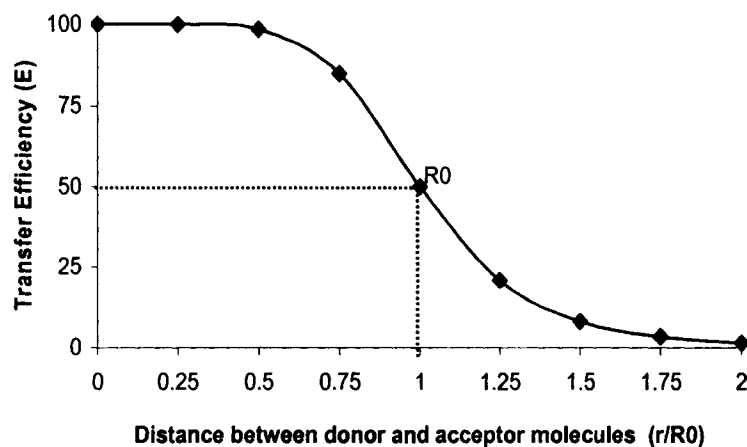


Figure 3.3. Effect of the distance between donor and acceptor molecules (r) on the energy transfer efficiency (E); where R_0 is the Förster distance.

Energy transfer efficiency (E) is generally measured using relative fluorescence intensity of the donor in the absence (F_D) and in the presence of acceptor (F_{DA}), as given in Equation 3.5. Fluorescence lifetimes are also used under similar conditions to estimate E value. The relationships are given as,

$$E = 1 - \frac{F_{DA}}{F_D} \quad \text{and} \quad E = 1 - \frac{\tau_{DA}}{\tau_D} \quad (3.5)$$

These mathematical representations highlight the main advantages of using FRET as a transduction mechanism; it is highly sensitive to the distance between two molecules, and the ratiometric nature allows variations in instrumental parameters, assay component concentrations, and measurement configuration to be internally compensated.¹²³ In recent years, FRET has been applied in various fields of biochemistry, such as single molecule FRET for detecting conformational changes and molecular interactions,¹²⁴ distance measurements in α -helical melittin,¹²⁵ protein folding measurements,¹²⁶ orientation of the

protein bound peptide,¹²⁷ nanoscale biosensors using organic,²² and quantum dot^{128,129} FRET donors, etc.

In this project, FRET is used as a transduction mechanism in a glucose sensing system, which is based on the competitive binding process. In particular, FRET is used as a readout technique for translating the changes in the distance between D and A molecules in the absence/presence of glucose. The following sections will demonstrate the theory behind a glucose sensing system, which is based on the combination of competitive binding and FRET techniques.

3.2 Competitive Binding Process

The competitive binding process, depicted in Figure 3.4, involves three components, (i) receptor/substrate (Con A), (ii) competing ligand/analyte-analog (dextran), and (iii) analyte (glucose). When a receptor is exposed to a ligand, they will be in close proximity because of the binding affinity (Figure 3(a)). However, in the presence of glucose the receptor/ligand complexes will be dissociated (Figure 3.4(b)), as the receptor has greater affinity toward the target-analyte over ligand. This process generates relatively more free ligand and receptor/glucose complexes. Generally, free ligand concentration (or the average distance between receptor/ligand) is monitored to estimate glucose concentrations.

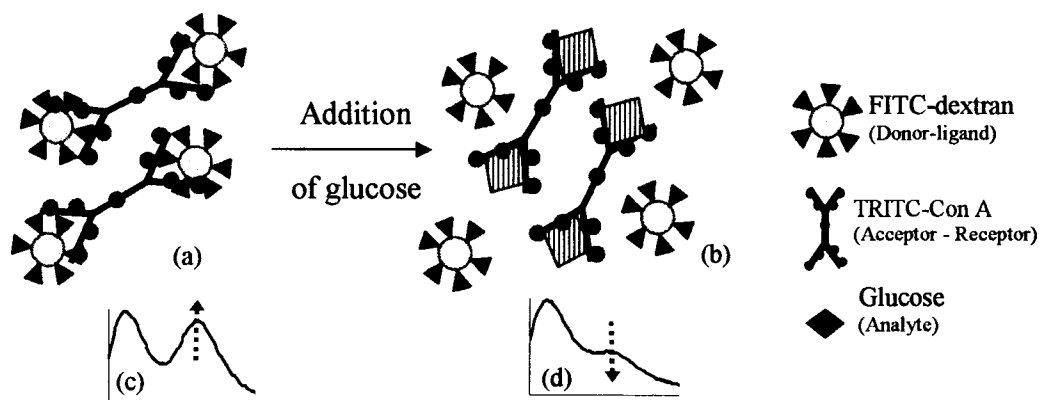


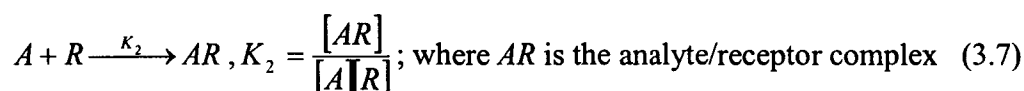
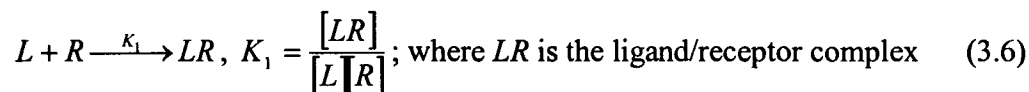
Figure 3.4. Schematic representation of the combination of FRET and competitive binding techniques: (a) FITC-dextran/TRITC-Con A complexes, and (b) displacement of dextran from Con A in the presence of glucose; (c) strong donor and acceptor peaks (d) strong donor peak relative to acceptor peak in the presence of glucose.

3.2.1 Competitive Binding Theory

Theoretical models for the above described sensing system were developed to hypothesize the effects of different parameters.¹³⁰⁻¹³⁵ Different heterogeneous models were generated for two different cases, (a) immobilized receptor,^{130,133} and (b) immobilized ligand.¹³¹ The theoretical modeling of the receptor-immobilized competitive binding system is given below. The only difference in this model compared to the above described competitive binding mechanism is that the receptor is immobilized on the solid gel. However, this is of little consequence when taking the assumptions of this model into consideration. The assumptions in this system are: (1) the single binding site on receptor molecules is available even after the immobilization process, (2) both the ligand and analyte are competing for the same binding site on a receptor molecule, (3) only monovalent interactions occur between receptor and ligand, and (4) equilibrium exists at all times. As mentioned above, with the addition of more analyte there is an increase in the free ligand concentration in the solution. Thus, the free ligand concentration can be measured independent of the analyte concentration. A calibration curve can be obtained

for this sensor system by plotting bulk free ligand concentration with respect to the increasing analyte concentration.^{130,133}

The competitive binding reactions between the analyte (A), immobilized receptor (R), and ligand (L), and the corresponding association constants (K_1 & K_2) are given as,



In the current model design, all the sensing elements are conserved within the transducer, as given below,

$$[R_t] = [R] + [LR] + [AR] \quad (3.8)$$

$$[L_t] = [L] + [LR] \quad (3.9)$$

$$[A_t] = [A] + [AR] \quad (3.10)$$

where R , L , and A represent the concentrations of free acceptor-labeled receptor, donor-labeled ligand, and analyte, respectively, and subscript 't' denotes total concentrations.

The free receptor concentration $[R]$, which is not bound to either ligand or analyte, can be written in terms of dissociation constant, and total and free (unbound) ligand concentrations as given below.

$$\text{From Equations 3.6 and 3.9, we have, } [R] = \frac{[L_t] - [L]}{[L]K_1} \quad (3.11)$$

The analyte/receptor complex concentration $[AR]$ can be written in terms of dissociation constant and free analyte and receptor concentrations as given below,

$$\text{From Equation 3.7, we have } [AR] = [A][R]K_2 \quad (3.12)$$

From Equation 3.9 and 3.8, we have

$$1 = \frac{[L]}{[L_t]} + \frac{[R_t] - [R] - [AR]}{[L_t]} \quad (3.13)$$

Substituting Equation 3.12 into Equation 3.13, we have

$$\frac{[L]}{[L_t]} + \frac{[R_t]}{[L_t]} - \frac{1}{[L_t]} ([R] + [A][R]K_2) = 1 \quad (3.14)$$

This can be reduced as shown below,

$$\frac{[L]}{[L_t]} + \frac{[R_t]}{[L_t]} - \frac{[R]}{[L_t]} (1 + [A]K_2) = 1 \quad (3.15)$$

Substituting Equation 3.11 into Equation 3.15 and reducing the equation, we obtain

Equation 3.18,

$$\frac{[L]}{[L_t]} + \frac{[R_t]}{[L_t]} - \frac{[L_t] - [L]}{[L][L_t]K_1} (1 + [A]K_2) = 1 \quad (3.16)$$

$$\frac{[L]}{[L_t]} - 1 + \frac{[R_t]}{[L_t]} - \frac{[L_t] - [L]}{[L][L_t]K_1} - \frac{[L_t] - [L]}{[L][L_t]K_1} [A]K_2 = 0 \quad (3.17)$$

$$\frac{[L]}{[L_t]} - 1 + \frac{R_t}{[L_t]} - \frac{1}{[L]K_1} + \frac{1}{K_1[L_t]} - \frac{[A]K_2}{[L]K_1} + \frac{[A]K_2}{[L_t]K_1} = 0 \quad (3.18)$$

Multiplying the above Equation 3.18 by $[L]/[L_t]$, we obtain a dimensionless equation,

$$\left(\frac{[L]}{[L_t]} \right)^2 - \frac{[L]}{[L_t]} + \frac{[L]}{[L_t]} \frac{[R_t]}{[L_t]} - \frac{1}{[L_t]K_1} + \frac{[L]}{[L_t]} \frac{1}{K_1[L_t]} - \frac{[A]K_2}{[L_t]K_1} + \frac{[L]}{[L_t]} \frac{[A]K_2}{[L_t]K_1} = 0 \quad (3.19)$$

By further simplification, we obtain the below equation,

$$\left(\frac{[L]}{[L_t]} \right)^2 + \frac{[L]}{[L_t]} \left(\frac{[R_t]}{[L_t]} - 1 \right) + \frac{[L]}{[L_t]} \left(\frac{1}{K_1[L_t]} + \frac{[A]K_2}{[L_t]K_1} \right) - \frac{1}{[L_t]K_1} ([A]K_2 + 1) = 0 \quad (3.20)$$

The above equation can be simplified further,

$$\left(\frac{[L]}{[L_t]} \right)^2 + \frac{[L]}{[L_t]} \left[\left(\frac{R_t}{[L_t]} - 1 \right) + \frac{[A]K_2 + 1}{[L_t]K_1} \right] - \frac{[A]K_2 + 1}{[L_t]K_1} = 0 \quad (3.21)$$

$([L]/[L_t])$ and $([A]K_2+1)/([L_t]K_1)$ give the ratio of free to total ligand and dimensionless analyte concentration, respectively. A plot of Equation 3.21, which gives the relationship between dimensionless analyte and fraction of free ligand, is shown in Figure 3.5. It can be observed that the fraction of free ligand is dependent on the analyte concentration, and also on the ratio of total ligand/receptor concentration. For example, if the required dimensionless analyte concentration range is from 0 to 40, then the total ligand/receptor ratio must be maintained in the range of 0.01-0.1 to obtain good sensitivity across the range of interest. This information, which is critical in tailoring the sensor parameters according to specified applications, is used in optimizing sensor response characteristics, such as sensitivity, detection range, etc.

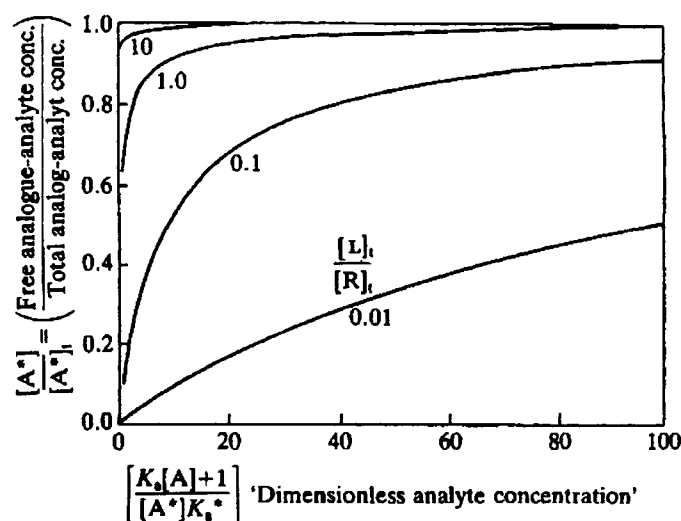


Figure 3.5. Effect of dimensionless analyte concentration and the total ligand/receptor (L_t/R_t) ratio on the response of competitive binding based assay.¹³⁴

Effect of total assay concentration

From the above discussion, it is obvious that the ratio of ligand to receptor has a significant effect on the sensor response. Apart from this, the total assay concentration may also have a considerable effect on the sensitivity, though this point was not

previously appreciated. In order to study this variation in total assay concentration, while maintaining the constant ligand to receptor ratio, we have simplified Equation 3.21 to

$$y^2 + y[c - 1 + A_d] - A_d = 0 \quad (3.22)$$

where relative sensor response = $y = (L/L_t)$, constant = $c = (R_t/L_t)$, and dimensionless analyte concentration = $[A_d] = ((K_{a1}[A] + 1)/(L_t K_{a2}))$.

The effect of total assay concentration on sensor response was tested by plotting sensor response versus dimensionless analyte concentration at different total ligand and receptor concentrations. The results are given in Table 3.1. It is important to note that the ratio between ligand/receptor is maintained constant in all cases. It can be observed that, for each case, a quadratic equation is derived (Table 3.1) and the corresponding plots are shown in Figure 3.6. From these results, the concentrations of the assay elements needed for any application can be estimated based on the required detection range.

Table 3.1. Parameters used to study the effect of total assay concentration on sensor response.

Receptor, R_t	Ligand, L_t	Constants	Equation
1* R_t	1* L_t	$c=10; A_d=20$	$y^2 + y[29] - 20 = 0$
2* R_t	2* L_t	$c=10; A_d=20$	$y^2 + y[76] - 40 = 0$
10* R_t	10* L_t	$c=10; A_d=20$	$y^2 + y[1100] - 200 = 0$
29* R_t	29* L_t	$c=10; A_d=20$	$y^2 + y[8149] - 580 = 0$
100* R_t	100* L_t	$c=10; A_d=20$	$y^2 + y[92000] - 2000 = 0$

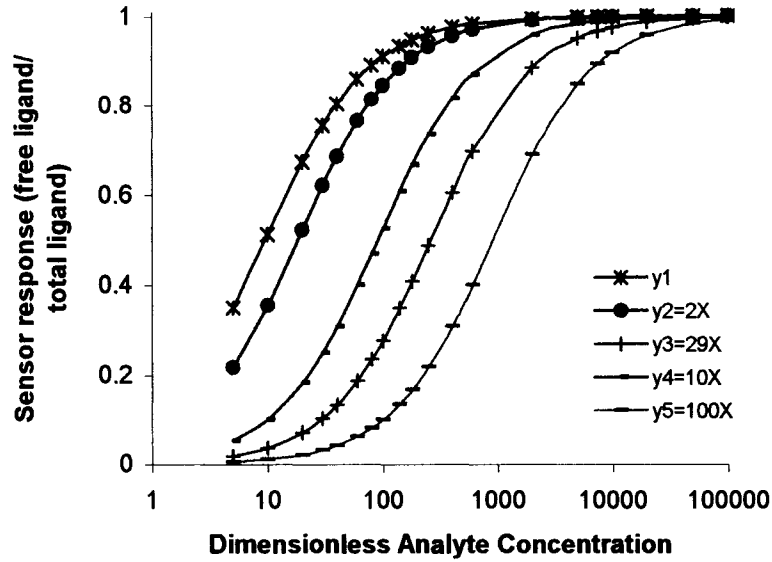


Figure 3.6. Effect of the total assay concentration on sensor response.

Hsu et al., further extended this work on theoretical modeling of affinity sensors, to study the effect of various parameters on the sensor response, such as ligand and receptor concentrations, variation in the ratio between ligand/receptor, type of receptor, etc. In this system, the receptor is assumed to be immobilized in a resin with volume V_r . They derived a cubic equation (Equation 3.23) instead of quadratic, for analyzing the sensor response due to the variations in several parameters.

$$Y^3 + Y^2(1/a + 1/ab - 1 - (1+X)/(1-c)) + Y\{(X+1-1/a-1/ab)/(1-c) - 1/ab\} + 1/ab(1-c) = 0 \quad (3.23)$$

where, $Y = \frac{[L]}{[L_t]}$, $X = \frac{[A_t]}{[L_t]}$, $a = \frac{[L_t]}{r[R_t]}$, $b = \frac{r[R_t]}{K_1}$, $c = \frac{K_2}{K_1}$, $K_1 = \frac{[L][R]}{[LR]}$, $K_2 = \frac{[A][R]}{[AR]}$,

and $r = \frac{V_r}{V_t}$ where V_t is the total volume (resin + buffer).

The above Equation 3.23 is derived similar to the quadratic equation (Equation 3.21), using Equations 3.6 to 3.13, and writing A in terms of A_0 , K_2 , and R , which can be

obtained from Equations 3.7 and 3.10. The variable signal that is being measured in this system is the concentration of ligand in the bulk solution ($[L]$). Using the above cubic Equation 3.23, the dimensionless signal, defined as $Y (L/L_i)$ can be obtained as a function of varying analyte concentration $X (A_i/L_i)$, for any given values of a , b , and c .

Equation 3.23 was used to build calibration curves (Figure 3.7) for the proposed affinity sensing system. The asymptotic minimum values of the signals represent the initial condition, where, in the absence of the analyte, the equilibrium concentration of the ligand produces the background. However, with the addition of analyte, ligand is displaced from the receptor and thus, the ligand concentration in the bulk increases with the increase in analyte concentration, which can be observed in Figure 3.7. Eventually, the dimensionless signal (or ligand in the bulk) reaches saturation indicating the displacement of all the ligand molecules with the addition of analyte. All the graphs shown in Figure 3.7 are produced using the cubic Equation 3.23, thus they are influenced by the three parameters, a , b , and c . The effect of these individual parameters on sensor response was studied by varying one parameter at a time and holding the other two parameters constant.

The effect of changing parameters a , b , and c (Equation 3.23) one at a time, while holding the other two parameters constant, is shown in Figure 3.7. In practice, parameters a , b , and c , can be tailored by changing the initial concentration of the loaded ligand (L_i), the amount of the immobilized receptor or by choosing the receptor with different binding affinity (K_d), and by choosing a receptor, which has different (more or less) affinity towards ligand compared to analyte, respectively. In this system, sensitivity is considered as the change in the dimensionless signal resulting from changes in analyte

concentration. Detection range is the range of analyte concentration in which there will be a significant change in the dimensionless signal with an increase in analyte concentration.

It can be observed from Figure 3.7(a) that the background signal generated was observed to increase with a , but the sensitivity and detection range were correspondingly decreasing. Also, the calibration curve is shifting to the right ($a < 1.0$), which indicates that the sensor is suitable for detecting high analyte concentrations. Also, when $a > 10$, there is a significant drop in sensitivity and detection range rendering the system unsuitable for practical cases. It is obvious from these results that a compromise must be made between the signal strength and the sensitivity of the sensor when choosing the initial concentration of the ligand.¹³⁰ It is noteworthy that the results obtained in this section (Figure 3.7(a)), match with the results obtained by the Schultz group using a quadratic equation (Figure 3.5). In both the cases, it is shown that with the increase in ligand concentration (i.e., increase in ligand/receptor ratio), there is an increase in background signal and a drop in sensitivity and detection range values.

It can be observed from Figure 3.7(b) that the effect of parameter b on the sensor response is contrary to the effect of parameter a . The increase in b results in lower signal, but increased sensitivity and detection range.¹³⁰ Again, the compromise must be made between the signal strength, detection range, and the sensitivity of the sensor when choosing the concentration of the receptor.¹³⁰

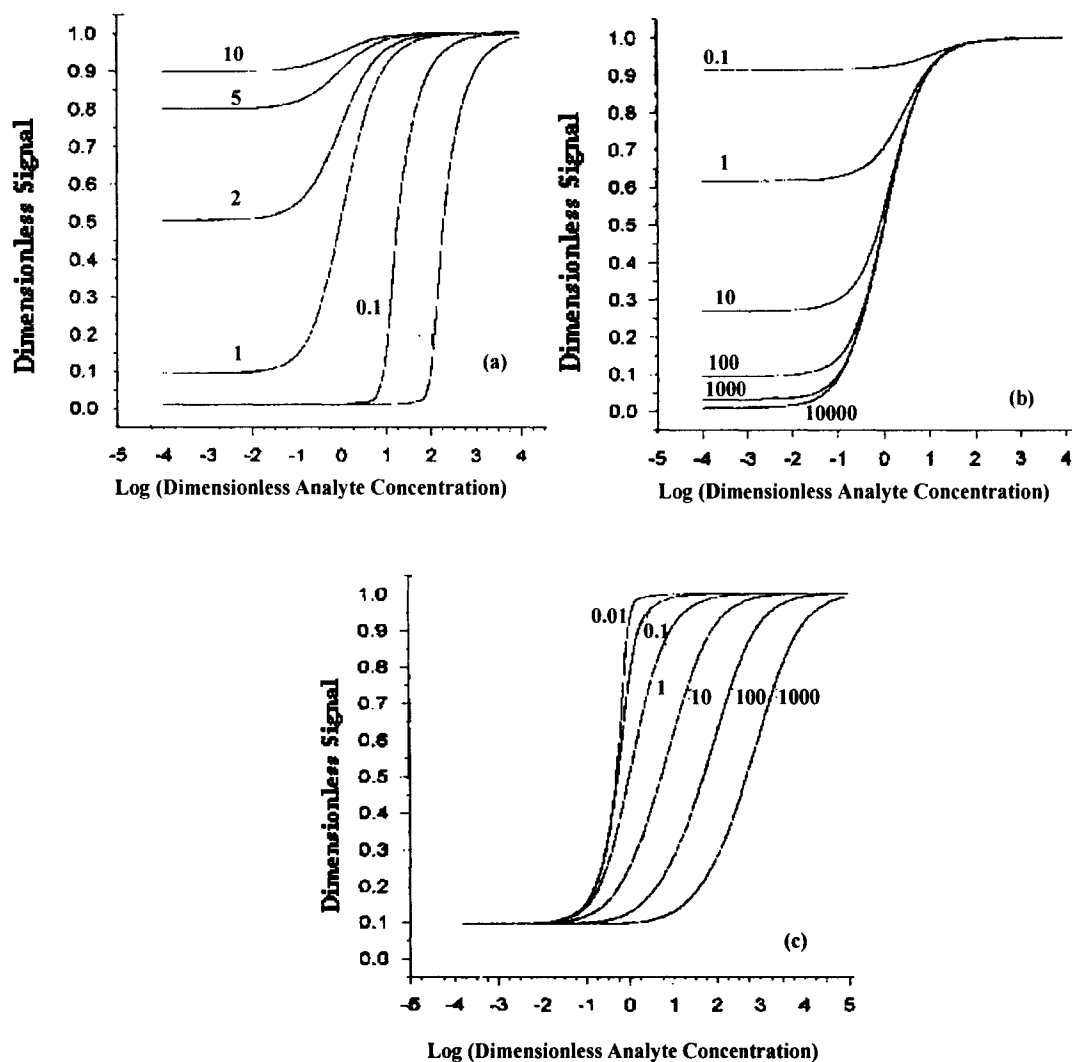


Figure 3.7. Effect of (a) parameter a , with constant $b=100$ and $c=1.01$; (b) parameter b , with constant $a=1$ and $c=1.01$; (c) parameter c , with constant $a=1$ and $b=100$; on the calibration curves obtained from the theoretical model (Equation 3.19). Values of the variable parameters are given in the corresponding graph.¹³⁰

Unlike the previous two cases, the asymptotic minimum signal value is independent of the parameter c , which can be observed in Figure 3.7(c). It can be observed that sensors designed with a lower c value will be useful for detecting lower analyte concentrations. In order to increase the range to a higher level, it is highly desirable to increase the value of c by choosing a different receptor.¹³⁰ Also, the results obtained in this section (Figure 3.7(c)) appear to be similar to the results shown in Figure 3.6 (obtained using quadratic Equation 3.22), even though the variables in both cases are

not identical. The response curves in Figure 3.7(c) were obtained by varying the parameter c (or choosing a different receptor), whereas the response curves in Figure 3.6 were obtained by varying the total assay concentrations. Thus, the detection range of the sensor can be controlled by varying two different parameters, total assay concentrations and choosing different receptor protein.

Thus, these theoretical models for competitive binding based sensing systems are essential for choosing the initial assay element concentrations and are also very helpful during the optimization of the sensor response characteristics.

3.3 Combination of FRET and Competitive Binding Techniques

In order to combine the FRET and competitive binding (CB) techniques, ligand and receptor were labeled with donor and acceptor fluorophores (FRET pair), respectively. This process is demonstrated in Figure 3.4. In the absence of analyte, ligand and receptor will be in close proximity (Figure 3.4(a)), which results in significant energy transfer from donor to acceptor, and is indicated by the strong emission peaks corresponding to donor and acceptor molecules (Figure 3.4(c)). With the addition of analyte, ligand is displaced from the receptor increasing the distance between two fluorophores (Figure 3.4(b)), and eventually reducing the energy transfer from donor to acceptor; this is indicated by a strong donor peak relative to acceptor (Figure 3.4(d)). The combination of competitive binding and FRET techniques is very attractive as it can retain the advantages of both techniques, such as the non-consumption of analyte, absence of reaction by-products, and the ratiometric nature of the FRET analysis.

3.3.1 Theory-Combination of FRET and CB Techniques

The information obtained in section 3.2 regarding the change in the fraction of free ligand concentration with the increase in analyte concentration can be converted into the relative amount of fluorescence that is being transferred from donor to acceptor molecules, by using FRET efficiency values.¹³³ The relation between the relative fluorescence and the ratio of free to total ligand concentration is given as,

$$\text{Relative Fluorescence} = \left[1 - \left(1 - \frac{[L]}{[L_t]} \times \text{efficiency} \right) \right] \quad (3.24)$$

The combined results of competitive binding and FRET are shown in Figure 3.8. It can be observed that at constant ligand/receptor ratio, FRET efficiency has significant effect on the sensor response characteristics. In Figure 3.8, the sensitivity curves are shown for two different ligand/receptor ratios. It can be observed that with the increase in FRET efficiency, there is increase in linear response. The main parameters influencing FRET efficiency, other the necessary conditions (such as, overlap integral, distance between the fluorophores, etc.), are the labeling ratios of acceptor and donor molecules. Thus, the fluorophore conjugation can have significant effect on the sensor response characteristics.

These modeling results emphasize the importance of each parameter in achieving the desired sensor parameters, mainly sensitivity and detection range. It helps in deciding the labeling ratio of the donor and acceptor molecules and sensing assay concentrations, in order to obtain the required sensor response characteristics. Thus, these theoretical models for competitive binding and FRET based sensing systems are very helpful in hypothesizing and optimizing the sensor response characteristics.

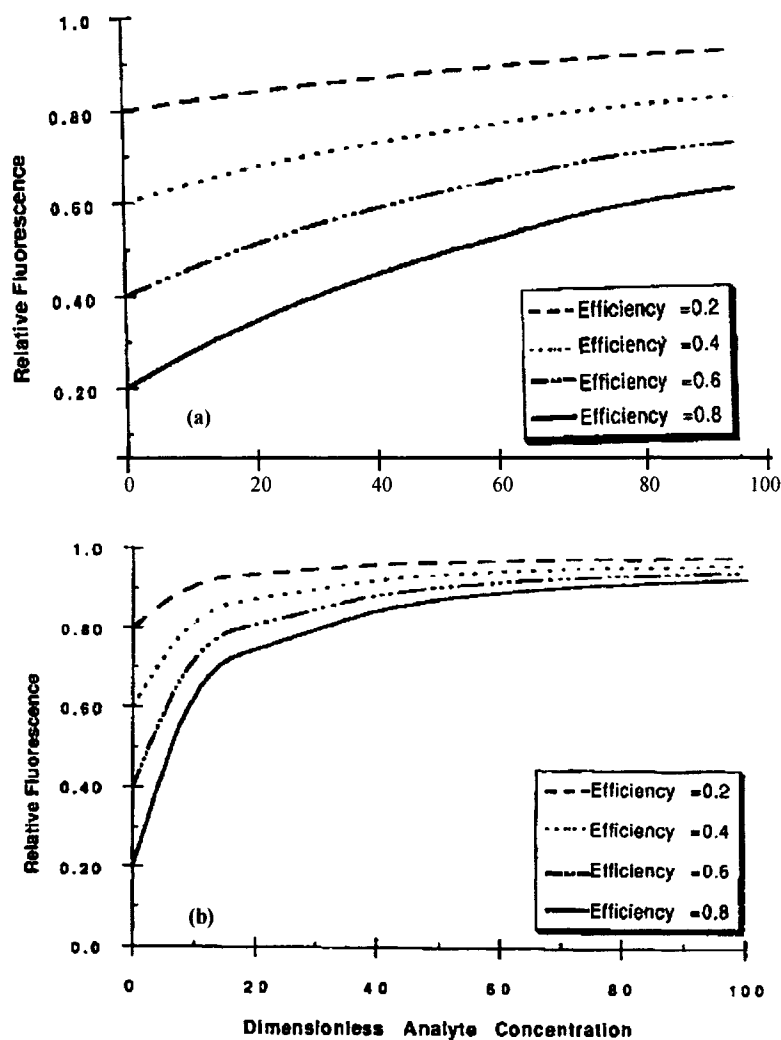


Figure 3.8. Effect of dimensionless analyte concentration and FRET efficiency on the relative fluorescence when the total ligand/receptor ratio is (a) 0.01, and (b) 0.1.¹³³

In conclusion, this chapter discussed the theoretical modeling involved in energy transfer based competitive binding based sensing systems and has highlighted the significance of the individual and total assay concentrations and binding affinities in determining the sensitivity and detection range of the sensors. Chapters four to seven will discuss experimental work for several variations of the energy transfer based competitive binding sensors which involves the demonstration of the design, fabrication, and characterization of microcapsule based sensors.

CHAPTER 4

LECTIN/SACCHARIDE BASED

GLUCOSE SENSOR

Since 1988, several variations of Concanavalin A (Con A)-based fluorescence resonance energy transfer (FRET) glucose sensors have been reported in the literature. However, most of the reports demonstrated Con A-based glucose sensitivity in solution phase, which will not achieve the final goal of an implantable glucose sensor, because the sensing assay chemistry is not enclosed in any microcontainer. Schultz et al., proposed several variations of Con A/dextran based fiber-optic glucose sensors. However, the length and diameter of a completed sensor are ~ 6cm and ~0.4mm, respectively, making them inappropriate for transdermal monitoring. After a decade of investigation into this transduction mechanism, in 1999, Russell et al., proposed a sensing design close to the clinical application, which involves the encapsulation of sensing assay in hydrogel microspheres.²⁷ There was also another report in 2003 by the Schultz group based on the changes in fluorescence intensity due to the exposure of Con A loaded sephadex beads to glucose.⁹⁷ Nevertheless, even this system requires microdialysis tubing. Other than the above-mentioned sensing mechanisms with the potential for achieving transdermal sensing, there were no previous reports on Con A-based implantable sensors.

This chapter demonstrates a Con A-based FRET glucose sensing assay encapsulated in true microscale capsules. This work expands on previous work by elaborating on the precise assembly of Con A/dextran multilayers on planar substrates to microcapsules,⁷² and packaging of these dynamic nanoassemblies within permeable polymeric capsules. This study was completed to characterize the self-assembly properties and, in particular, the glucose sensitivity of self-assembled Con A/dextran multilayer films. Furthermore, the glucose sensitivity of the tetramethylrhodamine isothiocyanate (TRITC)-Con A and fluorescein isothiocyanate (FITC)-dextran-coated particles and capsules was demonstrated by measuring changes in FRET between FITC and TRITC resulting from titration of glucose. Such micro/nano scale systems containing Con A/dextran multilayers may potentially be used for *in vivo* glucose sensing, if appropriately designed to eliminate concerns over Con A toxicity.

4.1 Sensor Design

A schematic of the glucose microsensor fabrication process is shown in Figure 4.1. To produce hollow capsules containing the assay components, soluble microparticles are coated with multilayers of FITC-dextran and TRITC-Con A thin films, followed by sequential deposition of oppositely charged polyelectrolytes. In the final step of fabrication, the particle core is dissolved, resulting in hollow capsules with immobilized Con A and dextran as the interior wall. The advantage of hollow capsules is the decreased diffusion barrier provided by the interior, which should give rise to rapid equilibrium and more uniform distribution of glucose in the films. As shown in Figure 4.1, strong fluorescence peaks due to both FITC and TRITC are present after assembly of the films, indicating there is considerable energy transfer. With the addition of glucose, dextran is

displaced from Con A, resulting in a decrease in energy transfer efficiency as indicated (Figure 4.1) by a stronger FITC peak relative to TRITC. The details of experiments investigating these properties are given in the following sections.

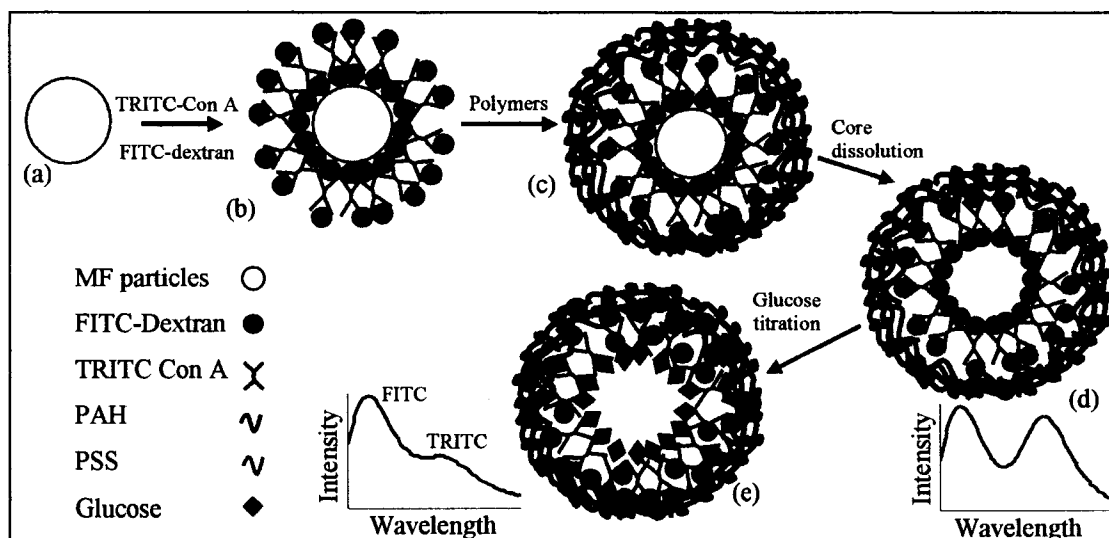


Figure 4.1. Fabrication process flow diagram (LbL assembly) of the biosensor (a) Microparticle as positively-charged substrate (b) Deposition of dextran (anionic) and Con A layers alternatively (c) Adsorption of the polymer multilayers (d) Dissolution of core to yield capsules (e) Titration of glucose to displace dextran from Con A.

4.2 Experimental Section

Materials. Poly(allylamine hydrochloride) (PAH, 15kDa), poly(dimethyldiallyl ammonium chloride) (PDDA, MW 200kDa), and poly(styrene sulfonate) (PSS, MW 70kDa) from Aldrich were used as polyelectrolytes. Solutions of 2 mg/mL in DI water were prepared for each polymer, and these were used at neutral pH. An aqueous dispersion, 10 wt% of 5 μm diameter melamine formaldehyde (MF) dissolvable resin particles, was obtained from Microparticles GmbH (Germany). FITC Dextran (MW 9kDa, 150kDa and 2MDa) and Succinyl-Con A (MW 54kDa) were purchased from Aldrich and EY Labs, respectively. Aqueous stock solutions of 0.5 mg/mL and 1mg/mL

were prepared in DI water for dextran and Con A, respectively, and the pH was adjusted to 8.5 by titrating with NaOH. Tetramethylrhodamine isothiocyanate (TRITC) was purchased from Molecular Probes to label succinyl-Con A using a standard amine-labeling protocol.¹³⁶ Glucose, from Sigma, was dissolved in DI water at neutral pH, to prepare a 100mg/mL stock solution. All solutions used in the experiments involving Con A contained 1 mM concentrations of calcium chloride (CaCl₂) and magnesium chloride (MgCl₂) salts to preserve Con A and glucose binding.⁶⁴

Instrumentation. A quartz crystal microbalance (QCM, USI-System, Japan) was used to study the self-assembly of Con A/dextran thin films. Absorbance spectra were collected using a UV-Vis absorbance spectrometer (Perkin Elmer Lambda 45). Zeta-potential measurements were taken using a ZetaPlus photon correlation spectroscopy and microelectrophoresis instrument (Brookhaven Instruments). A scanning fluorescence spectrometer (QM1, Photon Technology International) was used to collect fluorescence emission spectra from the sample using excitation at 488 nm. The microparticles and capsules containing FITC-dextran/TRITC-Con A were imaged using a confocal microscope (Leica Microsystems).

4.3 Methods

4.3.1 Assembly on QCM Resonator

To confirm the ability to form multilayer films from dextran and Con A, the LbL assembly of Con A/dextran was first monitored with QCM by constructing multilayer films on a quartz resonator. When a mass is adsorbed on the resonator there is a shift in resonant frequency, which is related to the adsorbed mass by the Sauerbrey equation.¹³⁷

According to this relationship, the change in frequency (ΔF , Hz) is related to the total mass of the adsorbed thin film layer (Δm , ng) as $\Delta m = -0.87\Delta F$.

QCM resonators were used as substrates for alternate assembly of FITC-dextran /Succinyl-Con A thin films. The resonator was a silver electrode, with a surface area of 0.16 cm^2 and natural resonance frequency of 9 MHz. During the assembly procedure, each resonator was dipped in the solution of polymer to be deposited for 15 min. The resonance frequency, was measured after rinsing the crystal with water and drying with nitrogen. Precursor films of (PAH/PSS)₂/PDDA were deposited to obtain a smooth and uniformly charged substrate prior to the addition of the polysaccharide/protein multilayers. For FITC-dextran (MW 2MDa) and succinyl-Con A deposition, the resonator was immersed in bulk solution for 25 min to allow enough time for the adsorption. The change in resonance frequency was monitored for each adsorption step.

Following the completion of the layering process, the resonator was used to test the sensitivity of the Con A/dextran thin films to glucose by immersing the resonator in 1.5mL of 100mg/mL glucose solution. After dipping the resonator in the glucose solution, the frequency change was monitored every hour over a period of 7.5 hrs. After completing the assembly process on the resonator, absorbance measurements were performed on all the solutions used for deposition, including the glucose solution, to assess the desorption of the layered thin film components into the bulk solutions.

4.3.2 Assembly on Microspheres

The techniques used for successful assembly of Con A/dextran multilayers on the planar surfaces of QCM resonators were applied to form Con A/dextran multilayers on the surface of $5 \mu\text{m}$ MF particles. FITC-dextran (2MDa, 0.5mL) was added to $10 \mu\text{L}$ of

the MF particle suspension. After allowing 20 min for complete adsorption saturation, the sample was rinsed using DI water and centrifuged at 4000 rpm for 8 min. This rinse process was repeated twice for each assembly step. Then, 0.5 mL of 0.5 mg/mL TRITC-Con A was added to the sample, and after a 20 min exposure, the sample was again rinsed twice. This assembly process was repeated to deposit multiple bilayers of TRITC-Con A/FITC-dextran, such that the outer surface was FITC-dextran.

To assess the charge of the adsorbed material and, therefore, determine the relative contribution of electrostatic attraction to the assembly process, multiple surface-potential measurements were taken after depositing and rinsing each layer. Fluorescence emission spectra were also collected from the suspension after depositing each layer, allowing tracking of the layering process and observation of FRET efficiency with each additional component of the nanofilms. Finally, the layered microparticles were imaged using a confocal microscope after each bilayer addition of FITC-Dextran/TRITC-Con A. A 5 μ L drop of the suspension was pipetted onto a glass microscope slide, and sequential confocal images were taken with a 63X oil objective by exciting FITC at 488 nm and TRITC at 543 nm using Ar/ArKr and green HeNe lasers, respectively.

4.3.3 Glucose Effect on Con A/Dextran Coated MF Particles

After completing the assembly of FITC-dextran and TRITC-Con A multilayers, fluorescence spectra of the particles and surrounding medium were collected. This was performed to determine the relative contribution of particles to fluorescence signals and to observe whether significant amounts of fluorophore-tagged macromolecules were present in the solution in free form. To assess the glucose-binding properties of the assembly, glucose was added to the continuously-stirred particle suspension in an attempt

to displace FITC-dextran from TRITC-Con A. After each addition, fluorescence emission measurements were performed to observe the change in energy transfer. After the final step of adding glucose, the particles were centrifuged and the fluorescence was observed in order to assess the effect of the dissociation of FITC-dextran from TRITC-Con A on film stability. A comparison of the supernatant fluorescence spectra before and after addition of glucose was used to demonstrate the sensitivity of the Con A/dextran nanoassemblies to glucose. These experiments were completed in parallel to the studies with the QCM measurements, such that the two sets of data could confirm the assembly and dissociation of dextran/Con A multilayers both on planar surfaces and spherical microtemplates.

4.3.4 Encapsulation and Hollow Capsule Formation

Following the successful demonstration of dextran/Con A multilayer glucose sensitivity and observation of the partial decomposition of these films, an ultrathin polymer shell was constructed around the Con A/dextran-coated particles to stabilize the localization of the polysaccharide and protein molecules. As the outer layer was FITC-dextran, and zeta-potential measurements confirmed that the surface charge was anionic, the coated microparticles were first suspended in a solution of the polycation PAH. After 15 min of exposure, the sample was rinsed twice in DI water, and the surface potential was measured. This procedure was repeated to deposit a total of four bilayers of PAH and PSS plus one additional outer layer of PAH. Thus, the final film architecture on the surface of the particles at the conclusion of the assembly was {(FITC-Dextran/TRITC-Con A)₃/FITC-dextran/ (PAH/PSS)₄/PAH}. Following the completion of polymer layer deposition, MF core particles were dissolved by adding 0.5mL of HCl at pH 1.1 to the

particle suspension.¹³⁸ Finally, the capsules were centrifuged and rinsed with DI water to remove residual MF monomer.

4.3.5 Glucose Effect on Capsules Containing Con A/Dextran Multilayers

After encapsulation of the dextran/Con A films within the polymeric shells and removal of the solid MF cores, the glucose response of the capsules was studied using the same procedures that were applied to the coated particles. The key comparisons made between the two cases (dextran/Con A films on solid particles versus hollow capsules with dextran/Con A multilayers inside a shell of polyelectrolyte multilayers) were the change in FRET following exposure to glucose, and the decomposition of the dextran/Con A layers, releasing molecules into the surrounding medium. To observe the glucose sensitivity of the microcapsules, 20 μ L additions of 100mg/mL glucose stock solution were given to 1 mL of a continuously-stirred capsule suspension (200mg/dL per step). To observe the change in energy transfer, fluorescence spectra were collected after each addition of glucose by exciting the sample at 488 nm and collecting the emission spectra from 500 nm to 650 nm. After the final step of glucose addition, the capsules were centrifuged and the supernatant fluorescence was measured to observe if displaced dextran was released from the capsules. Confocal microscopy was also used to observe the change in FRET within the capsule due to the addition of glucose, and to determine whether FITC-dextran was released into the interior of the capsule when displaced from Con A.

4.4 Results and Discussion

4.4.1 QCM Results

Mass measurements performed after depositing each layer are shown in Figure 4.2. This graph presents, in the first phase, the change in adsorbed mass due to deposition of the following multilayer architecture: $\{(PAH/PSS)_2/PDDA/(TRITC-Con A/FITC-Dextran)_3/Glucose\}$. The precursor polymer layers exhibited the expected linear stepwise growth. The average stepwise increase in mass for Con A and dextran addition, which is not quite linear, corresponds to an average of ~ 60 ng ($\sim 10^{11}$ molecules) and ~ 40 ng ($\sim 10^9$ molecules), respectively. In spite of having a higher MW compared to that of Con A, the average mass of dextran deposited per step was found to be less. This was expected, because the multiple glucose residues of dextran allow association with glucose binding sites on multiple Con A molecules. Thus, the dextran may assemble into a configuration more parallel to the surface, effectively covering more surface area per molecule.

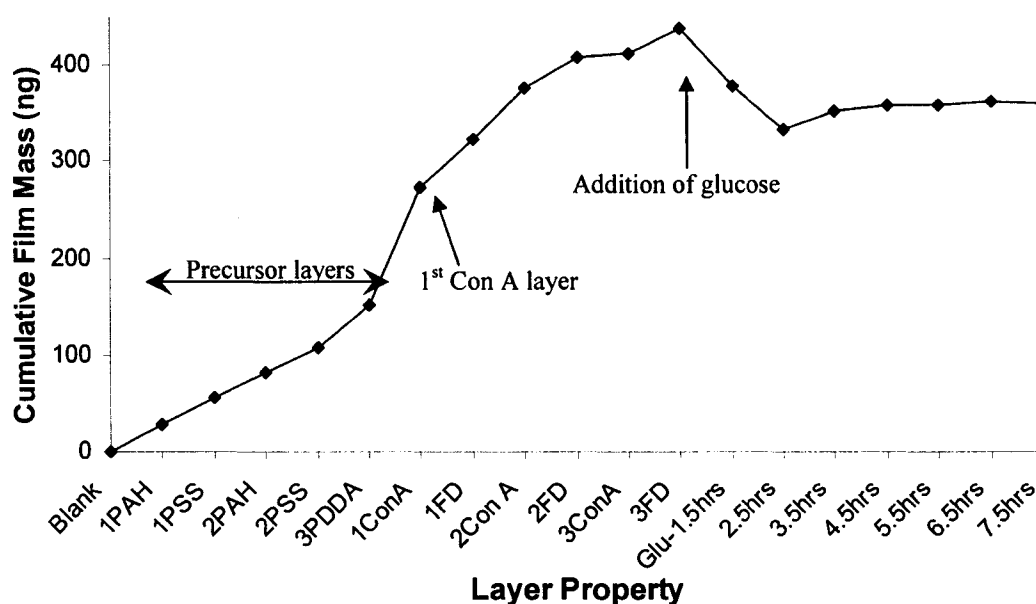


Figure 4.2. Mass deposited and released during adsorption of polyelectrolytes, FITC-dextran, and succinyl-Con A on the QCM resonator, and exposure of multilayer films to glucose.

Due to the small number of glucose binding sites on Con A molecules and the repulsive electrostatic force present between dextran and Con A, it is expected that the adsorption of Con A onto dextran films would be weakly enforced. Thus, it was also hypothesized that dextran could pull some Con A from the resonator surface when the films with Con A outer layers were exposed to dextran solution. To test this theory, absorbance measurements of the solutions used for layering the QCM resonator were performed. These measurements, presented in Figure 4.3, show that the absorbance spectrum of FITC-dextran assembly solution, after exposure to films with an outer layer of Con A, possessed an absorbance peak at 280 nm. This confirms that some protein was removed from the surface into the solution during this immersion period. In contrast, the Con A solution, following exposure to films containing a FITC-dextran outer layer, did not contain an absorbance peak at 490 nm. Thus, the opposite effect (Con A removing dextran) was negligible. This is also logical, as the dextran molecules likely bind with multiple Con A molecules on the surface, and these multiple parallel associations per molecule make the adsorption much more stable.

In experiments to assess the glucose response of the films, the QCM resonators with dextran/Con A multilayers were exposed to 100mg/mL glucose solution for 7.5 hrs, which resulted in an increase in resonance frequency corresponding to a decrease in adsorbed mass (Figure 4.2). This was expected behavior as glucose has been shown to displace dextran in competitive binding,⁸⁵ and these experiments demonstrate saturation of the mass change after ~2.5 hours. It is interesting that the response is so slow to equilibrate. This cannot currently be explained with confidence, but may be related to the diffusion barrier provided by the surface and the total mass of glucose present.

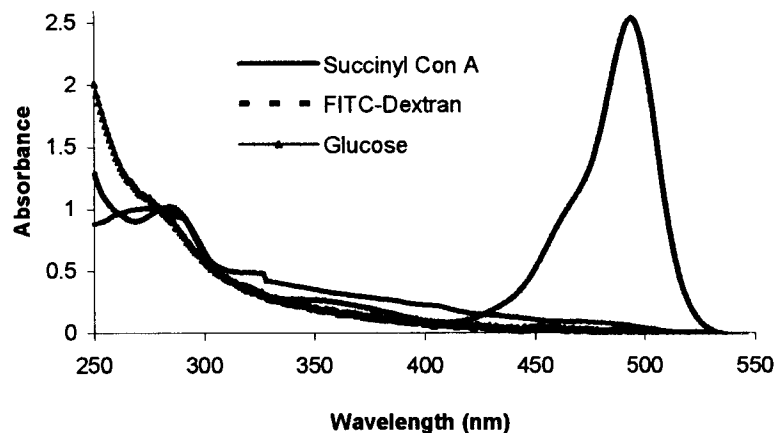


Figure 4.3. Normalized absorbance spectra of FITC-dextran, succinyl-Con A, and glucose solutions used for assembling on QCM resonator, and testing their glucose sensitivity (scaled up with factors of 12.5X, 25X, and 1000X, respectively).

Quantitatively, the total decrease in the film mass was 78.3 ng, which must correspond to the difference in glucose mass bound to the films and the dextran and/or Con A removed from the surface. In this case, glucose apparently displaced dextran from Con A, as absorbance measurements of the glucose solution after immersion of the QCM resonator (shown in Figure 4.3) possessed weak absorbance at 490 nm. In addition, an absorbance peak at 280 nm suggests the presence of Con A in solution as well. This was also expected, as glucose displacement of dextran from all glucose binding sites of a Con A molecule could free it from the film if other attractive forces are negligible. Thus, the QCM studies demonstrated that the affinity-binding nanoassemblies of dextran/Con A behaved as expected and further investigation was warranted.

4.4.2 Microparticle Coating Results

The surface potential of MF particles was measured to determine the contribution of electrostatic forces to dextran-Con A association for deposition of the multilayers with the architecture: $\{(FITC\text{-Dextran/TRITC-Con A})_3/FITC\text{-Dextran}/(PAH/PSS)_4/PAH\}$. The average and standard deviation of the multiple zeta potential measurements for the

particles after addition of each layer are given in Figure 4.4. The first layer of FITC-dextran (anionic) was bound to the MF (cationic) particles' surfaces, primarily due to electrostatic forces of attraction. However, the continuous negative potential values measured for Con A/dextran multilayers (1FD to 4FD in Figure 4.4) correspond to the adsorption of materials with negative charge. Although these values do not confirm successful deposition of the materials, the QCM data (Figure 4.4) suggest film assembly, and the fluorescence spectra of the particles (Figure 4.5(a)) directly confirm alternate assembly of Con A/dextran in multilayers. Thus, taken together, these data confirm that layer-by-layer assembly of FITC-Dextran and TRITC-Con A can be performed under neutral conditions in spite of both molecules carrying a net negative charge, and that the association between Con A and dextran molecules is due to binding affinity. The attractive forces involved in this association are sufficient to overcome electrostatic repulsion.

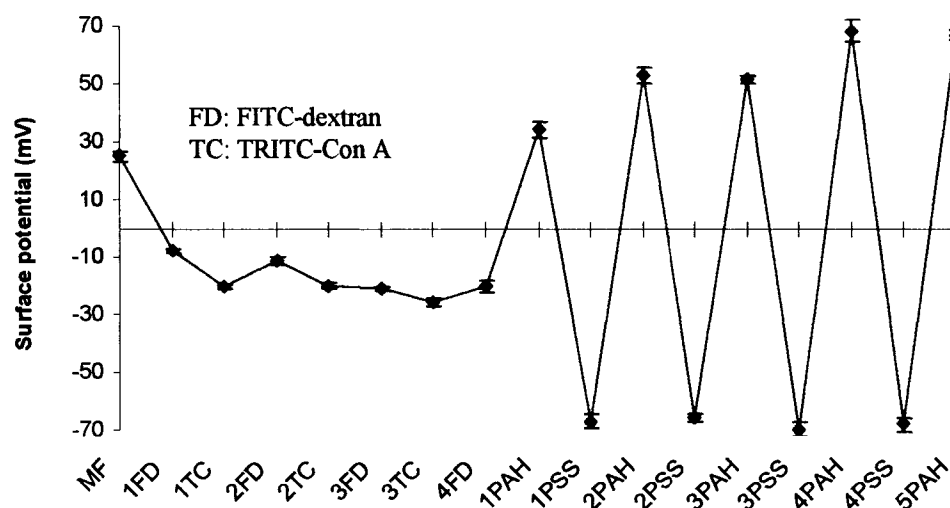


Figure 4.4. Mean and standard deviation values for zeta potential measurements of coated MF particles. Film architecture: {(FITC-Dextran/TRITC-Con A)₃/FITC-Dextran/(PAH/PSS)₅}

It can be observed from Figure 4.5(b) that the FITC:TRITC peak intensity ratio decreases with the addition of each layer up to two bilayers of FITC-dextran and TRITC-Con A, indicating that there is increase in energy transfer from FITC to TRITC. After two bilayers, the peak intensity ratio remained constant, suggesting that a constant level of energy transfer is achieved due to consistent association of dextran and Con A molecules with similar average distance between FITC and TRITC.

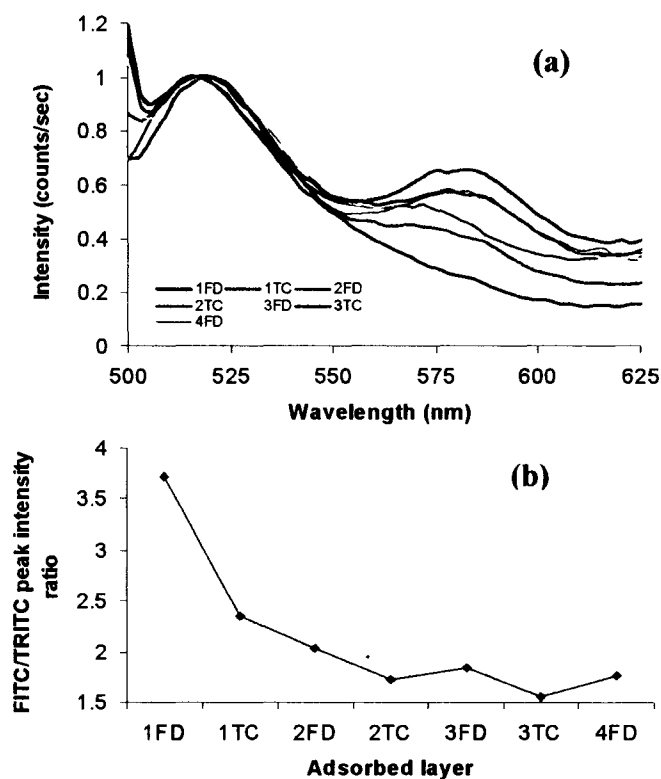


Figure 4.5. (a) Normalized fluorescence spectra of particle suspension after depositing fluorescent materials FITC-dextran (FD) and TRITC-Con A (TC); (b) FITC:TRITC peak intensity ratios after adsorbing each layer on MF particles

To observe if free dextran and Con A molecules were present in the sample, the fluorescence of the coated particles was compared with the supernatant fluorescence following separation by centrifugation. It can be observed from Figure 4.6(a) that the supernatant fluorescence had a prominent FITC peak compared to TRITC, and the total

emission intensity was an order of magnitude less than the suspension fluorescence. In comparing the fluorescence of the particles and the supernatant after adding glucose (Figure 4.6(b)), the relative FITC fluorescence of the supernatant increased significantly. Thus, it is apparent that when glucose was added to the sample, it was bound to Con A and displaced dextran into the bulk solution. By combining these observations with the QCM data presented earlier, the glucose interaction process may be described as follows: as dextran is released, the films partially decompose, and Con A-glucose complexes are also released. The absence of TRITC fluorescence in the supernatant after adding glucose indicates that the TRITC-Con A released into the supernatant is associated with glucose, not dextran, and therefore significant RET is not present.

Because ultrathin films based on electrostatic LbL self assembly are known to swell with increasing salt concentration,¹³⁹ additional experiments were performed to assess whether the observed changes in FRET and the release of FITC-dextran could have resulted from nonspecific effects of ionic strength or other properties of the environment. Fluorescence spectra of the particles (MF particles with FITC-dextran and TRITC-Con A multilayer films, without polymer coatings) and supernatant, following the addition of NaCl (up to 0.5 M) and dilution with water showed that there was no change in the FITC:TRITC peak intensity ratio. Therefore, the change in FRET observed for the nanoassembled Con A/dextran multilayer films likely arises specifically due to glucose and, thus, the displacement of dextran from Con A is believed to be a result of the competitive binding of glucose rather than a nonspecific change in the films. It is expected that these assemblies will have the same selectivity for glucose over other sugars as has been shown in other work,⁸⁵ though this property is not investigated here.

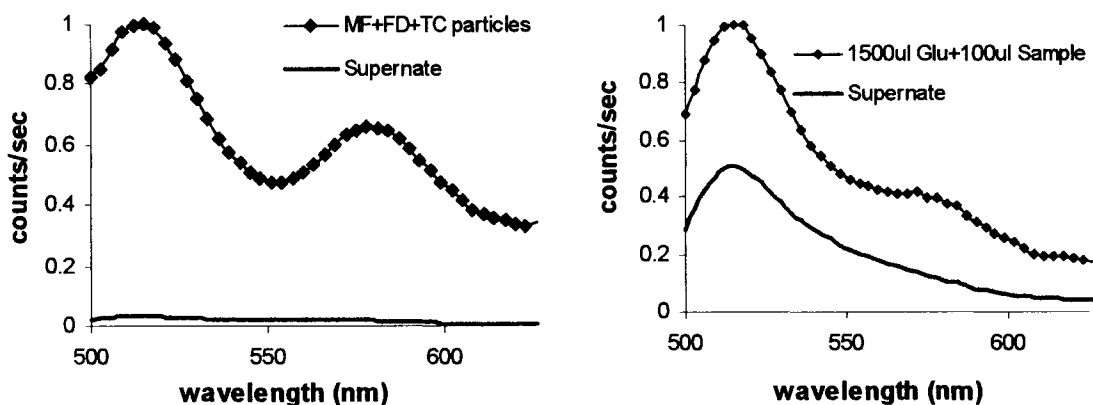


Figure 4.6. Fluorescence spectra of MF particle suspension coated with {(FITC-dextran/TRITC-Con A)₃/FITC-dextran}, along with supernatant a) prior to addition of glucose, and b) after glucose titration.

4.4.3 Polymer-Coated Microcapsules

The charged polymers were deposited on top of the Con A-dextran multilayer films via electrostatic self assembly and the charge was varied from positive to negative in alternate fashion. The alternation of surface potential values (Figure 4.4, 1PAH to 5PAH) corresponds to the adsorption of the positive (PAH) and negative (PSS) species, respectively. Confocal fluorescence images of the 5- μm capsules formed by MF dissolution are shown in Figure 4.7, from which it can be observed that the capsule walls remain intact after core dissolution. In addition, there does not appear to be significant amounts of free fluorescent molecules inside or outside the capsules indicating that the Con A/dextran assemblies remain mostly intact. The fluorescence intensity line scans of the capsules show the spatial distribution of fluorescence emitted from the image plane for both FITC and TRITC. These data clearly show the dimension of the capsules is approximately 5 μm and the fluorescence arising from the walls is much stronger than the background from the capsule interior and exterior.

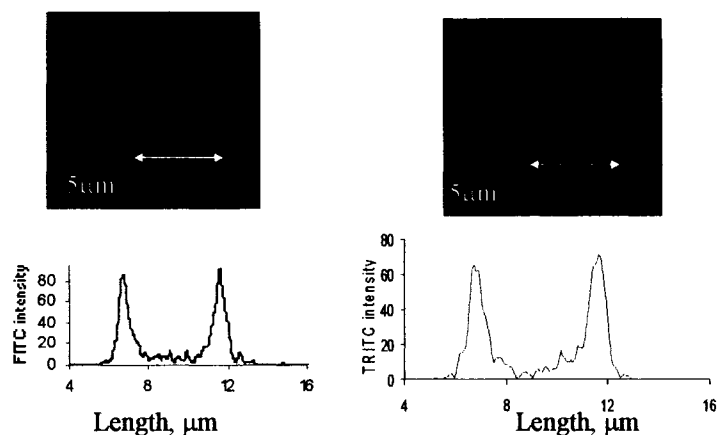


Figure 4.7. Confocal microscope images of capsules with {(FITC-dextran/TRITC-Con A)₄/FITC-dextran/(PAH/PSS)₄/PAH} as shell structure, and corresponding intensity line scans of capsules, showing FITC (left) and TRITC (right) intensities

It was hypothesized that the dextran in these capsules would be displaced from Con A by glucose. By this process, increasing the glucose concentration in the suspension of hollow capsules would result in an increase of free FITC-dextran concentration and, hence, increasing of the FITC fluorescence was expected from the suspension. Correspondingly, the average distance between dextran and Con A was expected to increase resulting in a decrease in the energy transfer between FITC and TRITC, due to which the relative fluorescence of TRITC would decrease.⁸⁷

To test these expectations, fluorescence emission spectra of polymer-coated capsules were monitored with increasing glucose concentration. The FITC:TRITC peak intensity ratio plotted versus glucose concentration is shown in Figure 4.8. It can be observed that the FITC fluorescence did, in fact, increase relative to the TRITC fluorescence, up to approximately 1200mg/dL glucose. Over this range, the sensitivity curve shows approximately linear increase in FITC:TRITC fluorescence peak intensity ratio with glucose concentration. The slope of the sensitivity curve in the linear region was calculated to be 4×10^{-4} ratio units/(mg/dL), which corresponds to ~7-10% of the total

ratio change for each step of 100mg/dL of glucose. Above the linear range, the signal appears to plateau, indicating the saturation of Con A binding sites with glucose. This sensitivity is near to that of the best case reported in the literature using intensity measurements of FRET, and was achieved without any attempt to optimize sensitivity or signal-to-noise ratio. Therefore, these results are encouraging and suggest further work may lead to improvements in the system properties related to measurement performance.

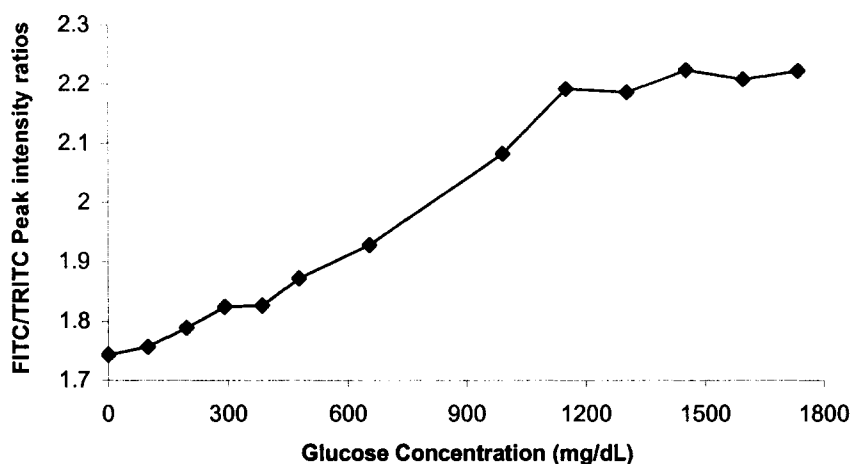


Figure 4.8. Effect of glucose titration into suspension of capsules comprising {(FITC-dextran/TRITC-Con A)₄/FITC-dextran/(PAH/PSS)₄/PAH} as shell layers

In addition to testing response to glucose measured by changing FRET, the stability of the structures was investigated. After completing the addition of glucose, the capsules were centrifuged and the supernatant was collected to determine the loss of fluorescent molecules from the microcapsules. The emission intensity of the supernatant was two orders of magnitude lower than the emission from the capsules and, because the peak ratio was identical to that of the capsules, even this small signal can be attributed to inefficient separation of capsules from supernatant. This is in contrast to the findings when assessing FITC-dextran/TRITC-Con A assemblies on MF particles without the

polymer shell, as noted above, where significant loss of FITC-dextran was seen in the supernatant. These results highlight the improved stability of the polysaccharide/protein films encapsulated by polymer nanofilms, and supports further development of this technology. However, further investigation will focus on quantitatively determining whether FITC-dextran or TRITC-Con A is released from the microcapsules.

The results of the response of the microcapsule suspension to glucose, taken together, indicate that the presence of glucose did result in separation of Con A and dextran, such that the energy transfer between FITC and TRITC was decreased. Also, this result corroborates with the theoretical model results in Chapter Three (Figure 3.5), which shows that there is an increase in the fluorescence from free-ligand with the increase in analyte concentration. Using the Förster distance for FITC and TRITC fluorophores as 55\AA ,¹¹⁶ the estimated change in the average distance between FITC and TRITC molecules was found to be 3.5\AA with the addition of $\sim 0.1\text{M}$ glucose, which is a reasonable number given the size of a glucose molecule ($\sim 10\text{\AA}$). These small displacements could easily be achieved without significant rearrangement of the ultrathin films, and could be a result of the movement of glucose residues on dextran to accommodate for glucose molecules binding to the Con A sites.

Further confirmation of the stability of the microcapsules was provided by the confocal microscope images of the capsules after adding glucose. Still, these did not show any significant fluorescence inside or outside the capsules. There could be several reasons for not observing free molecules after the glucose addition. The dextran and Con A molecules may be moving apart such that there is a change in FRET, but they remain immobilized within the films. Thus, the films are sufficiently deformable that they can

accommodate this change. This is a reasonable assumption given the previous calculation of 3.5Å for average displacement which could not be resolved with microscopic measurements. Alternatively, the dextran and Con A molecules may be completely separated, but the free FITC-dextran molecules may be stuck in the polymer layers due to their large size. Regardless of the true physical arrangement of the molecules in the films, which will be the subject of further studies, the results here demonstrate the concept of FRET-based glucose sensing using dextran-Con A multilayers, and further work to investigate these novel nanostructured materials is warranted.

4.5 Conclusion

In conclusion, a novel glucose sensing system based on the LbL self assembly competitive binding and FRET techniques is demonstrated in this chapter. Glucose-sensitive Con A/dextran multilayer films were successfully assembled on planar substrates and microparticles due to the affinity between molecules. Hollow capsules containing Con A/dextran multilayers showed a glucose sensitive decrease in FRET with a detection range from 0 to 1800 mg/dL and a sensitivity of 4×10^{-4} ratio units/(mg/dL). It was estimated from the data that with the addition of ~0.1M glucose solution to the capsule suspension the Con A and dextran molecules moved apart by an average distance of approximately 3.5 Å, which corresponds to a 27 % increase in the FITC:TRITC intensity ratio. These findings show that the combined use of FRET, competitive binding, and LbL principles is a promising approach to build sensors, and this should be a more generally useful method for building many other biosensor elements beyond the model Con A-dextran system. Depending upon the structural dynamics of the ultrathin films in response to the analyte, similar approaches could potentially be used to realize drug

carriers for controlled delivery. In spite of all the above-mentioned advantages of this sensor design, there are some inherent disadvantages of using Con A as one of the elements in the sensing assay, such as toxicity, aggregation, and specificity. Therefore, there is an urgent need to develop a new sensor design or find a replacement for Con A in the existing design. The next chapter demonstrates a sensor design by replacing Con A with another glucose binding protein, which is highly specific to glucose and is not toxic.

CHAPTER 5

FLOURESCENT GLUCOSE SENSORS

OPERATING IN VISIBLE REGION

To overcome the limitations of Con A, we have developed an alternative approach to the regular Con A-based competitive binding assay using an inactive form of the enzyme glucose oxidase (apo-GOx) as the glucose-binding protein, which is highly specific to β -D-glucose.²³ Apo-GOx was previously used as a biosensor based on its ability to reconstitute into a holoenzyme with the addition of semi-artificial cofactors.^{140,141} Apo-GOx was also used for glucose sensing by itself,²³ as it was shown that there was a decrease in the intrinsic fluorescence of apo-GOx/apo-GOD with the addition of glucose. This kind of sensing method cannot be corrected for inner filter effects as it is not ratiometric. Furthermore, any decrease in intensity could be partially due to the effect of assay dilution. Also, as UV light is used for excitation, complex instrumentation may be required, and also there could be interference from different proteins in biological samples.

This chapter demonstrates, for the first time, a FRET assay for glucose which utilizes the affinity of apo-GOx toward glucose. This system may potentially be used for *in vivo* glucose monitoring, if properly encapsulated. Furthermore, these sensors may be

used in drug delivery applications, wherein the glucose sensitive apo-GOx/dextran dissociation results in variable material properties that determine drug release.

5.1 Sensor Design

The working principle of the sensing system is illustrated in Figure 5.1. Briefly, apo-GOx is prepared from GOx by removing the FAD cofactor.²³ When apo-GOx is tagged with TRITC and exposed to FITC-dextran, strong fluorescence peaks due to considerable RET between FITC and TRITC are observed. Because of the high affinity of the glucose towards apo-GOx, the addition of glucose will result in the displacement of dextran from apo-GOx, which is indicated by a decrease in the energy transfer efficiency (Figure 5.1) by a stronger FITC peak relative to TRITC. In this study, the glucose sensitivity of the TRITC-apo-GOx/FITC-dextran was demonstrated by measuring changes in RET between FITC and TRITC resulting from titration of glucose.

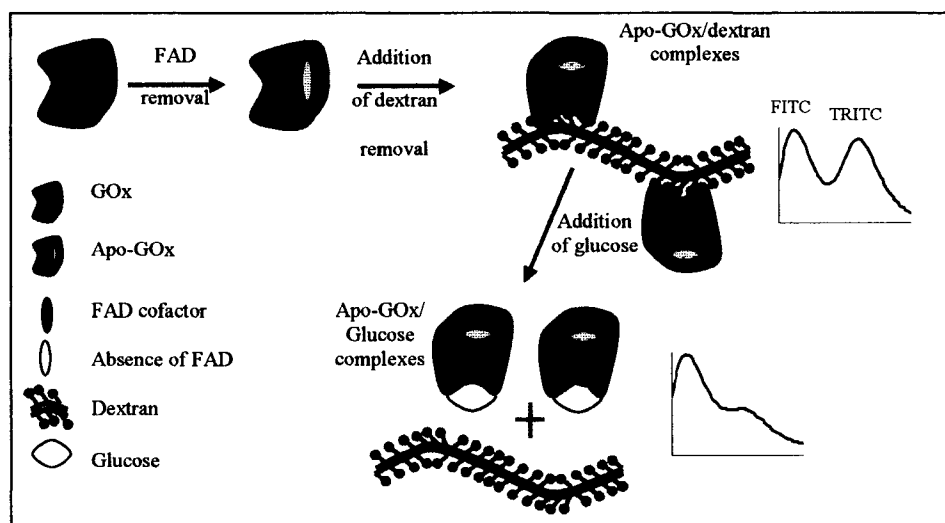


Figure 5.1. Schematic of a glucose assay based on competitive binding between dextran and glucose for binding sites on apo-GOx.

This system retains the advantages of the competitive binding approach: selectivity to the analyte of interest, elimination of reaction byproducts, and no consumption of the analyte during the sensing process.

5.2 Experimental Section

Materials. FITC-dextran (FD, MW 2MDa, 500kDa), glucose oxidase (GOx, G-2133), sodium poly(styrene sulfonate) (PSS, MW ~1MDa), poly(allylamine hydrochloride) (PAH, MW 70kDa), β -D-glucose, mannose, α -D-glucose, sucrose, sodium bicarbonate, dimethyl formamide, ammonium sulfate, peroxidase and sodium acetate buffer were obtained from Sigma. Tetramethylrhodamine isothiocyanate (TRITC, Molecular Probes) was used to label apo-GOx.¹³⁶ Diazo-resin (Diazo-10, 4-diazodiphenylamine/formaldehyde condensate hydrogen sulfate-zinc chloride salt, DAR) was purchased from PC Associates, NJ. All reagents were used as received. MnCO_3 (5 μm) particles were prepared as previously described.¹⁴²

Instrumentation. A UV-Vis absorbance spectrometer (Perkin Elmer Lambda 45) was used to collect absorbance spectra and perform catalytic activity tests. The slit size (4 nm) and scanning speed (480 nm/min) were held constant throughout all the experiments. A scanning fluorescence spectrometer (QM1, Photon Technology International) was used to collect fluorescence emission spectra by exciting the sample at 480 nm. A 100-W longwave UV lamp (Blak-ray[®] Model B 100AP, Entela) was used to irradiate the microcapsules for photocrosslinking PSS and DAR layers in the capsule walls. Confocal images were taken with a Leica TCS SP2, equipped with a 63X objective and Ar/ArKr, HeNe lasers. Counts of microcapsules were obtained with a Beckman Coulter counter.

5.3 Methods

5.3.1 Preparation of Apo-GOx

The basic procedure for apo-GOx preparation was followed as previously described.²³ GOx (20mg) was dissolved in 1mL of sodium acetate buffer and 10mL of prepared ammonium sulfate (25% saturated, pH 1.4) solution was added. The sample was then incubated in an ice bath with continuous stirring for 2 hrs. Excess $(\text{NH}_4)_2\text{SO}_4$ salt was added to the solution to separate protein and FAD. The protein without FAD cofactor (apo-GOx) was precipitated by centrifuging (twice) at 4500 rpm and 4°C. The supernatant was then removed and sodium acetate buffer was added to redissolve and neutralize. Finally the apo-GOx was labeled with TRITC using a standard amine labeling procedure¹³⁶ to obtain 1.67 moles of apo-GOx per mole of TRITC.

5.3.2 Assessment of FAD Cofactor Removal

Absorbance measurements were performed on the prepared apo-GOx solution to quantify the amount of FAD, which has a characteristic peak at 300 nm. In addition, apo-GOx activity measurements were performed to observe the decrease in activity compared to native GOx, using a standard colorimetric assay based on the oxidation of *o*-Dianisidine through a peroxidase coupled system on absorbance spectrometer. During continuous stirring with a magnetic bar, apo-GOx was added to the assay to achieve 0.17 μM concentration and the absorbance at 500 nm was monitored as a function of time, resulting in a catalytic profile for the apo-GOx. This experiment was repeated for GOx and TRITC-apo-GOx.

5.3.3 Solution Phase Experiments

Observations of RET between FITC-dextran (FD) and TAG were performed with a fluorescence spectrometer using 488 nm excitation with emission scans collected across the range of 500-625 nm. Initially, ~270pM FD was added to 1mL DI water, and fluorescence spectra were then collected after each titration of TAG into the sample solution. To determine the nature of the energy transfer (non-radiative, radiative, or both), fluorescence measurements were also performed after dilution with DI water. Finally, to assess the relative affinity of apo-GOx for glucose and FD, RET changes were observed during stepwise addition of aliquots of 100mg/mL β -D-glucose solution into the sample containing FD/TAG complexes. Sensitivity curves of the fluorescence peak ratio versus glucose concentration were constructed.

The effect of dextran molecular weight was studied by performing the same sensitivity experiments with equal molar concentrations (270pM) of 500kDa and 2MDa FITC-dextran. The effect of FD/TAG complex concentration on displacement behavior was investigated by repeating the same procedure at different total concentrations of FD-500kDa/TAG complexes, and maintaining an approximately constant 1:1 ratio of glucose moieties on FD-500kDa:TAG. In order to demonstrate the specificity of the sensor for glucose, the RET glucose sensitivity measurements were repeated with the titration of mannose, α -D-glucose, and sucrose into a solution of (FD-500kDa)/TAG complexes, maintaining all other parameters constant.

In Chapter Four, layer-by-layer (LbL) self-assembly was used to entrap Con A/dextran multilayers into microcapsules. Unlike Con A, apo-GOx has only one binding site, which prevents the construction of the multilayers of apo-GOx and dextran. Hence,

the procedure used for Con A/dextran assay is not applicable for the encapsulation of apo-GOx/dextran assay. Therefore, a new encapsulation technique is developed to encapsulate apo-GOx/dextran complexes into microcapsules using photo-sensitive materials, which is described in detail below.

5.3.4 Fabrication of Diazo-resin-Based Hollow Microcapsules

This approach employs the elegant LbL self-assembly¹⁴³ approach for the fabrication of microcapsules comprising photocrosslinkable materials (DAR and PSS) in the shell structure, which are used for stable entrapment of RET assay elements. Solutions of PSS (anionic), PAH (cationic), and DAR (cationic) used for assembling {PSS/PAH} and {PSS/DAR} multilayers were prepared in DI water at 2mg/mL. To obtain monodispersed samples, MnCO₃ particles (5μm) dispersed in DI water were sonicated for 10min prior to LbL assembly. As the core particles are positively charged, they were coated with one bilayer of {PSS/PAH}, and then three bilayers of {PSS/DAR}, followed by one layer of {PSS/PAH/PSS} as the outer layer, as illustrated in Figure 5.2(a-d). During each adsorption step, the particles were suspended in the polymer solution for 15min, followed by rinsing with DI water for three times to remove excess polyelectrolyte. The final architecture of the shell structure was {(PSS/PAH)(PSS/DAR)₃(PSS/PAH/PSS)}.

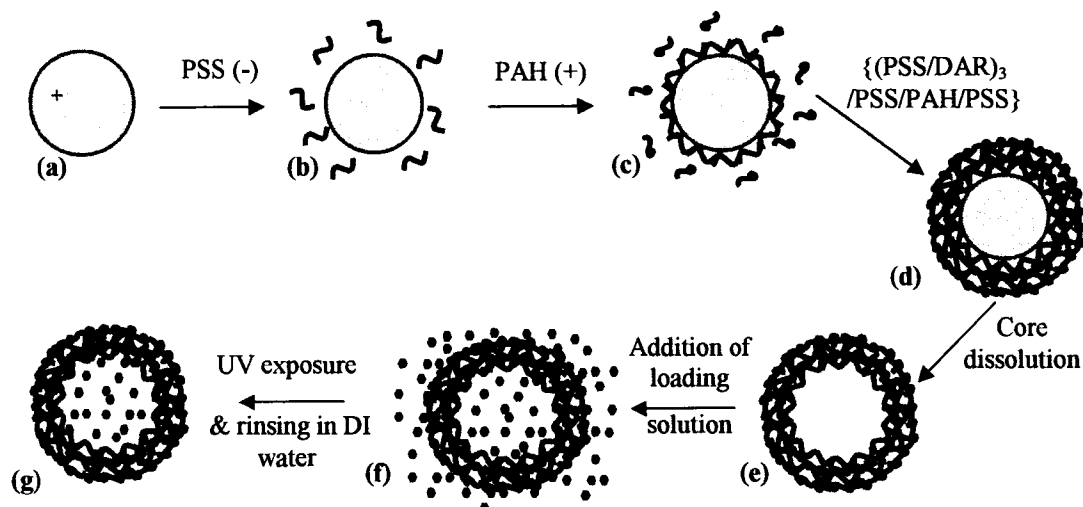


Figure 5.2. Fabrication of microcapsules and encapsulation of FD/TAG complexes.

It is noteworthy that the weak interaction between PSS/DAR layers could result in the disintegration of the capsule wall during the core dissolution process. To avoid this potential problem, initial and final bilayers of PSS/PAH were used to obtain a more stable shell structure.¹⁴⁴ Hollow microcapsules were obtained by dissolving the MnCO_3 cores in 0.1M hydrochloric acid (HCl) solution for 20min, followed by rinsing in DI water using centrifugation process four times to remove excess HCl solution, as depicted in Figure 5.2(e).

5.3.5 Encapsulation of Sensing Chemistry in DAR-Based Microcapsules

Microcapsules prepared as described are permeable to macromolecules, such as enzymes, prior to UV irradiation but become impermeable after photocrosslinking.¹⁴⁴ In order to encapsulate FD-500kDa/TAG and FD-2MDa/TAG complexes in the hollow shells, the capsule suspension was split into two different batches with approximately an equal number of capsules ($\sim 10^7$). In the first case, the microcapsule suspension was mixed with the $0.95\mu\text{M}$ FD-500kDa solution for 5min, followed by the addition of the

12.5 μ M TAG solution. The capsule suspension was incubated in the mixture of FD/TAG solution for 60 min, which allowed enough time for diffusion of the loading molecules into the capsule interior (Figure 5.2(f)). Confocal microscopy was used to visualize the loading process of the FD/TAG complexes into the microcapsules. A similar procedure was followed for complexes containing the larger dextran, with 0.3 μ M of FD-2MDa and 12.5 μ M of TAG. In each case, the capsules were irradiated while still in the FD/TAG loading solution, using a UV lamp for 10 min to crosslink the DAR and PSS layers of the capsule walls. Ultraviolet exposure was observed to result in a decrease of the permeability of the multilayer wall, which stopped the outward diffusion of the encapsulated molecules from the microcapsule. The loaded capsules were then rinsed in DI water using centrifugation process three times to remove residual loading solution (Figure 5.2(g)).

5.3.6 Estimation of the Encapsulation Efficiency

The procedure outlined below is the standard method used to calculate the loading efficiency of sensing assay elements in microcapsules. It is well understood that encapsulation of the sensing elements is based on diffusion from the loading solution and the loading rate is, therefore, directly proportional to the initial concentration of the loading solution. However, estimation of the final amount of loading solution encapsulated in the microcapsules is important in order to study the effects of ligand molecular weight on sensor response. The FD and TAG concentrations in the loading solution (C_{load}) were determined using UV-Vis absorbance spectroscopy prior to the addition of hollow microcapsules. As described above, following the suspension of the microcapsules in the loading solution and exposing them to UV light, the capsules were

rinsed thrice in DI water using centrifugation process and the supernatants were collected after each rinse. For each component, the concentrations in all the supernatants (e.g. $C_{rinse} = C_{rinse1} + C_{rinse2} + C_{rinse3}$) were determined by UV-Vis and subtracted from C_{load} to estimate the amount of the encapsulated (C_{encap}) material. Encapsulation efficiency (E) was estimated as the ratio of the total number of FD or TAG moles loaded to number of capsules N in the corresponding sample.

$$\begin{aligned} C_{encap} &= C_{load} - C_{rinse} \\ E &= \frac{C_{encap}}{N} \end{aligned} \quad (5.1)$$

5.3.7 Stability of Encapsulation

For potential use as sensors, it is important for the encapsulated material to be retained in the microcapsule over time. An experiment for the assessment of the stability of the encapsulated material was performed on two sets of capsules loaded with FD-500kDa/TAG and FD-2MDa/TAG complexes, respectively. To estimate the percentage of loaded material lost from the capsules, leaching studies were performed by separating the supernatant solution from the microcapsules via centrifugation and measuring the fluorescence from the supernatant. After each measurement, the supernatant solution was placed back with the microcapsule suspension in DI water. In order to reduce photobleaching effect and preserve the biomolecule activity all samples were covered and stored at 4-8°C under dark conditions, until the completion of all the experiments. Three replicate measurements were collected for each sample at 0, 2, 4, 10, 20, 30, and 50 hrs. Standard solutions of 26 nM FD-500kDa, 8 nM FD-2MDa, and 333 nM TAG were also measured at each point in time to correct for instrumental drifts over time and also to estimate the supernatant concentration as a percentage of a standard. The FD peak was

obtained by exciting the supernatant at 480 nm and collecting emission from 500 to 650 nm, while the TAG peak was obtained by exciting at 543 nm and collecting from 555 to 650 nm. FD and TAG peaks of the standard solutions were obtained in a similar manner. From loading efficiency and capsule counts, the FD and TAG concentrations present were calculated and the percentage of the leached FD and TAG were estimated.

5.3.8 Sensor Response in Microcapsules

A fluorescence spectrum of the microcapsules loaded with the FD/TAG complexes dispersed in DI water was collected as the starting point. Fluorescence spectra were then collected after each addition of 100mg/mL glucose to the microcapsules. The change in FITC to TRITC peak intensity ratio was calculated from each spectrum and plotted with respect to the increments in glucose concentrations. To observe the effect of molecular weight on sensor response and also to determine the feasibility of tailoring the sensor response, glucose sensitivity experiments were repeated for two different ligand sizes and three different concentrations of capsules. In the first case, capsules loaded with (FD-500KDa)/TAG and (FD-2MDa)/TAG were assessed. Next, three different concentrations of (FD-500KDa)/TAG loaded capsules ($\sim 10^6$, 2×10^6 , 3×10^6 capsules/mL) were considered.

5.3.9 Reversibility

To test the reversibility of these sensors, loaded microcapsules were suspended in glucose solutions in random order with respect to concentration. To achieve this, FD/TAG-loaded microcapsules (4×10^5) were dispersed in DI water (0.5mL) and the glucose concentration of the suspension was increased by addition of glucose stock solution. The glucose levels were changed by rinsing the capsules to remove glucose

after each measurement and then again adding glucose to reach a new concentration. In each case, after addition of glucose to the desired concentration and measurement of the fluorescence, the suspension was centrifuged, the supernatant (glucose) solution was removed and, finally, an equal volume of fresh DI water was added. The change in FITC:TRITC peak ratio was obtained at each step by collecting a fluorescence scan. This procedure was repeated to cover the glucose concentration over the range of 0-90 mM, in the order of 0, 4.15, 0.35, 9, 2.8, 0.02, 5.5, 19, 13.56, 60, 26.45, and 95 mM.

5.4 Results and Discussion

5.4.1 Assessment of FAD Co-factor Removal

The absorbance spectra of GOx and apo-GOx are shown in Figure 5.3(a). The absorbance peaks above 300nm in the spectrum corresponding to GOx are due to the presence of FAD cofactors. It can be observed that there are no such peaks above 300nm in apo-GOx absorbance spectrum, indicating the successful removal of the FAD cofactors. Activity measurements were performed at regular time intervals after FAD removal to ensure that apo-GOx did not regain activity with time and similar measurements were performed with TAG and GOx to determine the relative catalytic rate of the molecules. The results of these activity measurements are shown in Figure 5.3(b). The catalytic activity of apo-GOx and TAG was observed to be three and four orders of magnitude lower than the native GOx, respectively. The activity of apo-GOx approximately doubled over four weeks, but remained two orders of magnitude lower than the native GOx. The TAG activity was observed to be less than the apo-GOx activity which is likely the result of the labeling procedure employed to conjugate TRITC.

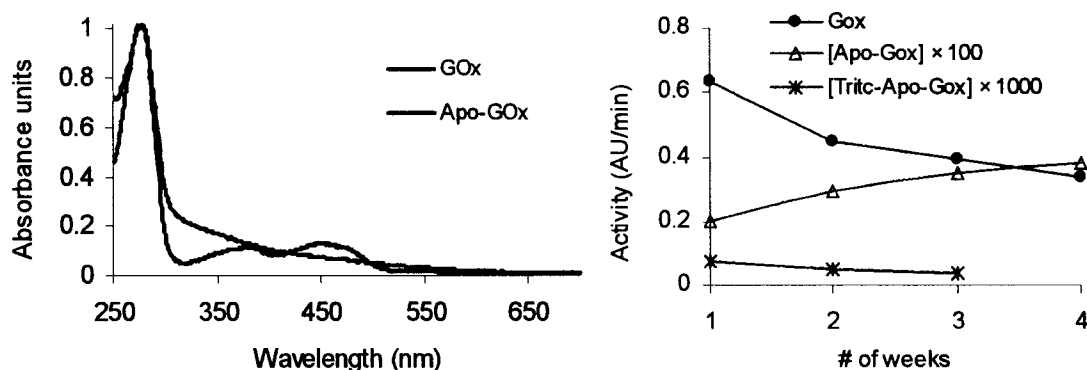


Figure 5.3. (a) Absorbance of GOx and apo-GOx. (b) GOx, apo-GOx, and TRITC-apo-GOx activities with respect to time.

5.4.2 Energy Transfer Experiments

Energy transfer from FITC to TRITC was monitored by collecting fluorescence spectra after each titration of TAG into FITC-dextran sample solution. Energy transfer was observed to increase with each titration of TAG, as shown in Figure 5.4(a). The spectra were normalized to the FITC peak at 515 nm to accentuate the changes in the TRITC fluorescence. From the data in Figure 5.4(c), it can be observed that the FITC:TRITC peak intensity ratio decreases with each addition of TAG. This does not directly indicate that energy transfer is non-radiative, as the same effect could be observed with radiative energy transfer. To determine that this change in peak intensity ratios was affected by radiative energy transfer, the assay was diluted with aliquots of DI water after the last addition of TAG. If the energy transfer is radiative, then the peak ratio should change with the dilution of the sample. The change in FITC:TRITC peak intensity ratios for the spectra after diluting the sample are given in Figure 5.4(c). The constant peak intensity ratio seen in Figure 5.4(c) after each addition of DI water confirms that the energy transfer between FITC-dextran and TAG is non-radiative.

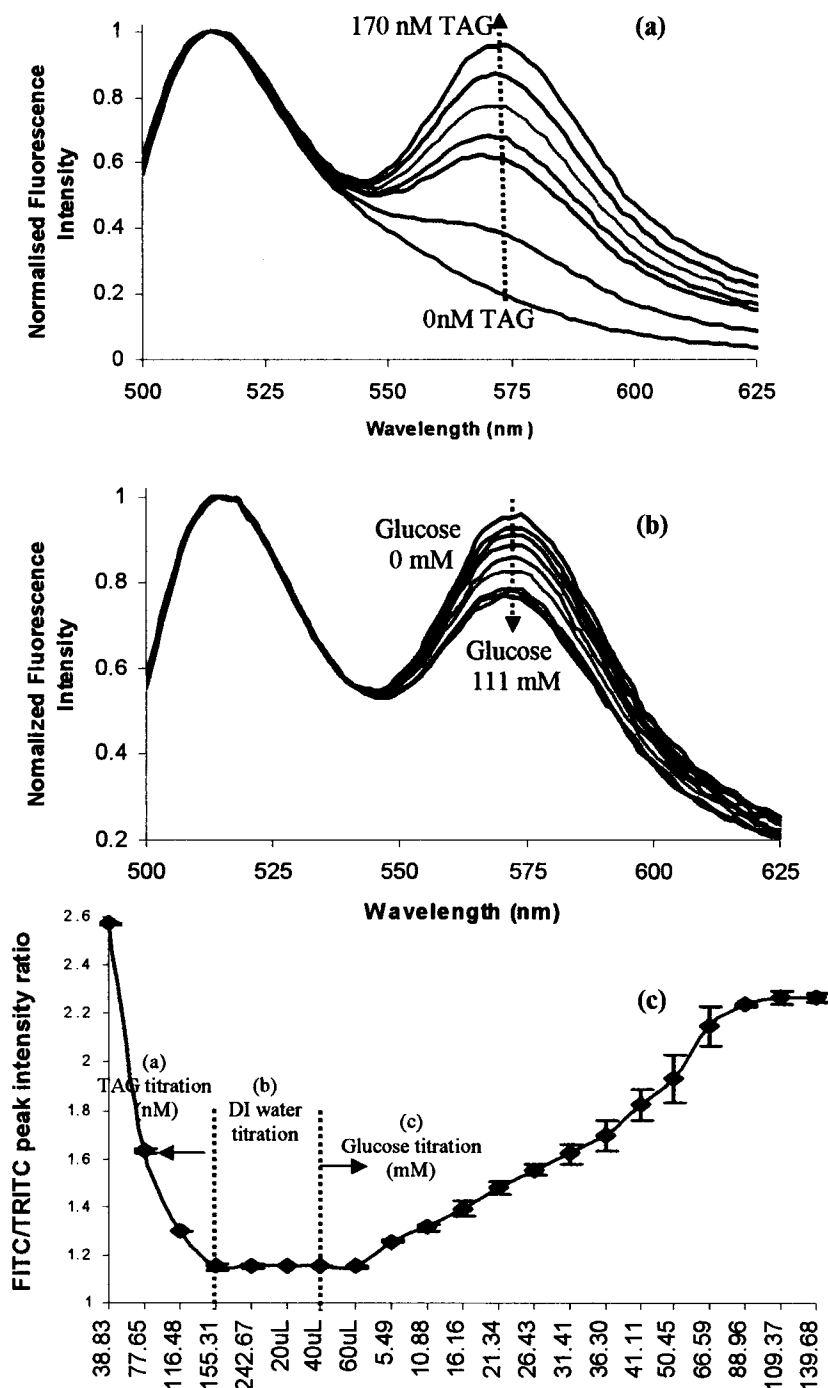


Figure 5.4. Normalized fluorescence spectra with the addition of (a) TRITC-*apo*-GOx (TAG) to FD-500kDa; (b) β -D-glucose added to the sample containing FD/TAG complexes. (c) Change in the FITC:TRITC intensity peak ratio with the addition of glucose.

The glucose sensitivity of the TAG/FITC-dextran samples was measured three separate times. The corresponding fluorescence spectra is shown in Figure 5.4(b) and the average FITC:TRITC peak ratio is plotted versus glucose concentration in Figure 5.4(c). The data clearly show a decrease in the energy transfer with increasing glucose concentration up to approximately 140 mM glucose. A 30% decrease in energy transfer was observed for a concentration of 90 mM glucose. These measurements verify that the apo-GOx and dextran molecules dissociated in the presence of glucose.

For easier comparison of different experimental results, sensitivity curves were obtained in all the RET experiments by plotting the percentage change in FITC:TRITC peak ratio versus glucose concentration (Figure 5.5), and the slope of the linear region was calculated as a measure of sensitivity response. In the case where FD-500kDa was used as the competitive ligand, a total change of 17% in energy transfer was observed due to 40 mM glucose, with a sensitivity of 0.5%/mM in the region of interest (0-40 mM). The same procedure was repeated with FD-2MDa, from which it was observed that there was a 7.5% change in RET with the addition of 40 mM glucose. The increase in dextran molecular weight was associated with ~2.5 times decrease in sensitivity and ~3 times increase in the dissociation constant, as shown in the inset of Figure 5.5.

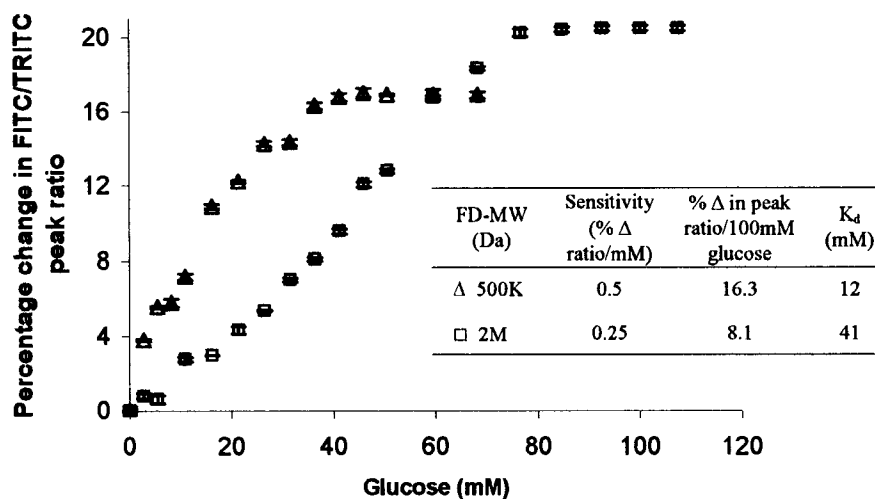


Figure 5.5. FITC:TRITC peak intensity ratio with the addition of glucose to FD/TAG complexes. Error bars show one standard deviation of three replicate measurements.

A key point to note for these data is that the calculated dissociation constants closely match reported values for glucose oxidase.¹⁴⁵ Thus, the processes required for cofactor removal and labeling of apo-GOx do not destroy the glucose binding behavior of the enzyme. This suggests that the binding of glucose and dextran is occurring in the active site as opposed to other regions of the enzyme that may be adhesive for sugars. Furthermore, this finding is critical for sensors intended for physiological monitoring, as the higher k_d values (millimolar range) more closely match the relevant range for glucose than the micromolar dissociation constants possessed by glucose binding proteins.

It is also noteworthy that the observed variation in the sensor response with different molecular weights of dextran could be due to an overall increase in the FD/TAG complex concentration in the sample. To achieve equal RET efficiency with different molecular weights of FD, the ratio of the number of glucose residues (proportional to FD-MW) on FD to the number of binding sites on TAG must be identical. As the number of TAG molecules that can bind to FD is directly proportional to glucose residues on FD,

the TAG concentration at which the energy transfer saturated during TAG titration increases proportionally with dextran molecular weight. This results in a total increase in the FD/TAG complexes present in the assay, which translates directly to a change in sensor response. This explains why the glucose sensitivity experiments (Figure 5.4(c)) show that 80 mM glucose is required to reach the saturation point for the larger dextran, whereas the saturation was reached with 40 mM glucose for the smaller molecule. Additional experiments conducted with lower FD molecular weights (77kDa and 250kDa) indicated that the sensitivity was increasing and the saturation concentration was lower with decreasing FD molecular weight (results not shown). These findings indicate that the sensitivity and range of the system can be “tuned” to some extent by controlling FD molecular weight.

5.4.3 Effect of Concentration on Sensor Response

To further explore the tunability of the system, sensitivity experiments were repeated at four different concentrations of FD-500kDa/TAG complexes. For these tests, the total FD/TAG complex concentration was varied over a wide range, but the ratio of FD/TAG mass was held constant in all experiments. An initial fluorescence spectrum was collected in each case for FD/TAG complex concentrations of 38pM/106 nm, 125pM/298 nm, 275pM/694 nm, and 1100pM/2620 nm, respectively. Fluorescence spectra were collected after each addition of glucose to the FD/TAG complexes and, as expected, there was a change in the FITC:TRITC peak ratio with the addition of glucose, which is plotted as percentage change in normalized peak ratio in Figure 5.6. In all cases, glucose solution was added until there was no further change in the FITC to TRITC peak ratio value indicating a saturated response, except for the highest concentration, where

the response did not reach saturation even with the addition of 300 mM glucose. The sensitivity and dissociation constant (k_d) for these four systems are plotted versus complex concentration over the range of 0-30 mM glucose concentration in Figure 5.7.

It is evident that the concentration of complexes that are present dramatically affects both the sensitivity and the range of the response. With approximately a thirty times increase in the FD/TAG complex concentration, the sensitivity was reduced by four times and the dissociation constant was increased by approximately five times the value for the lowest concentration. The required glucose concentration to reach the saturation point was increased approximately 10 times, from 30 mM to 300 mM, when the FD/TAG complex concentration was increased approximately 30 times (FD concentration from 38 to 1100pM).

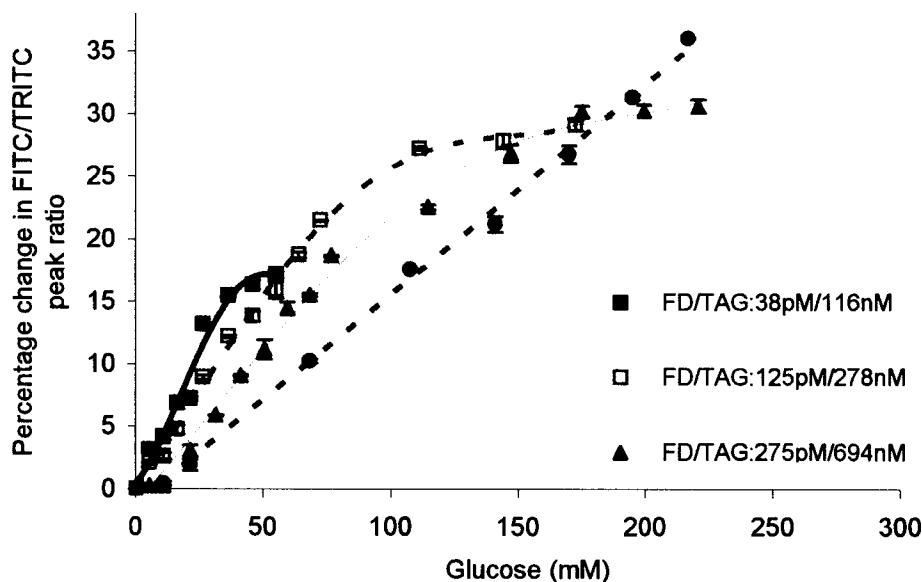


Figure 5.6. Percentage change in FITC:TRITC peak ratio with the addition of glucose into different FD/TAG complex concentrations. Lines are regression curves used only to clearly indicate the trend for each set of measurements. Error bars show one standard deviation of three replicate measurements.

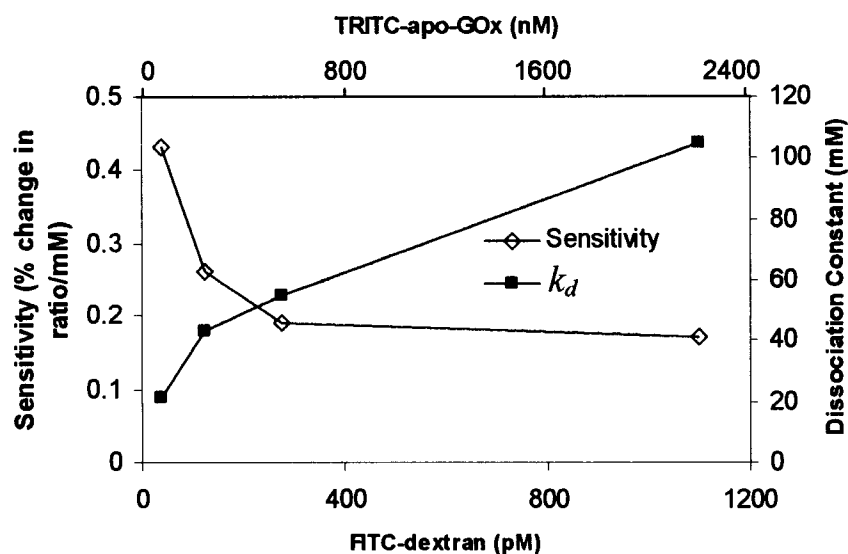


Figure 5.7. Relationship of sensitivity (%/mM) and dissociation constant (k_d) to concentration of assay components (constant mole ratio).

These results agree with the previous studies on the effect of receptor:ligand ratio on sensor response using a single dimensionless equation (discussed in Chapter Three (Figure 3.5)), which shows that there is an increase in the fluorescence from free-ligand with the increase in analyte concentration.¹⁴⁶ Also, with the increase in the total concentration of the assay elements while keeping the ligand/receptor ratio constant, there is drop in sensitivity and an increase in the detection range (Figure 3.6), which agrees with the results obtained in this particular experiment.

By comparing the results obtained in the current and previous sections, it can be concluded that the sensor response follows the same trend with the increase in dextran molecular weight and FD/TAG complex concentration, because the final condition in both cases is identical, i.e., there is an increase in FD/TAG complex concentration. Thus, the sensor properties can be tailored by varying the dextran molecular weight or FD/TAG complex concentration.

5.4.4 Specificity

It is known that glucose oxidase exhibits a high degree of specificity for β -D-glucose. It has been reported that α -D-glucose, D-mannose and D-fructose are also oxidized by the enzyme, but at least at a 20-fold reduced rate.¹⁴⁷ This suggests that the binding specificity for the molecules is likely to be different. However, in the case of the apo-enzyme, the specificity had to be experimentally determined as no previous reports were found. To observe the effect of different sugars on the response of the FD/TAG glucose assay, the sensitivity experiments were repeated with β -D-glucose, mannose, α -D-glucose, and sucrose. For these experiments, the starting concentrations for the assay complexes were 270pM:170 nm FD:TAG. To observe the specific nature of the sensor, the different sugar solutions were titrated into the sample in a stepwise manner until the RET reached saturation. The corresponding percentage change in FITC:TRITC peak intensity ratios versus sugar concentration are plotted in Figure 5.8. It can be observed from the response curves that the maximum sensitivity was achieved with β -D-glucose, and there was ~5–10 times lower sensitivity for mannose, sucrose, and α -D-glucose.

The total percentage changes in peak ratio with the addition of different sugars also follows the same trend as the sensitivity, i.e., with the addition of 50 mM β -D-glucose, mannose, α -D-glucose, and sucrose solutions there is 16.9%, 6.0%, 5.9%, and 2.5% change in RET, respectively. The dissociation constants for β -D-glucose, mannose, α -D-glucose, and sucrose were observed to be 14 mM, 24 mM, 46 mM, and 3 mM, respectively. It can be observed that in the case of sucrose, the linear region is reduced by more than 10X compared to glucose. This large difference in sensor response is attributed to the significant variation of the sucrose structure (disaccharide) from that of β -D-

glucose (monosaccharide), which results in very weak hydrogen bond interactions between sucrose and apo-GOx.¹⁴⁷ The above results prove that apo-GOx retains its binding specificity for β -D-glucose, and the presence of low levels of other sugars will not significantly interfere with accurate measurement of glucose concentration.

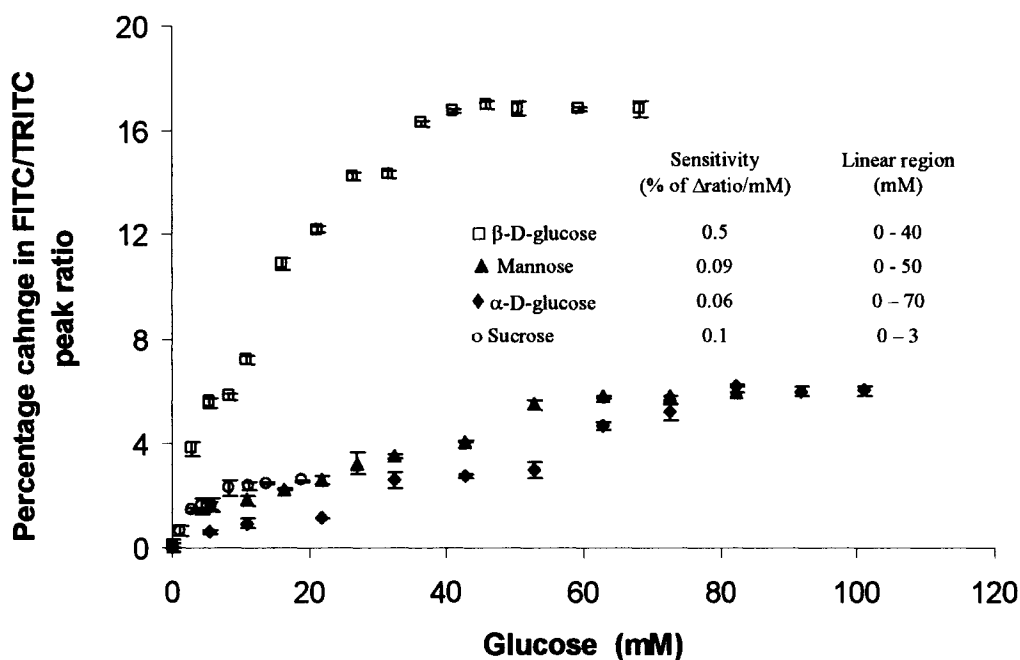


Figure 5.8. Percentage change in the normalized FITC:TRITC peak ratio values with the addition of different sugars. Error bars denote one standard deviation of three replicate measurements.

5.4.5 Encapsulation of FD/TAG Complexes in Microcapsules

Microcapsules with $\{(PSS/PAH)(PSS/DAR)_3(PSS/PAH/PSS)\}$ shell architecture were prepared as previously described and used for encapsulating FD/TAG complexes. Both FD-500kDa/TAG and FD-2MDa/TAG complexes were encapsulated in parallel experiments. Confocal images of representative polyelectrolyte microcapsules loaded with the glucose assay (there was no obvious difference between capsules loaded with FD-500KDa and FD-2MDa) are shown in Figure 5.9. It can be observed from the images

of capsules in loading solution (Figure 5.9(a-b)) and corresponding line scan in Figure 5.9(g), that there is equal concentration of FD/TAG in the interior and exterior of the capsules. This was expected because the semi-permeable capsule walls allow diffusion of macromolecules. However, the exposure of the microcapsules to UV light results in the crosslinking of the adjacent DAR and PSS layers in the capsule wall, decreasing the permeability of the capsule walls to FD/TAG complexes. As the final step, the capsules were rinsed to remove excess FD/TAG complexes, yielding microcapsules loaded with the sensing assay (Figure 5.9(c-f)). It can be observed from Figure 5.9(c-d) that the FITC and TRITC fluorescence is concentrated in the capsule interior and walls, indicating the immobilization of FD/TAG complexes inside and on the capsule walls. When UV light was not used to irradiate capsules before rinsing in DI water, the resulting capsules showed weak fluorescence from the capsule walls with no fluorescence from the solution in the interior of the capsules. High encapsulation in the walls could be due to a combination of electrostatics (residual charged residues of polyelectrolytes in walls), van der Waals forces, different solubility/partitioning, and physical entrapment of the sensing elements (upon crosslinking). Due to the relative magnitude of the forces, it is likely that electrostatic forces of attraction between negatively charged FD/TAG complexes and positive polymer layers in the capsule walls dominate all the other types of interactions. It is noteworthy that association with capsule walls is seen without the wall crosslinking, so the contribution of the latter effect is expected to be minimal.

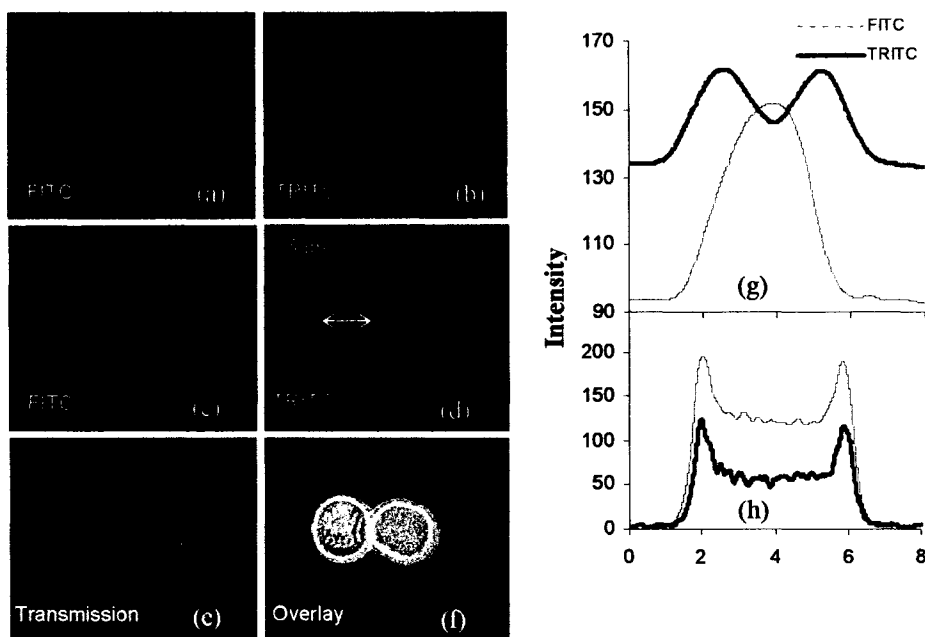


Figure 5.9 Confocal images of the microcapsules (a) & (b) in FD-500KDa/TAG complex loading solution; (c) & (d) after UV exposure and rinsing in DI water; (e) phase transmission image of the loaded microcapsules; (f) overlay of FITC, TRITC fluorescence and transmission mode image. Fluorescence line scan of the capsules (g) during loading process (from a and b) and (h) after encapsulation process (from c and d).

From Figure 5.9(e-f), which clearly show the capsule walls before and after encapsulation and from the line scans (Figure 5.9(g-h)) of the loaded and rinsed capsules, it can be observed that the encapsulated FD/TAG complexes are distributed uniformly in the hollow interior and on the capsule walls. The mismatch of the shapes of the line scans in Figure 5.9(g-h) is due to the loading protocol used. It can be observed from the intensity scales, that the average intensity value inside the capsule is almost the same. There are no peaks at capsule walls for FD-line scans because the dextran can readily diffuse into capsules without any entrapment in the walls. However, during the encapsulation of TAG after loading of FD, it was observed that a much stronger green fluorescence signal was associated with the capsule walls, as dextran could be attracted to TAG, which was entrapped in the walls due to its structure and charge. Therefore, after

rinsing, a fraction of the FD and TAG was entrapped in the capsule walls, which resulted in the strong peaks in the FD-line scans in Figure 5.9(g). It is noteworthy that the broad peaks of TAG in Figure 5.9(g) are due to the presence of TAG, still present when the image was collected. However, after the excess TAG was removed high intensity from the walls results in apparently sharper edges.

The encapsulation efficiency of FD/TAG complexes was estimated by measuring the absorbance of the rinse solutions and obtaining the capsule count using the Coulter counter. The results, presented in Table 5.1 prove that each capsule contains $\sim 10^{-17}$ and 10^{-15} moles of FD and TAG, respectively, in the capsules loaded with FD-500kDa/TAG and FD-2MDa/TAG complexes (the mass of the loaded FD and TAG was in the same order of magnitude for the two sets of capsules considered). It can be observed from Table 5.1 that the FD/TAG mole ratio is slightly higher in the case of the smaller dextran due to encapsulation of more FD-500kDa moles relative to FD-2MDa. Using the molecular weights of dextran and glucose molecules, it was estimated that there are 1.27×10^{-13} and 2.16×10^{-13} total glucose residues in the capsules loaded with FD-500kDa/TAG and FD-2MDa/TAG complexes, respectively. The greater number of glucose residues provide more binding sites for apo-GOx molecules, which is supported by the calculations in Table 5.1. It can be observed that there is a greater number of TAG molecules in the capsules loaded with FD-2MDa/TAG (1.07×10^{-15}) as compared to FD-500kDa/TAG (7.85×10^{-16}), because of a larger number of glucose residues in the former case. Even though there is a 1.7 times increase in the number of glucose residues in FD-2MDa/TAG loaded microcapsules over FD-500kDa/TAG loaded capsules, there is only 1.3 times increase in the corresponding TAG concentration. While this suggests that the

apo-GOx/dextran association does not scale linearly with the dextran length, further investigation on what factors affect encapsulation efficiency will be required to establish a clear mathematical relationship. However, these results do prove that the amount of sensing assay in the microcapsules does vary with molecular weight, and the sensor response characteristics depend upon the encapsulated assay concentration, ligand size, and FD/TAG ratio.

Table 5.1. Encapsulation efficiency parameters for FITC-dextran of two different molecular weights.

Calculated parameters	FITC-Dextran MW (Da)	
	500k	2M
# of FD-moles and mass (pg)/capsule	$5.1 \times 10^{-17}/25.4$	$2.2 \times 10^{-17}/43.3$
# of TAG moles and mass (pg)/capsule	$7.9 \times 10^{-16}/125.2$	$1.1 \times 10^{-15}/171.3$
FD/TAG mole ratio in a capsule	6.5×10^{-2}	2.0×10^{-2}
# of glucose residues/FD molecule	2500	10000
# of glucose moles/capsule	1.3×10^{-13}	2.1×10^{-13}
# of glucose residues/ TAG molecule	1.6×10^2	2.0×10^2

5.4.6 Leaching of Encapsulated Molecules from Microcapsules

Loss of FITC-dextran (FD) and TRITC-apo-glucose oxidase (TAG) molecules from microcapsules was quantified using fluorescence spectroscopy studies, where release of the encapsulated molecules from the microcapsules was observed as an increase in the fluorescence intensity of the supernatant. The results obtained from this experiment are given in Figure 5.10, where the percentage leached indicates the percentage of initially encapsulated FD and TAG molecules lost from the capsules to the supernatant solutions. These experiments were performed on capsules loaded with FD-500kDa/TAG and FD-2MDa/TAG complexes. It is clear from the data that the leaching is higher for the capsules loaded with FD-500kDa/TAG, but still less than 4%. This

result is intuitive because the diffusivity scales as the inverse of the square root of molecular weight, and both free and complexed forms of FD-500kDa will have larger diffusivity than the corresponding free and complexed forms of FD-2MDa. It is also noteworthy that dextran molecules, which possess a linear structure with branches, are expected to diffuse more readily through the capsule walls compared to apo-GOx molecules (globular structure) because of the lower hydrodynamic volume. This trend can be observed in Figure 5.10, which shows that the amount of FD leached is always greater than corresponding TAG concentration. Since the TAG is bound to FD, relatively few TAG (2M-TAG) molecules can diffuse out of the capsule in the case where TAG is bound to FD-2MDa.

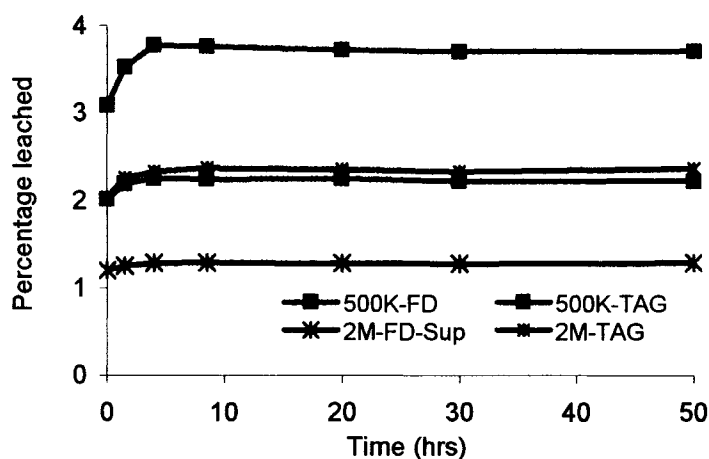


Figure 5.10. Percentage of the initially encapsulated FD and TAG in the microcapsules lost to the supernatant; (500K-FD and 500K-TAG) and (2M-FD and 2M-TAG) indicate the FD and TAG moles in the supernatant corresponding to the capsules loaded with (FD-500kDa/TAG) and (FD-2MDa/TAG) complexes, respectively.

It is very likely that the 4% loss in the loaded materials is due in part to molecules weakly trapped in or on the capsule walls, because there is no significant barrier present to resist diffusion of the assay molecules. It is noteworthy that in all cases there is only a small amount of leaching i.e., about 1 – 4% of the initially encapsulated molecules that

occurs during the first 10hrs of leaching studies, after which there was no change in the fluorescence intensities from the supernatant solutions. Thus, the photo-crosslinking technique appears to be an appropriate approach for stable encapsulation of the elements for the competitive binding assay.

5.4.7 Sensor Response to Glucose Addition in Microcapsules

Glucose sensitivity experiments were performed on the microcapsules loaded with FD-500kDa/TAG and FD-2MDa/TAG complexes. The fluorescence spectrum was collected after each addition of β -D-glucose to microcapsules loaded with FD/TAG complexes and the corresponding percentage change in the FITC:TRITC peak ratio was calculated for each case, as shown in Figure 5.11. It can be seen that there is a linear increase in the peak ratio with the addition of glucose up to 30 mM for the capsules loaded with FD-500kDa/TAG complexes, with a sensitivity of 2.75%/mM. The signal saturation after 30 mM indicates that all the available binding sites on apo-GOx were occupied by glucose molecules.

By closely examining the curves in Figure 5.11, it becomes obvious that there is a small difference between the glucose responses of the two sets of capsules. The sensitivity over the linear region (0-30 mM) for capsules loaded with FD-2MDa/TAG complexes was 2.5%/mM. A possible reason for this is the difference in encapsulation efficiency, which will be discussed below in more detail. By using the encapsulation efficiency and back calculating the number of FD and TAG molecules in both samples, it was found that the ratio (no. of glucose moieties/TAG) is approximately equal in the two sets of capsules loaded with FD-500kDa/TAG and FD-2MDa/TAG complexes (Table

5.2). Thus, the minimal variation in the sensor response of the two sets of microcapsules is attributed to the insignificant difference in the concentration of sensing assay elements.

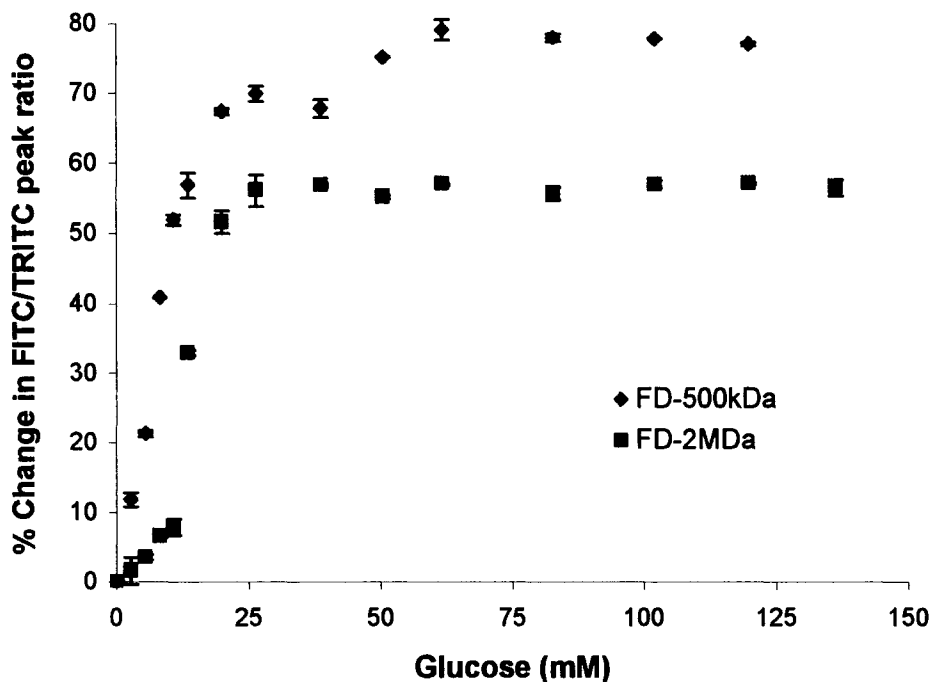


Figure 5.11. Percentage change in the normalized FITC:TRITC peak ratio with the addition of glucose to the microcapsules loaded with FD-500kDa/TAG and FD-2MDa/TAG complexes. Error bars show one standard deviation of three replicate measurements.

Table 5.2. Details of the sample used for testing sensor response in microcapsules.

Calculated parameters	FITC-Dextran MW (Da)	
	500k	2M
# of FD moles (picomoles)	20.5	6.7
# of TAG moles (picomoles)	315.5	329.5
# of glucose residues/FD	2500.0	10000.0
# glucose moles (picomoles)	51219.5	66659.5
# of glucose residues/TAG	162.3	202.0

It was previously found that there is a considerable variation in the sensitivity and dissociation constant with different molecular weights of dextran for solution-phase experiments, which is due to the high FD/TAG complex concentrations and not merely

due to the increase in molecular weight. In the case of microcapsules, however, the encapsulation efficiency is limited by the molecular weight of the loading materials and capsule size. Therefore, the loading procedure resulted in the encapsulation of almost an equal mass of FD and TAG per capsule in the capsules loaded with FD-500kDa and FD-2MDa (Table 5.1). As opposed to solution phase experiments, there is no significant variation in the sensing assay concentration with the encapsulation of FD-500kDa/TAG and FD-2MDa/TAG into microcapsules (Table 5.2). Thus, there is no significant difference in the sensor response of the two sets of capsules. This explanation agrees with the solution phase experimental results (Figure 5.4 and Figure 5.6), which show that there is a significant change in the sensor response mainly with the variation in FD/TAG complex concentration. Thus, it can be concluded that the sensor response is mainly dependent on the number of ligand and receptor molecules that are available, and not the size of the ligand molecule. The small difference in sensor response of the two sets of microcapsules could result from the difference in the encapsulation efficiency or the behavior of dextran molecules with different molecular weights due to the conformation of dextran chains in the capsule interior.

5.4.8 Effect of Capsule Concentration on Sensor Response

It was demonstrated in solution phase experiments that the sensor response can be tailored by varying the assay concentrations. In order to test the feasibility of tailoring the sensor response with the sensing assay encapsulated in microcapsules, the glucose sensitivity experiments were performed with FD-500kDa/TAG loaded capsules at three different concentrations: 1×10^6 , 2×10^6 , and 3×10^6 capsules/mL. Fluorescence scans were collected at each addition of glucose solution to the capsules, and the corresponding

changes in the FITC:TRITC peak ratios for all three samples are plotted in Figure 5.12. It is immediately evident that with a 3X increase in capsule concentration, there is a decrease in the total change in the percentage of RET from 73% to 58%, and also a higher glucose concentration is required to reach the FITC:TRITC peak ratio saturation point. It can be seen from Table 5.3 that a 3X increase in capsule concentration results in a 3.1X decrease in sensitivity and a 4X increase in dissociation constant. This trend corroborates the solution-phase experimental results. These results prove that the sensitivity can be tailored by changing the competitive binding assay concentration, regardless of the environment of the assay.

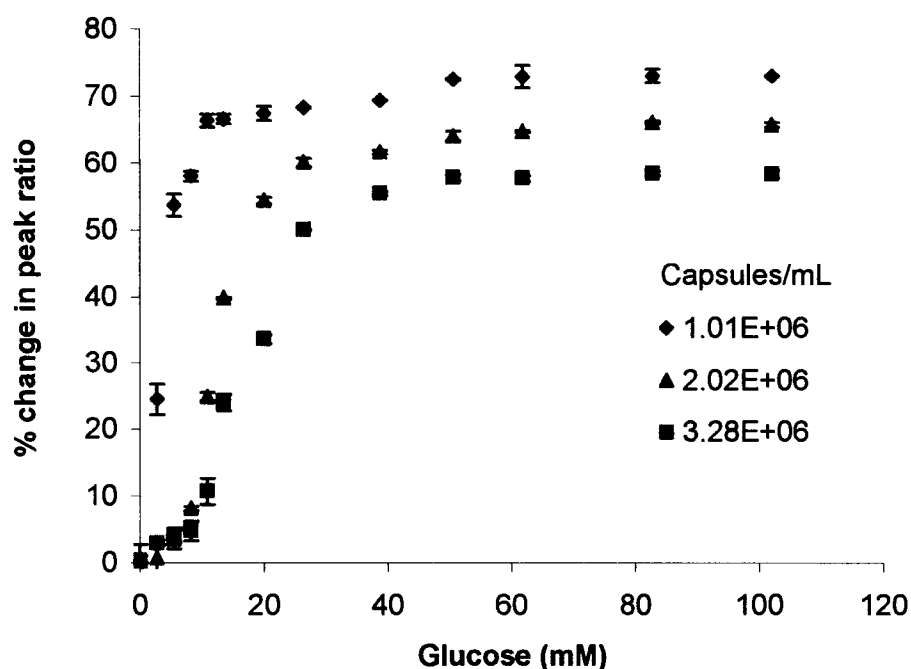


Figure 5.12. Effect of capsule concentration on the change in FITC:TRITC peak ratio with the addition of glucose solution. Error bars show one standard deviation of three replicate measurements.

Table 5.3. Change in sensitivity and dissociation constant with varying capsule concentration.

Capsules/ mL	FD (moles)	TAG (moles)	Sensitivity (% Δ ratio/mM)	Total change in peak ratio/100mM glucose (%)	Linear range (mM)	k_d (mM)
1.0×10^6	2.1×10^{-11}	3.2×10^{-10}	6.11	73	0 - 10	5
2.0×10^6	4.1×10^{-11}	6.3×10^{-11}	2.67	66	0 - 30	12
3.2×10^6	6.7×10^{-11}	1.0×10^{-9}	1.95	58	0 - 40	19

It can be observed from the microcapsule and solution phase glucose sensitivity experiments that there is approximately a two-fold increase in the sensitivity for the case of the microcapsules. This observation is the result of a low concentration of mobile sensing assay elements, due in part to the entrapment of ~70% of the total encapsulated molecules in the capsule walls. The apo-GOx and dextran molecules that are entrapped in the walls may not dissociate in the presence of glucose molecules. Thus, the total number of mobile molecules will be far less than in solution phase samples. This low concentration (~30%) of freely moving FD/TAG complexes is ultimately reducing the active sensing assay concentration which results in the increased sensitivity, as predicted by theory, and was experimentally verified by studying the effect of competitive binding assay concentration on response (Figure 5.7).

The response time of this system was not measured separately, because the sensor response was observed to reach steady-state in approximately 1-2 minutes which is the approximate time required for the collection of one fluorescence scan. There was no observable change in the response time with the variation in assay elements concentration and ligand molecular weight. The response kinetics will be the subject of future studies, but clearly the response occurs in a reasonable time and will not be a limiting factor for implementation of this system for glucose sensing.

5.4.9 Reversibility of the Glucose Sensors

The reversibility of the fabricated sensors was tested by exposing FD-500kDa/TAG loaded microcapsules to random glucose concentrations. Fluorescence spectra were collected after each addition and removal of glucose solution from the microcapsules and the corresponding changes in FITC:TRITC peak ratios are plotted in Figure 5.13. It is clear that there is a linear response in the 0-10 mM range and a decreased yet measurable response up to 20 mM, which covers much of the region of interest for glucose monitoring in diabetics. Sensitivity with random glucose concentrations was calculated to be 2.5%/mM with a total sensitivity of more than 50%, which is comparable to the sensitivity obtained with capsules exposed to a stepwise increase in glucose concentrations. These results show that the microcapsule based sensors are completely reversible without any significant loss in sensitivity. Further assessment of the forward and reverse response kinetics is currently being studied with a flow-through system.

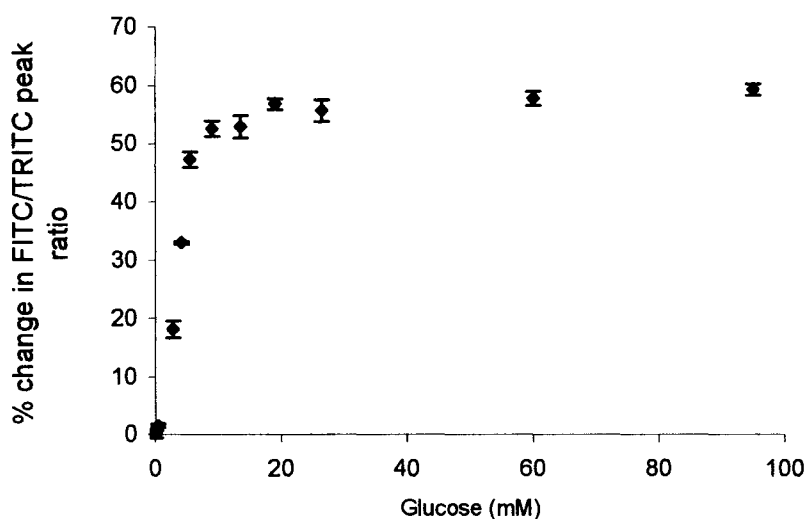


Figure 5.13. Percentage change in the normalized FITC:TRITC peak ratio with the addition of random glucose concentrations to the microcapsules loaded with FD-500kDa/TAG complexes. Error bars show one standard deviation of three replicate measurements.

In the above demonstrated system, the use of prefabricated microcapsules for carrying the sensing assay is advantageous, because it allows (a) for the free movement of sensing elements during competitive binding process, which is critical for proper functioning of the sensor that rely upon the equilibrium association and dissociation of free molecules, and (b) in maintaining the constant concentrations of the ligand and receptor with continuously varying analyte concentration. The generic sensor design described here opens the door for a wide variety of analytes to be sensed using the versatile sensing technique, which involves selection of analyte-specific enzyme and a competing ligand, and can be considered a platform technology for development of biosensors based on competitive-binding and fluorescence RET based techniques. Potential targets include neurochemicals, such as glutamate and choline, lipids, and estrogen.¹⁴⁸ The general approach to construction of specific “smart” responsive systems may be useful in other applications, such as drug delivery, wherein the apo-GOx/dextran dissociation determines release of an encapsulated compound in response to glucose.¹⁴⁹

The sensitivity of apo-GOx/dextran system was observed to be 10^3 times greater than Con A/dextran system that was demonstrated in Chapter four. Even though, the encapsulation techniques in both the cases are entirely different, we did not try to develop a Con A/dextran sensing system using the DAR based encapsulation technique, because of the demonstrated advantages of apo-GOx and its excellent sensor response characteristics. Even if a Con A/dextran system were to be demonstrated with comparable sensitivity to apo-GOx based system using different encapsulation techniques or FRET pairs, it would not be of any greater significance because of the disadvantages of Con A.

With specific reference to the glucose-sensing microcapsules described here, the sensors employing apo-GOx elements can potentially be used for *in vivo* glucose sensing without the concern of the toxicity associated with Con A. It is also noteworthy that the sensors can be easily extended into the NIR region by replacing the FITC-TRITC RET pair with an appropriate NIR donor-acceptor combination. It is also appropriate to note that these sensors could be interrogated using fluorescence lifetime measurements,^{21,90,91} which will be better suited to *in vivo* monitoring because they are less affected by the fluorophore concentration and optical properties of the medium.

5.5 Conclusion

A novel glucose sensing system based on competitive binding, resonance energy transfer, and polymer microcapsule technology has been demonstrated. Microcapsules containing FD/TAG complexes showed a decrease in RET due to the addition of glucose, with the sensitivity ranging from 2 – 6% /mM over the range of 0 to 40 mM. It was found that the key variable in tuning the response of the system (sensitivity and dissociation constant) to glucose is the concentration of FD/TAG complexes. The assay comprising an apo-GOx recognition element showed 5 to 10 times more sensitivity to β -D-glucose as compared to other sugars. Based on the sensitivity, specificity, dissociation constant values, and reversible response, this sensor system appears to be suitable for glucose monitoring in diabetic patients. The apo-enzyme based competitive binding assay described in this chapter can be used as a platform technology for developing different biosensors to detect several neurochemicals, such as, glutamate, choline and ascorbic acid using the respective enzymes (glutamate oxidase, choline oxidase, and ascorbate oxidase) as receptor molecules. Also, other analytes such as, cholesterol and lactate may also be

detected using this technology. These glucose-responsive FD/TAG complexes can also potentially be used in the future for controlled drug delivery studies, e.g.: insulin can be released due to apo-GOx/dextran dissociation in response to glucose.

In spite of the advantages of this sensor design, it may not be an ideal system for subcutaneous implantation, because of the use of dyes which fluoresce in the visible region. The main disadvantage of the prototype microcapsule-based glucose sensors is the use of FITC and TRITC as the energy transfer pair. While more photostable analogs of these dyes are available, these visible excitation/emission systems operate at short wavelengths where tissue is highly scattering. Even if fluorescence lifetime measurements are used for *in vivo* interrogation, it is desirable to replace the visible range fluorescent dyes with near infrared (NIR) fluorophores to increase penetration depth and decrease scattering losses. The next chapter demonstrates a similar sensor design using dyes that fluoresce in the orange/red region.

CHAPTER 6

FLOURESCENT GLUCOSE SENSORS OPERATING IN ORANGE/RED REGION

This chapter is the extension of the sensor design demonstrated in Chapter Five in to longer wavelength (orange/red) region. This chapter describes the investigation of glucose sensitivity of TRITC-dextran/cyanine(Cy5)-apo-GOx complexes encapsulated in polyelectrolyte microcapsules using fluorescence spectroscopic and imaging techniques, and compares their performance characteristics with those obtained for the FITC:TRITC energy transfer pair to determine the sensor response characteristics after replacing the green/orange dyes with the orange/red fluorescence RET pair.

6.1 Sensor Design

The transduction mechanism used in this sensor is similar to the one illustrated in Figure 5.1. The basic procedure for apo-GOx preparation was followed as previously described.²³ The apo-GOx prepared by this method was observed to maintain its reduced catalytic activity and preserve its binding capacity for at least four weeks. The close proximity of Cy5-apo-GOx (CAG) and TRITC-dextran (TD) in the absence of glucose results in strong fluorescence peaks due to energy transfer from TRITC to Cy5. As apo-GOx has higher affinity for glucose over dextran, the addition of glucose results in the

displacement of dextran from apo-GOx, accompanied by a decrease in the energy transfer efficiency, which will be indicated by a stronger TRITC peak relative to Cy5. It is noteworthy that this apo-enzyme sensing approach retains the advantages of competitive binding assays (no analyte consumption) and RET-based sensors (ratiometric, high sensitivity) while adding the high specificity of enzymatic sensors and reduced scattering due to the employment of longer wavelength fluorophores.

6.2 Experimental Section

Materials. Amino-dextran (MW 500kDa), GOx (G-2133), sodium poly(styrene sulfonate) (PSS, MW ~1MDa), poly(allylamine hydrochloride) (PAH, MW 70kDa), β -D-glucose, mannose, α -D-glucose, sucrose, sodium bicarbonate, dimethyl formamide, ammonium sulfate, and sodium acetate buffer were obtained from Sigma. Tetramethylrhodamine isothiocyanate (TRITC) and Cyanine bis-NHS ester (Cy5) were obtained from Molecular Probes and conjugated to amino-dextran and apo-GOx, respectively, using standard amine labeling procedures.¹³⁶ Diazo-resin (Diazo-10, 4-diazodiphenylamine/formaldehyde condensate hydrogen sulfate-zinc chloride salt, DAR) was purchased from PC Associates, NJ. All reagents were used as received. MnCO_3 (5 μm) particles were prepared as previously described as templates for the polymer microcapsules.¹⁴²

Instrumentation. A UV-Vis spectrometer (Perkin Elmer Lambda 45) was used to collect absorbance spectra. The slit size (4 nm) and scanning speed (480 nm/min) were held constant throughout all the experiments. A scanning fluorescence spectrometer (QM1, Photon Technology International) was used to collect fluorescence emission spectra by exciting the sample at 543 nm. A 100-W longwave UV lamp (Blak-ray[®])

Model B 100AP, Entela) was used to irradiate the microcapsules for photocrosslinking the PSS and DAR layers in the capsule walls. Confocal images were taken with a Leica TCS SP2 microscope equipped with a 63X oil immersion objective and green and red He-Ne excitation lasers. Counts and sizes of microcapsules were obtained with a Beckman Coulter counter (Z2) using a 100 μ m aperture. A YSI biochemical analyzer was used to measure the glucose concentrations.

6.3 Methods

6.3.1 Solution Phase Experiments

All glucose sensitivity experiments were performed in PBS (0.01M phosphate buffer, 0.0027 potassium chloride, and 0.137M sodium chloride) solution maintained at pH 7.4. The apo-GOx and amino-dextran used in all experiments were conjugated to Cy5 and TRITC, with a labeling ratio of 1.14 and 1.12, respectively. In all experiments, the changes in energy transfer from TRITC-dextran (TD) to Cy5-apo-GOx (CAG) were monitored at every step using a fluorescence spectrometer to collect emission across the range of 560-725 nm. Initially, 17 picomoles of TD (donor) were added to 0.4 mL of PBS, which was followed by the stepwise addition of 80 picomoles of total CAG into the sample solution. To observe the dissociation of dextran and apo-GOx complexes with the addition of glucose, RET changes were observed with the titration of 100 mg/mL β -D-glucose solution aliquots into the sample containing TD/CAG complexes.

It is known that glucose oxidase (GOx) exhibits at least a 20X higher specificity for β -D-glucose over other sugars (e.g. α -D-glucose, D-mannose, D-fructose).¹⁴⁷ Previously in Chapter five (Figure 5.8), the specificity of the glucose sensor based on (FITC-dextran, FD)/(TRITC-apo-GOx, TAG) was found to be five to ten times more

specific to β -D-glucose compared to other sugars. The specificity of the new sensor was investigated in this report because the amine conjugation efficiency of Cy5 is much greater than TRITC, which could result in a different degree of labeling near glucose binding sites and this could ultimately change the binding properties. The specific nature of the sensor for glucose was demonstrated by performing similar RET measurements with the titration of β -D-glucose, α -D-glucose and mannose into the solution of TD/CAG complexes, maintaining all other parameters constant. Sensitivity curves were obtained by plotting the percentage change in TRITC: Cy5 peak ratio versus analyte concentration. The slope of the linear region was calculated as a measure of response sensitivity.

6.3.2 Formation of Hollow Microcapsules

Solutions of PSS (anionic), PAH (cationic), and DAR (cationic) used for assembling {PSS/PAH} and {PSS/DAR} multilayers were prepared in DI water at 2mg/mL. As described in detail in Figure 5.2, the positively-charged manganese carbonate (MnCO_3) particles were coated with the ionic polymers to obtain a final architecture of {(PSS/PAH)(PSS/DAR)₃(PSS/PAH/PSS)}. Hollow microcapsules were then obtained by dissolving the MnCO_3 cores using 0.1M hydrochloric acid (HCl) solution.

6.3.3 Encapsulation of Sensing Elements

The microcapsules prepared as described above contain porous walls, which are permeable to sensing elements (TD and CAG) prior to UV irradiation, but become impermeable after photocrosslinking.¹⁴⁴ The microcapsule suspension was incubated in the mixture of 1 μ M TD and 6 μ M CAG for 60min, which allowed sufficient time for

diffusion of loading molecules into the capsule interior. In order to encapsulate the TD/CAG molecules in microcapsules, DAR and PSS layers in the capsule walls were crosslinked by exposing the microcapsules in loading solution to UV light. As the final step, the capsules were rinsed in DI water three times using centrifugation process to remove excess TD/CAG complexes, yielding microcapsules loaded with the sensing assay elements, with a final form as illustrated in Figure 6.1.

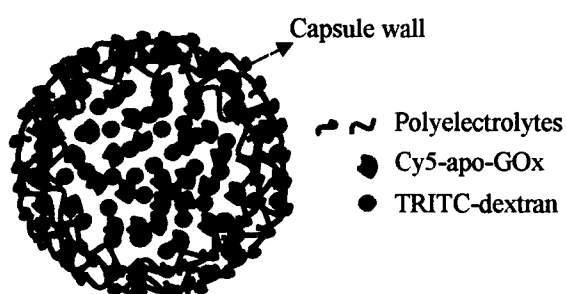


Figure 6.1. Schematic of the microcapsules loaded with dextran/apo-GOx complexes.

6.3.4 Sensor Response to Random Glucose Concentrations in Microcapsules

Glucose sensitivity experiments were performed on the microcapsules loaded with TD/CAG complexes to demonstrate a reversible sensor response. The sensing assay-loaded microcapsules were exposed to random glucose concentrations, after collecting an initial fluorescence spectrum with TD/CAG loaded microcapsules in PBS buffer. The random glucose concentrations were achieved by repeating two steps several times: (1) increase the glucose concentration with the addition of stock solution to microcapsules in buffer, then collect the fluorescence spectrum, and (2) reduce the glucose levels in the suspension by centrifuging and removing the supernatant (glucose) solution, measuring the actual glucose concentration of this solution with the biochemical analyzer, then

adding an equal volume of fresh PBS buffer without glucose. Fluorescence spectra were collected after each addition and removal of glucose solution from the microcapsules and the corresponding changes in TRITC: Cy5 peak ratios are calculated for changing glucose concentration. This procedure was repeated to cover the glucose concentration in the range of 0-2800mg/dL, in the order of 0, 164, 56, 108, 632, 433, 813, 1980 and 2800mg/dL.

6.4 Results and Discussion

6.4.1 Solution Phase Glucose Response Tests

Titration of TRITC-dextran up to 43 nM into 200 nM of CAG in PBS solution led to strong fluorescence emission peaks corresponding to TRITC and Cy5 at 543 nm excitation; implying significant energy transfer from TRITC to Cy5. To observe the displacement of dextran from apo-GOx with the addition of glucose, spectra were measured after the titration of 100mg/mL β -D-glucose solution aliquots into the sample containing TD/CAG complexes. As hypothesized, the glucose in the solution displaced dextran from apo-GOx resulting in decreased energy transfer from TRITC to Cy5, as indicated by the increase in TRITC peak relative to Cy5 (Figure 6.2(a)). The percentage change in TRITC: Cy5 peak ratio (relative to the baseline ratio, at zero glucose) as a function of glucose concentration is shown in Figure 6.2(b), from which it can be observed that there is a total change of 15% in energy transfer due to 360 mg/dL glucose. The data clearly show that the response is linear in the range of 0-540 mg/dL, with a sensitivity of 0.06%/(mg/dL). These measurements confirm that apo-GOx and dextran molecules were dissociated in the presence of glucose, though the overall change in

signal is only about one fourth of that observed when FITC and TRITC were used as the donor and acceptor, respectively.

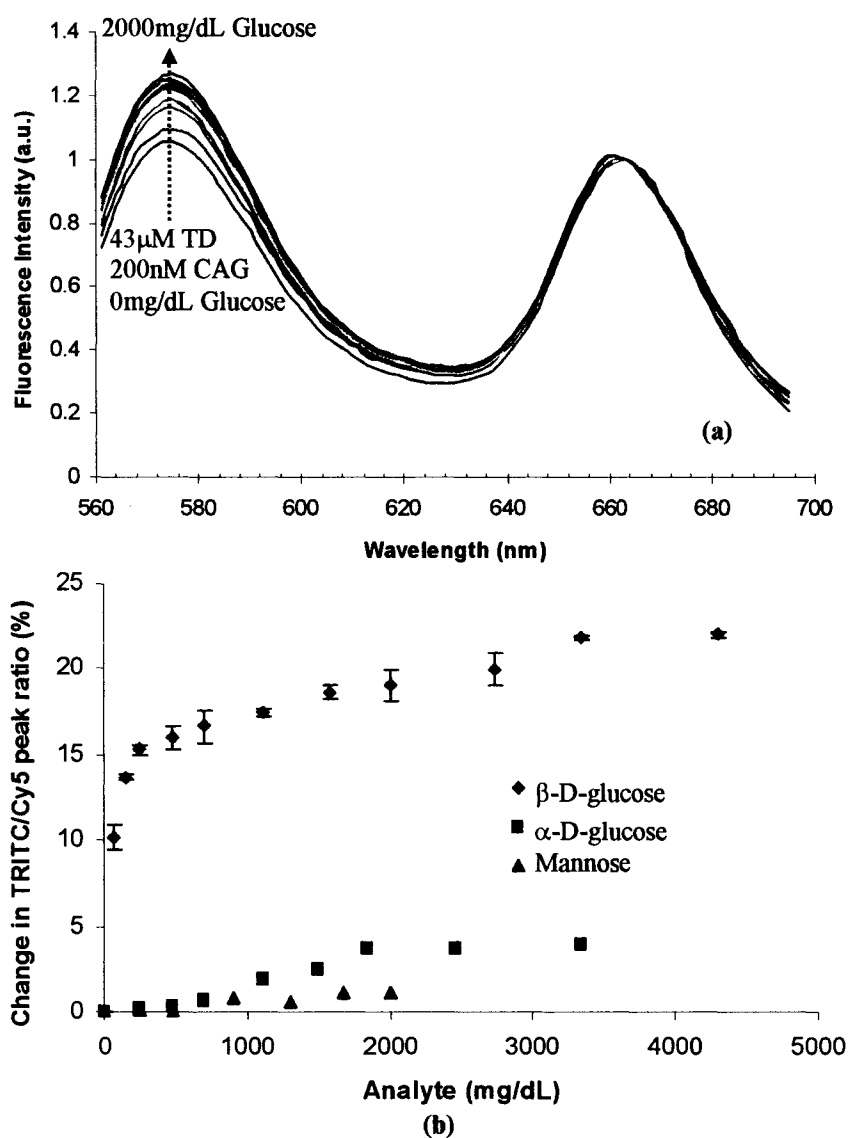


Figure 6.2. (a) Normalized fluorescence spectra with the addition of β -D-glucose to TD/CAG complexes in PBS buffer, (b) Percentage change in TRITC: Cy5 peak ratio with the addition of β -D-glucose, β -D-glucose, and mannose solutions. Error bars show one standard deviation of three replicate measurements.

6.4.2 Sensor Specificity

To demonstrate the specificity of the TD/CAG based glucose sensor, the RET measurements were performed with the titration of β -D-glucose, mannose, and α -D-glucose, into solutions of 50 nM:200 nM TD:CAG complexes. The corresponding percentage change in TRITC:Cy5 peak intensity ratio versus analyte concentration is plotted in Figure 6.2(b), from which it can be observed that the maximum sensitivity was achieved with β -D-glucose, and there was \sim 5–10 times lower sensitivity for mannose and α -D-glucose. This agrees with the previous results (Figure 5.8), and proves that the apo-GOx retains its binding specificity for β -D-glucose in spite of exposing the sensing elements to several chemical processes, such as protein precipitation, conjugation, etc.

6.4.3 Encapsulation of Sensing Chemistry in Microcapsules

Microcapsules with $\{(PSS/PAH)(PSS/DAR)_3(PSS/PAH/PSS)\}$ shell architecture were prepared as described and used for encapsulating TD/CAG complexes. Confocal images of polyelectrolyte microcapsules loaded with the glucose assay are shown in Figure 6.3, from which it can be observed that the TRITC and Cy5 fluorescence is concentrated in the capsule interior and walls, indicating the immobilization of TD/CAG complexes inside and on the capsule walls. High encapsulation in the walls could be due to a combination of electrostatics (residual charges of polyelectrolytes), van der Waals forces, different solubility/partitioning, and physical entrapment of the sensing elements (upon crosslinking). It is noteworthy that association with capsule walls occurs prior to wall crosslinking, so the contribution of the latter effect is expected to be minimal.



Figure 6.3. Confocal fluorescence images of typical microcapsules loaded with TRITC-dextran and Cy5-apo-GOx; (a) TRITC and (b) Cy5 fluorescence; (c) Overlay of the TRITC and Cy5 fluorescence.

6.4.4 Demonstration of Reversible Sensor Response

To test the reversibility of these sensors, loaded microcapsules were exposed to random glucose concentrations. The fluorescence spectra were collected after each addition and removal of glucose solution from the microcapsules, and the corresponding changes in TRITC: Cy5 peak ratios are plotted in Figure 6.4. It is clear that there is a linear response in the 0-720mg/dL range with a sensitivity of 0.05%/(mg/dL), which is comparable to the sensitivity obtained in solution-phase experiments. The dissociation constant in the case of TD/CAG was observed to be 202mg/dL, which is comparable to that obtained with FD/TAG complexes.

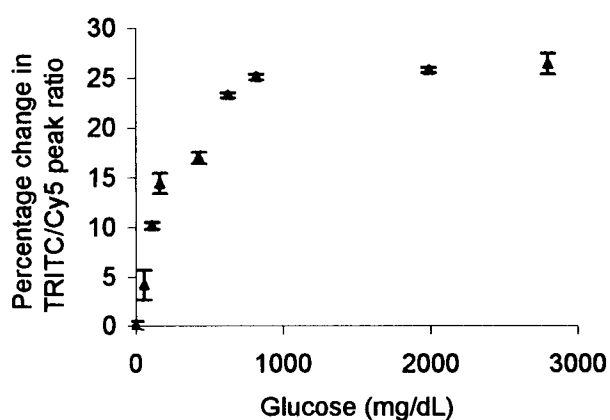


Figure 6.4. Percentage in TRITC: Cy5 peak ratio with the addition of random β -D-glucose concentrations to the TD/CAG loaded microcapsules. Error bars show one standard deviation of three measurements.

After comparing the results obtained with the current sensor design (TD/CAG) and previously reported FD/TAG based sensor, it was observed that there is a drop in sensitivity by a factor of three to four due to the replacement of FITC:TRITC dyes with TRITC: Cy5. This decrease in sensitivity may be attributed to several factors. First, the labeling ratio for dextran varied between the commercially-available FITC-dextran (24.5) and custom-labeled TRITC-dextran (1.12). Considering equal molar concentrations of FD/TAG and TD/CAG complexes, this variation in dextran labeling ratio could logically result in a lower average RET efficiency for bound dextran in the latter case. Consequently, with the addition of glucose, the total percentage change in energy transfer would reduce, translating into lower sensitivity. This reasoning is supported by the theory discussed in Chapter Three, which explains the significance of labeling ratio and RET efficiency. It was shown in the model that the decrease in RET efficiency, which is dependent on the labeling ratio of ligand and receptor molecules, will result in a significant drop in the sensitivity and detection range (Figure 3.8). Second, the TRITC-dextran used in this study was prepared using amino-dextran (cationic), whereas the FITC-dextran (from Sigma) was anionic. Because apo-GOx is anionic at pH 7.4, it is possible that a fraction of the cationic dextran used in this study could complex with apo-mGOx on the basis of electrostatic forces in addition to affinity forces. If the ionic complexes do not dissociate with the addition of glucose, this will contribute a strong static baseline signal for all of the measurements, resulting in decreased sensitivity. Finally, there is a significant variation in the conjugation reaction of apo-GOx with Cy5 compared to TRITC. For this study, the Cy5 bis-NHS ester can simultaneously bind to two amine groups on apo-GOx, whereas the isothiocyanate group of TRITC can only

react with a single amine. Binding multiple amine groups on the protein could partially disrupt the conformation of the apo-GOx and alter binding properties, resulting in a decreased glucose affinity. However, given the agreement between the dissociation constants obtained from the two studies, this last possibility is less likely to be a significant factor. Determination of the major contributing factors and sensitivity optimization will be part of future work.

The system demonstrated here carries the advantages of using (a) prefabricated microcapsules for carrying the sensing assay, because it allows for the free movement of the sensing elements during the competitive binding process, and in maintaining the concentrations of the ligand and receptor constant in the presence of continuously varying analyte concentration, and (b) orange/red dyes which will enable the use of longer excitation wavelengths where by tissue scattering is reduced making the sensor more appropriate for *in vivo* applications. It is noteworthy that even though there is a 3X drop in sensitivity with the use of longer wavelengths, this is not a large concern when the expected improvement in signal intensities measured through the skin is taken into consideration. It is also appropriate to note that these sensors could be interrogated using fluorescence lifetime measurements,⁹⁰ which will be better suited to *in vivo* monitoring because they are less affected by the fluorophore concentration and optical properties of the medium. Ongoing studies include complete sensor response characterization, including long-term stability analysis, and careful investigation of the reasons for sensitivity loss when longer-wavelength dyes are employed. The successful demonstration of apo-GOx/dextran based assay by replacing FITC/TRITC (as

demonstrated in Chapter five) with TRITC/Cy5 indicate that this assay can be modified according to the required application.

6.5 Conclusion

A novel glucose sensing system based on competitive binding, resonance energy transfer, and polymer microcapsule technology operating in the long wavelength region has been demonstrated. This glucose assay, comprised of apo-GOx/dextran complexes, showed ~5-10 times more sensitivity to β -D-glucose compared to other sugars. Microcapsules containing TRITC-dextran/Cy5-apo-GOx complexes showed a decrease in RET due to the addition of glucose, with a sensitivity of 0.06%/(mg/dL) over the range of 0-720mg/dL. Based on the sensitivity, specificity, and reversible response in the region of interest (0-360mg/dL), this sensing system can be used for glucose monitoring in diabetic patients. It is postulated that a 3X loss in sensitivity with the use of longer wavelength dyes will be compensated for by an increase in the intensity levels and a decrease in the signal to noise ratio. Therefore, future studies will aim at discovering the reasons for the sensitivity loss with longer wavelength dyes and focus more on the improvement of sensor response characteristics. These glucose-responsive systems can also potentially be used in future for “smart” drug delivery studies, e.g.: insulin may be released in response to apo-GOx/dextran dissociation.

CHAPTER 7

FLUORESCENT NEAR INFRARED

GLUCOSE SENSORS

In previous chapters, FRET based glucose sensors operating in visible and long-wavelength regions were demonstrated. In order to further extend this work to clinical studies, a glucose sensor operating in the near infrared (NIR) region is more appropriate because of the reduced light scattering in the dermis. However, the broad excitation spectrum of the available NIR dyes makes it impossible to find an efficient FRET pair for the NIR region. Therefore, this chapter employs the apo-GOx/dextran based competitive binding assay discussed in previous chapters, but now used in conjunction with a different transduction (quenching) mechanism. This chapter describes the investigation of an NIR glucose sensor comprised of competitive binding assay encapsulated in polyelectrolyte microcapsules, and compares their performance characteristics with those obtained for the FITC/TRITC, TRITC/Cy5 energy transfer pair to determine the sensor response characteristics with NIR dyes.

7.1 Sensor Design

A schematic of a glucose sensor based on the quenching mechanism is shown in Figure 7.1. The dyes used in this sensing mechanism are Alexa Fluor (AF) 647, QSY21,

and AF750. AF647 emits in the range of 650-720nm, which overlaps with the QSY21 absorbance spectrum. Therefore, when AF647 and QSY21 are in close proximity, QSY21 significantly quenches the fluorescence of AF647. As QSY21 is not fluorescent, there is only one fluorescent peak, preventing ratiometric analysis of the data. Therefore, AF750 is used as a reference dye, as it can be partially excited at 640nm (which is also the excitation wavelength for AF647). Also, AF750 is not influenced by the quenching and the presence of glucose. When apo-GOx tagged to AF647 is exposed to QSY21-dextran (QSY-dex), they will be in close proximity due to the binding affinity between apo-GOx and dextran. This results in the weak fluorescent peak at 675nm due to the quenching of AF647 by QSY21. Because of the high affinity of glucose towards apo-GOx, the addition of glucose will result in the displacement of dextran from apo-GOx, decreasing the quenching effect on AF647, which is indicated by a stronger AF647 peak (Figure 7.1). In this study, the glucose sensitivity of the AF647-apo-GOx (AF-AG)/QSY-dex complexes entrapped in microcapsules along with AF750 was demonstrated by measuring the changes in fluorescence intensities of AF647 relative to the reference dye (AF750).

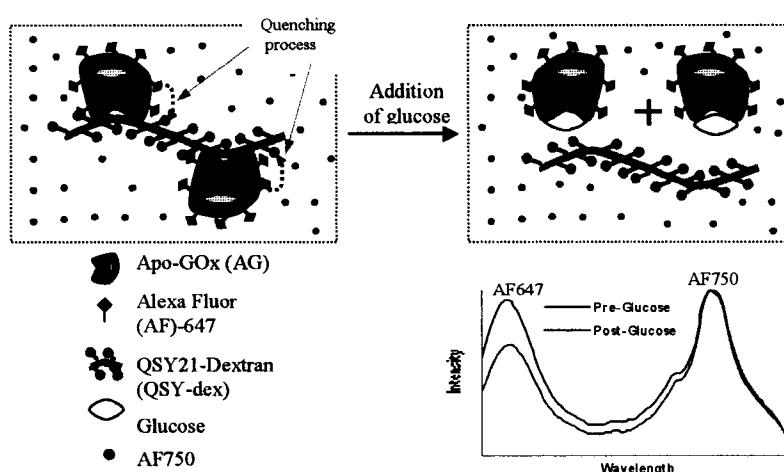


Figure 7.1. Schematic of the RET quenching system for glucose monitoring based on the competitive binding between dextran and glucose for binding sites on apo-GOx.

7.2 Experimental Section

Materials. Glycidyl 3-(trimethoxysilyl)propyl ether (glycidyl-silane), GOx (G-2133), sodium poly(styrene sulfonate) (PSS, MW ~1MDa), poly(allylamine hydrochloride) (PAH, MW 70kDa), β -D-glucose, sodium bicarbonate, dimethyl formamide, ammonium sulfate, sodium acetate buffer were obtained from Sigma. Alexa Fluor (AF) 647, AF 750, and QSY21 from Molecular Probes, were used to label apo-GOx, PAH, and amino-dextran (500kDa, Molecular Probes), respectively, using a standard amine labeling procedure.¹³⁶ All reagents were used as received. MnCO_3 (5 μm) particles were prepared as previously described.¹⁵⁰

Instrumentation. A UV-Vis spectrometer (Perkin Elmer Lambda 45) was used to collect absorbance spectra. The slit size (4 nm) and scanning speed (480 nm/min) were held constant throughout all the experiments. A scanning fluorescence spectrometer (QM1, Photon Technology International) along with a new photomultiplier tube (R928) was used to increase the sensitivity in the longer wavelengths (650-800nm), and to collect fluorescence emission spectra by exciting the sample at 640 nm. Confocal images were taken with a Leica TCS SP2 microscope equipped with a 63X oil immersion objective and green and red He-Ne excitation lasers. Counts and sizes of microcapsules were obtained with a Beckman Coulter counter (Z2) using a 100 μm aperture.

7.3 Methods

7.3.1 Solution Phase Experiments

Assay optimization. The glucose assay concentration was optimized by performing a simple titration experiment to obtain maximum change in signal for a given analyte concentration. The concentrations of the sensing assay elements were optimized

based on the concentration dependent quenching of AF647 by QSY21. In order to observe the quenching pattern, 700nM QSY21-dextran (QSY-dex) was titrated into 40nM AF647-AG (AF-AG) in a stepwise manner. A fluorescence spectrum of AF-AG was collected after each addition of QSY-dex. It was hypothesized that there will be a significant drop in fluorescence due to non-radiative quenching compared to radiative. In the case of radiative quenching, higher quencher concentrations are required to observe a small drop in fluorescence intensity. Thus, the least amount of QSY-dex required to significantly (non-radiatively) quench AF-AG fluorescence is determined.

Glucose sensitivity. The apo-GOx and amino-dextran used in all experiments were conjugated to AF647 and QSY21, with a labeling ratio of 3.2 and 2.4, respectively. The quenching process between AF-AG and QSY-dex was monitored using the fluorescence spectrometer by exciting the sample at 640 nm and collecting the emission across the range of 650-750 nm. Initially, ~16.5 picomoles of AF647-AG were added to 0.4mL of DI water. The initial fluorescence spectrum was collected after titrating 143nM QSY-dex into the sample solution containing 41nM AF-AG. Finally, to assess the relative affinity of apo-GOx for glucose and QSY-dex, changes in the quenching efficiency were observed during the stepwise addition of aliquots of 100mg/mL β -D-glucose solution into the sample containing QSY-dex/AF-AG complexes. The effect of QSY-dex concentration on the displacement behavior was investigated by repeating the same procedure at different concentrations of QSY-dex. The reference dye (AF750) was not incorporated in this assay as the experiments were performed in solution phase and the dye was showing some anomalous effects on glucose response characteristics, such as delayed response (~20min). As there is no reference peak in this assay, fluorescence

changes in AF647 peak were corrected for dilution effects by diluting QSY-dex/AF-AG complexes with aliquots of DI water and subtracting the change due to water from that due to glucose. For all the experiments, sensitivity curves were constructed by plotting AF647 fluorescence peak intensity (corrected for dilution) versus glucose concentration.

After the successful demonstration of a near infrared glucose sensor using apo-GOx/dextran system in solution phase, the next step is to incorporate these assay elements into a microcontainer. In order to encapsulate the sensing elements, a new approach was used for entrapping the assay elements using glycidyl-silane. This process is superior to the DAR based encapsulation technique discussed in Chapter five when one considers the disadvantages of DAR such as, toxicity, and the inconvenient assembly conditions, as the assembly process must be performed in the absence of UV light.

7.3.2 Fabrication of Silane-Based Organo- Inorgano Microcapsules

The sensing assay along with the reference dye is encapsulated into microcapsules using a facile method based on glycidyl-silane hydrolysis and condensation. The permeability of the capsule walls is controlled by incorporating silane in the shell structure, wherein silane builds a crosslinking network by undergoing hydrolysis and condensation reactions, which is described in detail below.

Silane theory

The formation of interpenetrating network by glycidyl-silane is a two step process as shown in Figure 7.2. In step 1, glycidyl groups on silane are conjugated to amine groups on PAH upon mixing. During this conjugation step, the ring opening reaction of epoxy groups on glycidyl-silane will result in the formation of hydroxyl groups.

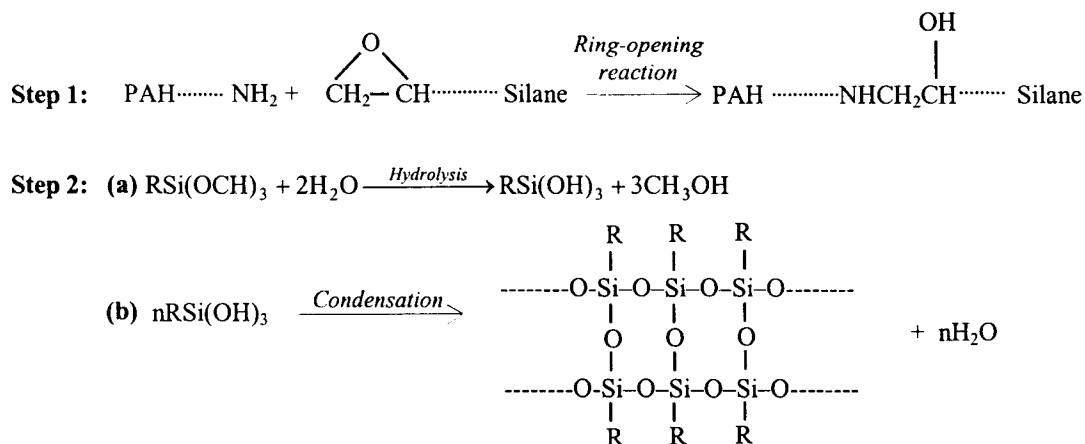


Figure 7.2. Chemical crosslinking of PAH and silane (step 1); Hydrolysis and condensation of silane in the presence of water (step 2).

Step two involves formation of the interpenetrating network through the formation of -Si-O- bonds. In the presence of water, silane undergoes hydrolysis which releases methanol, and condensation which releases water. It is hypothesized that the formation of the interpenetrating network is much slower than the conjugation reaction between glycidyl and amine groups. The condensation step may take several days to reach saturation, which offers a great opportunity for materials to penetrate into the microcapsules and become encapsulated.

Manganese carbonate (MnCO₃) particles, with 5 μm in diameter are used as sacrificial core material. Multilayers of PSS (cationic material) and PAH conjugated to glycidyl-silane (PAH-silane, anionic material) were deposited based on the LbL self-assembly process. The final film architecture (Figure 7.3(b)) on the surface of the template particles at the completion of the assembly was {(PSS/(PAH-silane))₄/PSS}. The change in surface potential with the deposition of each layer was measured using a zeta-potential analyzer. Following the completion of the polymer layer deposition, MnCO₃ core particles were dissolved (Figure 7.3(c)) yielding silane-based hollow microcapsules.

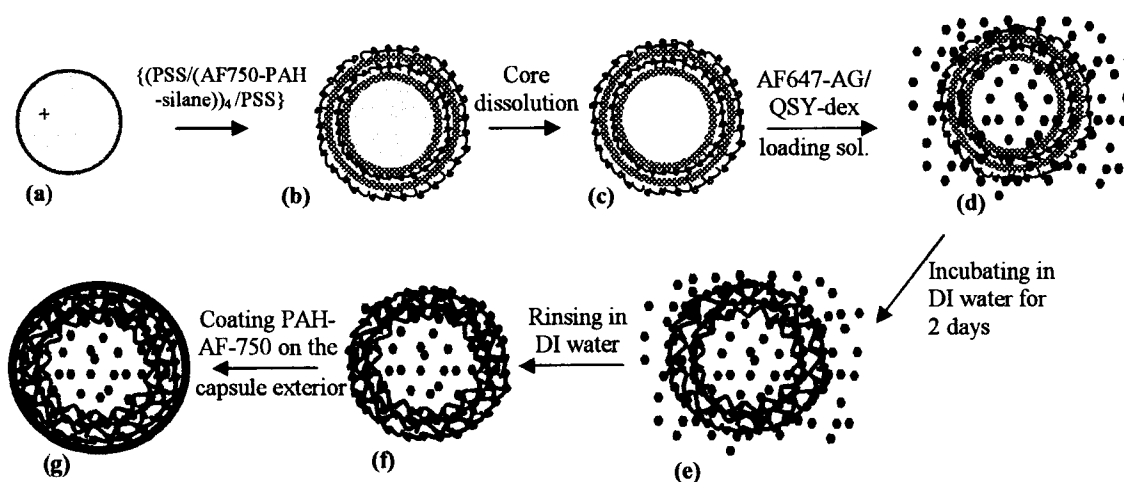


Figure 7.3. Fabrication of organic/inorganic hybrid microcapsules (a – c); encapsulation of AF647-AG/QSY-dextran into hollow microcapsules (d – f); and (g) incorporation of reference dye (AF-750).

7.3.3 Encapsulation of Sensing Chemistry in Organo/Inorgano Hybrid Microcapsules

Microcapsules with $(PSS/(PAH-silane))_4/PSS$ shell architecture were prepared as described and used for encapsulating glucose assay by dispersing microcapsules in a AF-AG:QSY-dex (230pM:990pM) complexes solution (Figure 7.3(d)). The concentration of the loading molecules inside the microcapsules was found to reach equilibrium with the exterior loading solution within minutes, because of the semi-permeable nature of the capsule walls. However, during the two-day period of the incubation of the microcapsules in the loading solution, there is enough time for the hydrolysis and condensation of silane to take place and thus, facilitate the formation of the interpenetrating network (Figure 7.3(e)). This network within the shell structure will result in a decrease in the permeability of the capsule wall, thus suppressing the leaching of the material that was loaded into the capsule interior. As the final step, the capsules were rinsed in DI water to remove excess loading molecules yielding microcapsules loaded with AF647-AG and QSY21-dextran (Figure 7.3(f)). Finally, the reference dye is incorporated into the

microcapsule walls by coating the outer layer (PSS) of microcapsules with PAH-AF750 (Figure 7.3(g)) by utilizing the electrostatic forces of attraction. The detailed description of the effect of silane on the formation of microcapsules and encapsulation of biomolecules is discussed elsewhere.¹⁵¹ Confocal microscopy was used to assess the loading of assay elements into microcapsules. Encapsulation efficiency was estimated as described in Chapter five (section 5.3.6). The NIR assay elements were not encapsulated into microcapsules using the DAR technique because the silane based method showed good loading efficiency and is not associated with toxicity problems and inconvenient assembling conditions.

Stability. This experiment is described in more detail in Chapter five (section 5.3.7). An experiment for the assessment of the stability of the encapsulated material was performed on the capsules loaded with QSY-dex/AF-AG complexes. As opposed to the procedure in Chapter five, leaching of the loaded assay elements was estimated at only one point, i.e., after five weeks from the day of encapsulation. A standard solution of 50 nM AF-AG was used to estimate the supernatant concentration as a percentage of a standard.

7.3.4 Sensor Response in Microcapsules

A fluorescence spectrum of the microcapsules loaded with the AF-AG/QSY-dex complexes and AF750 reference dye dispersed in DI water was collected as the starting point. Fluorescence spectra were then collected after each addition of 100mg/mL glucose solution to the microcapsules. The change in AF647 to AF750 peak intensity ratio was calculated from each spectrum and plotted with respect to the increments in glucose concentrations. To determine the feasibility of tailoring the sensor response, glucose

sensitivity experiments were repeated with three different concentrations of capsules, (4.3×10^5 , 8.6×10^5 , 1.72×10^6 capsules/mL).

7.3.5 Reversibility

To test the reversibility of these sensors, microcapsules loaded with sensing assay were suspended in glucose solutions in random order with respect to concentration. To achieve this, AF-AG/QSY-dex loaded microcapsules (2.88×10^6 capsules/mL) were dispersed in DI water and the glucose concentration of the suspension was increased by addition of glucose stock solution. The glucose levels were changed by rinsing the capsules in DI water to remove the glucose after each measurement followed by adding glucose to a new concentration. In each case, after addition of glucose to the desired concentration and measuring the fluorescence, the suspension was centrifuged three times, the supernatant (glucose) solution was removed and, finally, an equal volume of fresh DI water was added. The change in AF647/AF740 peak ratio was obtained at each step by collecting a fluorescence scan. This procedure was repeated to cover the glucose concentration in the range of 0-60 mM, in the order of 0, 5.3, 10, 13.5, 20, 33.1, 26.6, 32.5, 5.5, 44.6, 6.3, 61.6, 10 mM.

7.4 Results and Discussion

7.4.1 Solution Phase Experiments

Assay optimization. Fluorescence spectra collected during the titration of QSY-dex into AF-AG is shown in Figure 7.4. Because of the affinity between AF-AG and QSY-dex, AF647 and QSY dyes will be in close proximity which will result in the quenching of AF647 fluorescence by QSY21, which is indicated by a decrease in the AF647 peak. It can be observed from Figure 7.4 that there is a significant decrease in the

fluorescence corresponding to AF647-AG after adding 200nM QSY-dex, due to the close proximity of the AF647 and QSY dyes. Also, further additions of QSY-dex have a small quenching effect on the AF647 fluorescence, which could be most likely due to the radiative quenching because there is a smaller decrease in AF647 fluorescence with the addition of quencher concentrations, greater than 150nM.

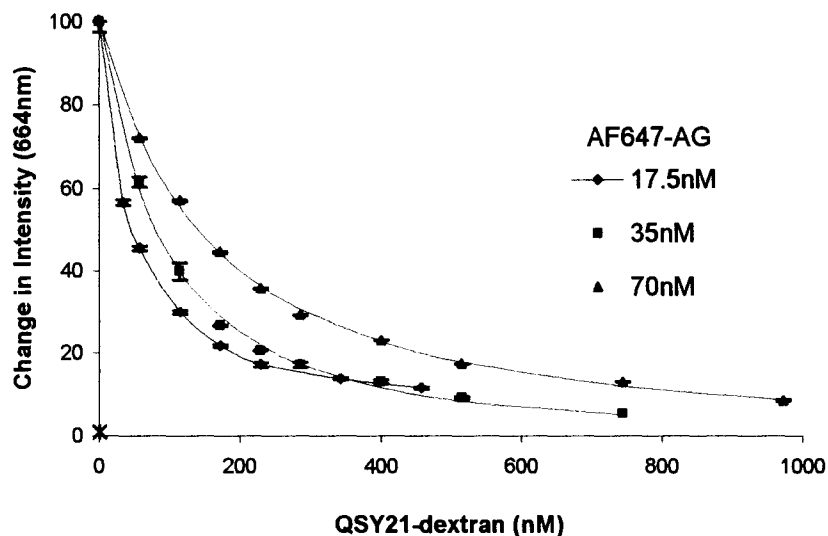


Figure 7.4. Quenching of AF647-AG due to increasing concentrations of QSY21-dextran.

Therefore, from the quenching pattern, it can be observed that maximum quenching (70%) due to non-radiative energy transfer can be obtained with the addition of 145nM QSY-dex into 35nM AF-AG. Similar experiments were performed at two different concentration of AF-AG (17.5nM and 70nM) to observe the effect of concentration on the quenching process. As expected, quenching in the case of higher AF-AG concentration required higher QSY-dex concentrations to reach saturation.

Glucose response tests. Taking the optimum assay concentrations obtained from the above experiment into consideration, 142 nM QSY-dex was titrated into 42 nM of AF-AG in DI water which led to a decrease in the AF647 fluorescence emission peak,

implying significant quenching of AF647 by the quencher, QSY21. To observe the glucose sensitivity of dextran/apo-GOx complexes, fluorescence spectra were measured after the titration of 100mg/mL β -D-glucose solution aliquots into the sample containing QSY-dex/AF-AG complexes. As hypothesized, the glucose in the solution displaced dextran from apo-GOx resulting in the decrease in quenching, as indicated by the increase in AF647 peak (Figure 7.5(a)).

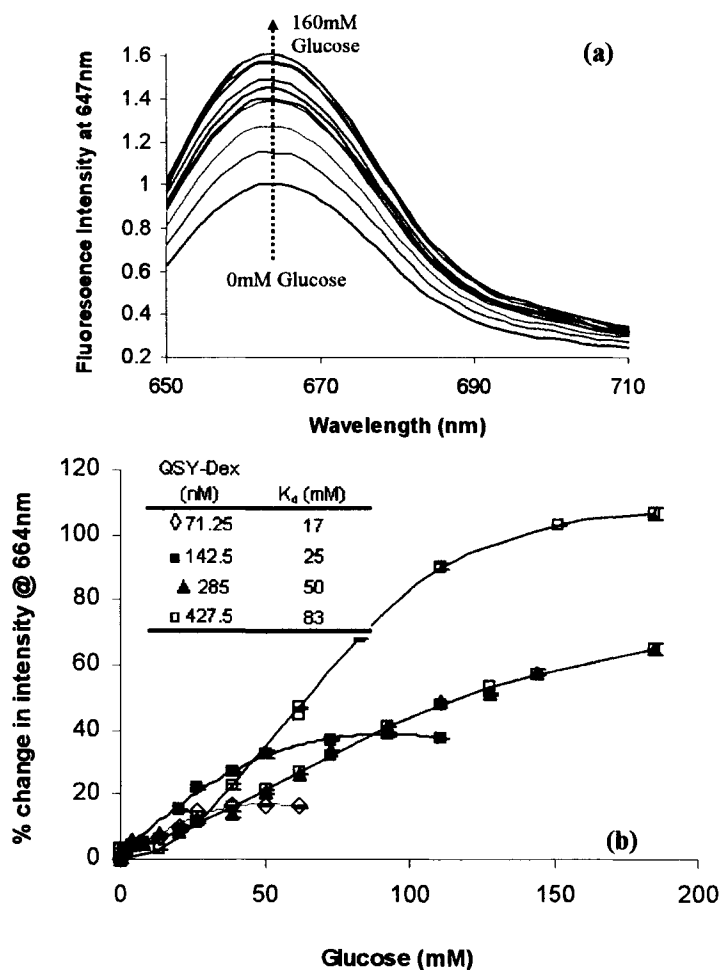


Figure 7.5. Normalized (a) Fluorescence spectra and (b) Percentage change in AF647:AF750 peak ratio with the addition of glucose into AF-AG/QSY-dex complexes with different dextran concentrations. Lines are regression curves used only to clearly indicate the trend for each set of measurements. Error bars show one standard deviation of three replicate measurements.

The percentage change in AF647:AF750 peak ratio (corrected for dilution) as a function of glucose concentration is shown in Figure 7.5(b) from which it can be observed that there is 25% increase in the AF 647 peak due to 30mM glucose with a sensitivity of 0.7%/mM. The data clearly show that the response is linear in the range of 0-30 mM. The most significant characteristic of this assay is that, in spite of the extension of this assay into NIR region, the sensitivity is comparable to the FD/TAG based glucose assay (Chapter five).

Effect of quencher concentration on sensor response. To observe the effect of quenching molecule concentration, similar glucose sensitivity experiments were performed with different concentrations of QSY-dex, while maintaining constant 42nM AF-AG concentration. The corresponding sensor response characteristics are shown in Figure 7.5(b). It can be observed from these results that the detection range and the sensitivity of this sensor can be significantly varied by changing the apo-GOx:dextran molar ratio. The reason for this observation is because of the two main consequences of an increase in QSY-dex concentration, (a) an increase in the number of dextran molecules associated with AF-AG, and (b) the total decrease in AF 647 signal due to quenching effect. Therefore, an increase in the total glucose concentration is required to dissociate all the QSY-dex/AF-AG complexes, which can be observed in Figure 7.5(b). Also, as the initial decrease in AF647 intensity is high for the case of high dextran concentrations, the signal reversal is also high with the addition of glucose, as more number of AF-AG molecules are being freed. It was calculated that with a 5X increase in QSY-dex concentration, there is a 4X times increase in dissociation constant and a 6.6X increase in the total percentage change in the signal.

Thus, the sensitivity in over a wide range of glucose (0-200mM) can be significantly varied by controlling the quencher concentration. However, the sensitivity in the region of interest (0-30mM) is almost same in all the experiments. Thus, the main parameter that can be varied by controlling quencher concentration is the dissociation constant (k_d) of the sensing assay. All these results corroborate with the modeling results explained in Chapter Three, which show that with the increase in ligand concentration there is an increase in the linear region and the total change in signal.

7.4.2 Encapsulation of AF-AG/QSY-dex Complexes in Microcapsules

As previously described, oppositely charged polymers were deposited on MnCO_3 particles via electrostatic self assembly. The reversal of the surface-potential with the addition of each layer, as shown in Figure 7.6(a), demonstrates the successful fabrication of the shell on the template particles. Microcapsules with $\{\text{PSS/PAH-sil}\}_4\text{PSS}\}$ shell architecture were prepared by core dissolution and used for encapsulating AF-AG/QSY-dex complexes and reference dye (AF750).

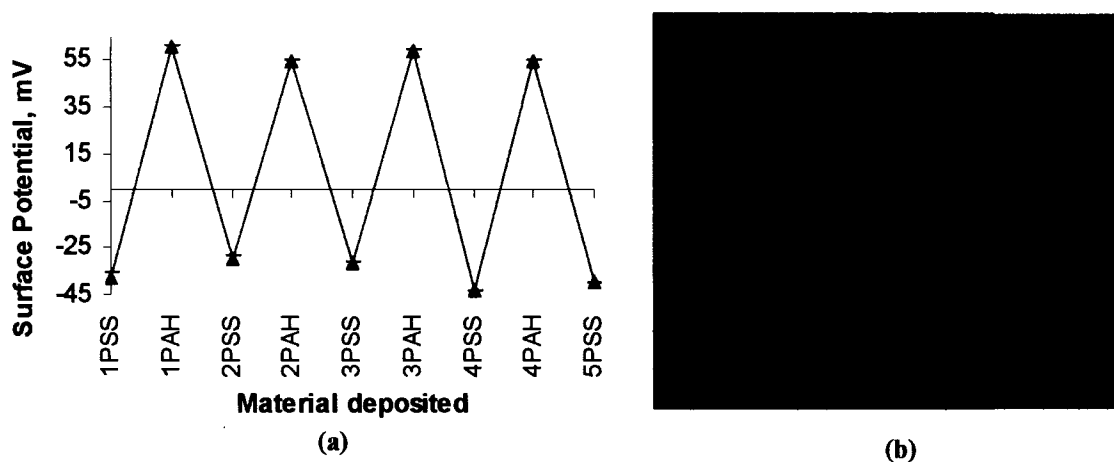


Figure 7.6. (a) Surface potential values obtained after coating each layer on MnCO_3 particles. Error bars show one standard deviation of three replicate measurements; (b) Confocal fluorescence images of microcapsules loaded with AF647-*apo*-GOx, QSY21-dextran and AF750-PAH with AF647 fluorescence.

Confocal images of representative polyelectrolyte microcapsules loaded with the glucose assay are shown in Figure 7.6(b). The encapsulation efficiency of AF-AG/QSY-dex complexes was estimated by measuring the supernatant concentrations and obtaining the capsule count using the Coulter counter and was found to be 1×10^{-16} and 1.34×10^{-16} AF-AG and QSY-dex moles/capsule, respectively.

From the leaching studies it was estimated that the number of moles of AF-AG in supernatant is 10^3 times lower than the AF-AG moles encapsulated in the microcapsules. Thus, it was estimated that only 0.12% of the initially loaded assay molecules have leached out over a five week period. Compared to the leaching studies on microcapsules loaded using DAR based encapsulation procedure, this data is highly promising as the leaching is reduced by 40 times. However, in order to study the leaching of loaded molecules over a period of time, leaching studies must be performed at regular time intervals over a five week period. These studies can help in accounting for the loss in sensitivity over long period of time.

7.4.3 Sensor Response to Glucose Addition in Microcapsules

To demonstrate the sensor response characteristics of microcapsules loaded with sensing assay and to test the feasibility of tailoring the sensor response with the microcapsule concentration, glucose sensitivity experiments were performed on three different concentrations of microcapsules (4.3×10^5 , 8.6×10^5 , 1.72×10^6 , 3.87×10^6 capsules/mL) loaded with AF-AG/QSY-dex complexes and reference dye (PAH-AF750). Fluorescence spectra were collected after each addition of β -D-glucose to the microcapsules loaded with AF-AG/QSY-dex complexes. The fluorescence spectra are normalized to a reference peak (776nm) to account for dilution and instrumentation

drifts, as shown in Figure 7.7. The corresponding percentage change in the AF647:AF750 peak ratio was calculated for each case, as shown in Figure 7.8.

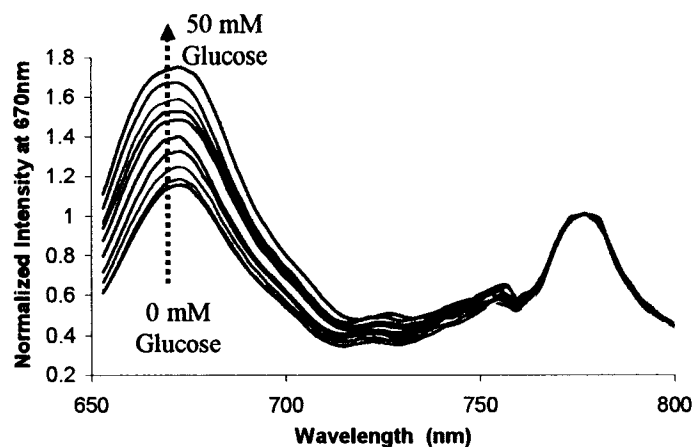


Figure 7.7. Fluorescence spectra of the microcapsules loaded with sensing assay and reference dye (AF750) with the addition of glucose solution. All the spectra are normalized to the reference peak at 776nm.

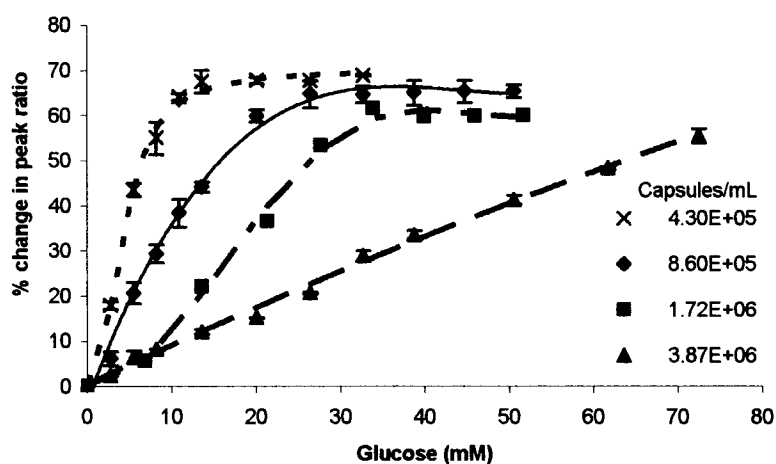


Figure 7.8. Effect of capsule concentration on the change in AF647:AF750 peak ratio with the addition of glucose solution. Error bars show one standard deviation of three replicate measurements.

For the case of the 8.6×10^5 caps/mL sample, it can be seen that there is a linear increase in the peak ratio with the addition of glucose up to 30mM for the capsules loaded with AF-AG/QSY-dex complexes, with a sensitivity of 2.67%/mM. It is noteworthy that even after extension the apo-GOx/dextran based competitive binding

assay from the visible (500-600nm) to the NIR region (650-800nm), there is no significant drop in the achievable sensitivity in the region of interest (0-30mM). It is immediately evident that with a 4X increase in capsule concentration, there is a decrease in the total change in the percentage of RET from 69% to 58%. Furthermore, it is clear that a higher glucose concentration is required to reach the AF647:AF750 peak ratio saturation point. It can be seen from Table 7.1 that a 3X increase in capsule concentration results in a ~ 3X decrease in sensitivity in the region of interest (0-30mM) and ~ 4X increase in dissociation constant. This trend corroborates with the previously demonstrated theoretical modeling results in Chapter Three. These results prove that the sensitivity can be tailored by changing the competitive binding assay concentration.

Table 7.1. Change in sensitivity and dissociation constant with varying capsule concentration.

Capsules/ mL	QSY-dex (moles)	AF-AG (moles)	Sensitivity (% Δ ratio/mM)	Linear range (mM)	k_d (mM)
4.3×10^5	1.8×10^{-11}	2.3×10^{-10}	5.15	0 - 10	4.1
8.6×10^5	3.7×10^{-11}	4.6×10^{-11}	3.09	0 - 30	10
1.72×10^6	7.3×10^{-11}	9.2×10^{-11}	1.97	0 - 40	20
3.44×10^6	1.84×10^{-10}	1.46×10^{-10}	0.8	0 - 80	60

7.4.4 Demonstration of Reversible Sensor Response

The reversibility of these sensors was tested by exposing the microcapsules (2.88×10^6 capsules/mL) to random glucose concentrations. Fluorescence spectra were collected after each addition and removal of glucose solution from the microcapsules and the corresponding changes in AF647:AF750 peak ratios are plotted in Figure 7.9. It is clear that there is a linear response in the 0 - 80 mM range, with a sensitivity of 0.83%/mM, which is comparable to the sensitivity obtained with capsules (same

concentration) exposed to a stepwise increase in glucose concentrations (Figure 7.8). These results show that the microcapsule based sensors are completely reversible, without any significant loss in sensitivity.

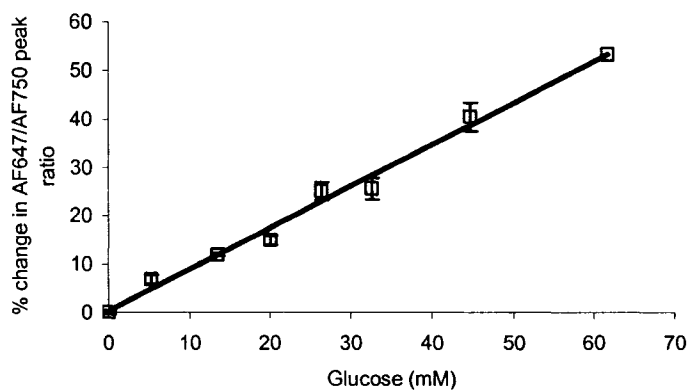


Figure 7.9. Percentage change in AF647:AF750 peak ratio with the addition of random β -D-glucose concentrations to the AF-AG/QSY-dex loaded microcapsules. Error bars show one standard deviation of three replicate measurements.

It can be observed from microcapsule and solution phase glucose sensitivity experiments that there is approximately a two-fold increase in the sensitivity for the case of the microcapsules. As explained in Chapter five, this observation is the result of a low concentration of mobile sensing assay elements, due in part to the entrapment of $\sim 72\%$ of the total encapsulated molecules in the capsule walls. The apo-GOx and dextran molecules that are entrapped in the walls may not dissociate in the presence of glucose molecules. Thus, the total number of mobile molecules will be far less than in the solution phase samples. This low concentration ($\sim 27\%$) of freely moving QSY-dex/AF-AG complexes is ultimately reducing the active sensing assay concentration, which results in the increased sensitivity as predicted by theoretical modeling of the effect of competitive binding assay concentration on response (Chapter Three (Figure 3.6)).

7.4.5 Photobleaching Effect

The long term functional stability of the above described glucose sensors greatly depends on the stability of the encapsulated or immobilized fluorophores. It has been previously demonstrated that there is only 0.12% leaching of the encapsulated assay molecules. Thus, leaching of the loaded elements is not a concern. However, the photostability of the sensors is a major concern, since the transduction scheme (energy transfer) involved in this work depends on measuring the intensity of the fluorophores. To assess the photobleaching behavior of the sensors in the presence and in the absence of glucose, two experiments were performed in which the sample was continuously excited at 640nm with 20mM glucose and 0mM glucose concentrations. The results of these experiments are given in Figure 7.10. It can be observed from the figure that the photobleaching rates of AF647 (-2.96%/min) and AF750 (-2.8%/min) are almost identical in the absence of glucose. However, with the addition of glucose AF647 (-1.12%/min) is bleaching rapidly compared to AF750 (-0.55%/min). This variation in the bleaching rates could be the effect of a decrease in energy transfer, which results in the observed decrease in the bleaching of AF750 dye. It can be observed from Figure 7.10b that there is 10% decrease in peak ratio in the presence of glucose, whereas in the absence of glucose there is no change in peak ratio. For example in Figure 7.9, there is 20% increase in signal with the addition of glucose. But if these sensors are exposed to light for 15 min, then there will be 10% decrease in the signal, resulting in the decrease in sensitivity. These results indicate that continuous exposure of the sensors to light in the presence of glucose may result in the loss of sensitivity. Therefore, in the future, during real time monitoring of the sensors this variation in bleaching rates has to be considered.

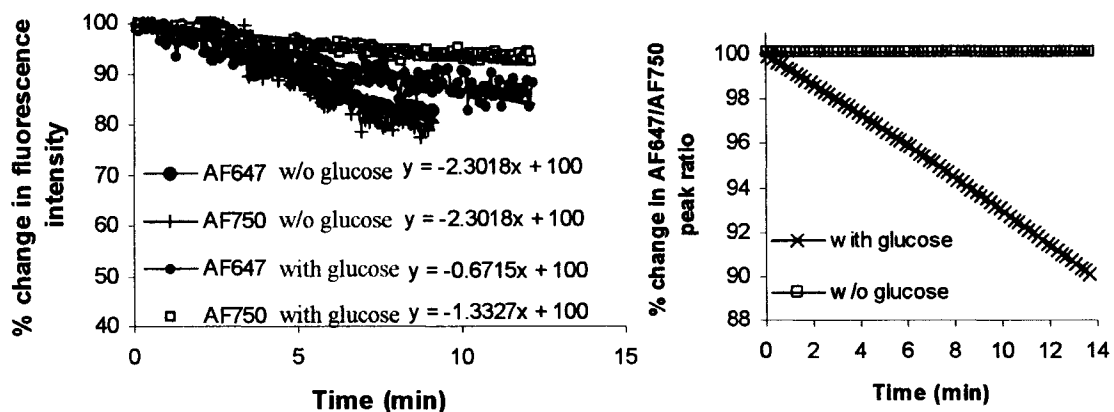


Figure 7.10. Photobleaching of the AF647-AG/QSY-dex and AF750 loaded microcapsules by continuously exciting at 640nm (a) with and without glucose, and (b) Change in the peak ratio with respect to time, with and without glucose.

7.5 Conclusion

A novel glucose sensing system based on competitive binding, quenching mechanism, and polymer microcapsule technology operating in near infrared region has been demonstrated. Sensing assay elements were entrapped in microcapsules using a silane based encapsulation procedure which could be less toxic,¹⁵² also there is no need for exposure of capsules to extreme conditions. Microcapsules containing QSY-dextran/AF-AG complexes showed glucose sensitivity of $\sim 2\text{-}5\%/mM$ over the range of 0-30mM. Thus, this assay is superior to all the other assays demonstrated in the previous chapters, because it has the advantages of, (a) non-toxic nature, which was the main problem with Con A based assays, (b) the silane based encapsulation procedure employed in this system is simple, and is free of toxic materials, (c) comparable and better sensitivity to FD/TAG and TD/CAG based assays, respectively, and (d) significant increase in the signal levels due to the use of NIR dyes. Based on the sensitivity, specificity, and reversible response in the region of interest (0-30mM), this sensing system can be used for glucose monitoring in diabetic patients.

Also, the successful demonstration of the extension of the apo-GOx/dextran based competitive binding assay into the NIR region indicates the potential to modify this assay according to the requirements of an application. By choosing appropriate apo-enzyme and competing ligand molecules, various biosensors can also be developed for detecting different analytes. Thus, the sensor design demonstrated in this chapter can be considered as a platform technology for designing biosensors based on competitive binding and energy transfer techniques.

CHAPTER 8

SUMMARY AND FUTURE WORK

8.1 Summary

This dissertation demonstrated a generic design for developing fluorescent biosensors based on the encapsulation of a competitive binding assay into a micro-container. A model biosensor for glucose monitoring was developed using this approach. Initially, a glucose sensor operating in the visible light region was demonstrated, which was then followed with the detailed discussion of the approaches pursued for extending the sensor operating region from the visible to the near infrared (NIR) region. Also, the disadvantages of each sensor prototype and the possible ways to overcome these limitations are summarized at the end of each chapter.

The first part of this project was focused on demonstrating a glucose sensor based on the encapsulation of previously reported FRET based FITC-dextran (FD)/TRITC-Con A (TC) assay in microcapsules. Even though the hollow microcapsules comprised of FD/TC multilayers showed reasonable glucose sensitivity (Table 8.1), there are some inherent disadvantages in using Con A as one of the elements in this assay, such as toxicity, aggregation, and specificity. Also, the total obtainable signal in this assay is limited by the amount that can be coated on the microparticle surface.

Table 8.1. Sensor response characteristics of different variations of competitive binding assays.

Receptor labeled- Ligand molecule	Acceptor labeled- Receptor molecules	Reference dye labeled polycation	Sensitivity (% Δ ratio/mM)	Dissociation Constant (k_d , mM)
FITC-Dextran	TRITC-Con A	-	0.3	50
FITC-Dextran	TRITC-Apo-Gox	-	2 , 6.2	20, 5
TRITC-Dextran	Cy5-Apo-Gox	-	0.83	12
QSY21-Dextran	AF647-Apo-Gox	AF750-PAH	0.8 - 5.2	4 - 60

In order to overcome the concerns regarding Con A, a glucose sensing system was proposed which replaces Con A in the above described sensing system with a deactivated enzyme glucose oxidase (apo-GOx). The use of deactivated enzyme makes this approach more generic as different analytes can be detected by choosing the corresponding enzyme (which can be deactivated) as the receptor molecule in competitive binding assay. Also, as the enzymes are highly specific towards their substrate molecule there will not be any concerns over toxicity. In addition, toxicity is not a concern when Con A is removed from the assay elements and the aggregation issue can be solved since enzymes bind to one substrate molecule at a time.

Another significant achievement is the encapsulation of a competitive binding assay comprised of dextran/apo-GOx complexes into microcapsules by incorporating photosensitive materials (diazoresin (DAR) and poly (styrene sulfonate) (PSS)) in the capsule wall structure. This encapsulation process resulted in the efficient loading of assay elements compared to FD/TC encapsulation. The employment of prefabricated microcapsules for entrapping the competitive binding sensing assay is advantageous, because it allows for the free movement of sensing elements during the competitive binding process while maintaining the concentrations of the ligand and receptor constant

in the presence of varying analyte concentration. Therefore, this approach is highly appropriate for developing smart tattoo systems.

Microcapsules containing FD/TRITC-apo-GOx (TAG) complexes showed a glucose sensitivity ranging from 2 – 6% /mM (Table 8.1). Also, FD/TAG based glucose assay is 10 times more sensitive compared to FD/TC assay and is also highly specific (5 – 10X more sensitive) towards glucose over other sugars. It was also found that the response of this system (sensitivity and dissociation constant) to glucose can be tuned by varying the concentration of FD/TAG complexes. In spite of these advantages, this sensor design may not be an ideal system for subcutaneous implantation because of the use of dyes which fluoresce in visible region, where tissue is highly light scattering.

In order to extend FD/TAG based glucose sensor into the longer wavelength region, FITC/TRITC pair was replaced with TRITC/Cy5 FRET pair. Microcapsules containing TRITC-dextran (TD)/Cy5-apo-GOx (CAG) complexes showed a sensitivity of 0.83%/mM, which is 3 – 4X lower than the sensitivity obtained with the FD/TAG assay. This drop in sensitivity could be due to the lower FRET efficiency between TRITC and Cy5, different labeling ratios, etc. Also, using the TRITC/Cy5 dyes extended the operating region by only 100nm, which may not result in a significant decrease in tissue scattering. In order to carry out implantation studies, it is highly desirable to extend the operating wavelength region more into the NIR region.

Another concern in the above mentioned apo-GOx/dextran systems is the use of DAR, which is toxic, and the inconvenient assembly conditions, as the assembly process must be performed in the absence of UV light. Also, the biomacromolecules which are loaded into microcapsules are exposed to UV light, which may result in the loss of

activity or binding affinity to certain molecules. Therefore, another approach has to be developed in order to improve the stability of the biomolecules in the microcapsules.

In order to extend the operating region into the NIR, various dyes operating in the NIR region were selected. Due to the difficulties in finding an efficient NIR FRET pair, quenching is used as the transduction mechanism in the dextran/apo-GOx competitive binding assay. The sensing assay elements, quencher (QSY21)-dextran/fluorescent (AF647)-apo-GOx and reference dye (AF750), were entrapped in microcapsules using a simple silane based encapsulation procedure. Unlike the DAR based encapsulation procedure, this silane based technique is very simple in terms of maintaining proper assembling conditions, and it also may not have the toxicity concern. Microcapsules containing labeled dextran/apo-GOx complexes showed glucose sensitivity of ~2-5%/mM (Table 8.1). Also, a significant achievement in this assay is that, in spite of the extension of the operating region from visible to NIR, its sensitivity to glucose is comparable to the assay operating in the visible region. Thus, this assay is superior to all the other assays demonstrated in this dissertation, because it has the advantages of, (a) non-toxic nature, which was the main problem with Con A based assays, (b) the silane based encapsulation procedure employed in this system is simple, and is free of toxic materials, (c) The sensitivity of this system is comparable to and better than FD/TAG and TD/CAG based assays and (d) a significant increase in the signal levels (signal to noise ratio) due to the decrease in light scattering resulting from the use of NIR dyes. Thus, the NIR glucose sensor is highly promising for conducting *in vivo* studies in a rat model.

The generic sensor design described here opens the door for a wide variety of analytes to be sensed using this versatile sensing technique which involves the selection

of an analyte-specific enzyme and a competing ligand. Therefore, this design can be considered as a *platform technology* for the development of biosensors based on competitive binding and RET techniques. Potential targets include neurochemicals, such as glutamate, choline, lipids, and estrogen. In conclusion, fluorescence affinity sensors were shown to be promising for monitoring glucose concentrations in diabetic patients.

8.2 Future Work

Optimization. The sensor response can be further optimized by varying the labeling ratio of apo-GOx and dextran molecules with donor and acceptor dyes. Also, apo-GOx molecule contains three reactive molecular groups, amine, thiol groups and carboxylic acid, that are candidates for conjugation of the FRET donor Alexa Fluor 647. This fact can be exploited to determine which molecular group needs to be labeled to achieve the desired sensitivity and different concentrations of assay molecules can be encapsulated into microcapsules using different concentrations of loading solutions. The stability of the encapsulated sensing elements in microcapsules should be measured over a long period of time.

Stability. The stability of the assay molecules encapsulated in microcapsules using silane based procedure must be tested by performing the leaching experiments as described in Chapter five (section 5.3.7). Also, sensor response must be monitored at regular intervals over a long time period to observe the magnitude of drift in the response.

Further experiments must be performed on the flow through system to more accurately test the reversibility and response time of the sensors. While using the flow through system, variations in the photobleaching rates of different dyes have to be considered, as the sample is continuously excited which may have significant bleaching

effect on the dyes. It would be appropriate to conduct fluorescence lifetime studies on these sensors because they are not concentration dependent and could also be the best approach for future *in vivo* experiments. Finally, the response of the sensors should be evaluated *in vivo*, first in the rat model, then in larger models with skin similar to that of humans (e.g., porcine models).

This work could be further used in detecting different metabolites other than glucose. For example, a lactate sensor can be designed by using apo-lactate oxidase and poly(lactic acid) as the receptor and ligand molecules, respectively. Also, this sensing mechanism can be further extended to develop drug-delivery systems; for example, insulin may be released in response to apo-GOx/dextran dissociation.

REFERENCES

- [1] D. L. Wise, *Applied Biosensors*, Butterworth, Stoneham, MA, 1989.
- [2] E. A. H. Hall, *Biosensors*, New York, 1991.
- [3] A. J. Cunningham, *Introduction to Bioanalytical sensors*, John Wiley & Sons, New York, 1998.
- [4] D. G. Buerk, *Biosensors Theory and Applications*, Technomic Publishing Comp., Inc, PA, 1993.
- [5] WHO, *Diabetics Action Now: An Initiative of the World Health Organization and the International Diabetes Federation*, 2004, WHO, Geneva, Switzerland.
- [6] D. G. Griffiths, G. Hall, *Biosensors – what real progress is being made?*, *Trends in Biotechnology*, 1993, 111, 122-130.
- [7] H. King, R. E. Aubert, W. H. Herman, *Global burden of diabetes, 1995-2025: prevalence, numerical estimates, and projections*, *Diabetes Care*, 1998, 21(9):1414-31.
- [8] J. C. Pickup, F. Hussain, N. D. Evans, N. Sachedina, *In vivo glucose monitoring: the clinical reality and the promise*, *Biosensors and Bioelectronics*, 2005, 20(10), 1897-902.
- [9] R. J. McNichols, G. L. Cote, *Optical glucose sensing in biological fluids: an overview*, *Journal of Biomedical optics*, 2000, 5 (1), 5-16.
- [10] Jeffrey D. Newman, Anthony P.F. Turner, *Home blood glucose biosensors: a commercial perspective*, *Biosensors and Bioelectronics*, 2005, 20 (11), 2310-2313.
- [11] D. M. Nathan, *Long-term complications of diabetes mellitus*, *New England Journal of Medicine*, 1993, 328, 1676-1685.
- [12] American Diabetes Association, *Self monitoring of blood glucose*, *Diabetes Care*, 1994, 17, 81-86.

- [13] J. C. Pickup, L. McCartney, O. Rolinski, D. Birch, In vivo glucose sensing for diabetes management: progress towards non-invasive monitoring, *British Medical Journal*, 1999, 319, 1-4 .
- [14] O. S. Khalil, Spectroscopic and Clinical Aspects of Noninvasive Glucose Measurements, *Clinical Chemistry*, 1999, 45(2), 165–177.
- [15] N. Sachedina, J. C. Pickup, Performance assessment of the Medtronic-Minimed continuous glucose monitoring system and its use for measurement of glycaemic control in type 1 diabetic subjects, *Diabetes Medicine*, 2003, 20, 1012-1015.
- [16] A. Maran, C. Crepaldi, A. Tiengo, Continuous subcutaneous glucose monitoring in diabetic patients. A multicenter study, *Diabetes Care*, 2002, 25, 347-352.
- [17] W. Kerner, Implantable glucose sensors: Present status and future developments, *Experimental and Clinical Endocrinology and Diabetes*, 2001, 109, S341-S346.
- [18] Y. Wickramasinghe, Y. Yang, S. A. Spencer, Current problems and potential techniques in in-vivo glucose monitoring, *Journal of Fluorescence*, 2004, 14, 513-520.
- [19] J. Wang, Glucose biosensors: 40 years of advances and challenges, *Electroanalysis*, 2001, 12, 983–988.
- [20] T. D. James, K. R. A. S. Sandanayake, R. Iguchi, S. Shinkai, Novel Saccharide-Photoinduced Electron Transfer Sensors Based on the Interaction of Boronic Acid and Amine, *Journal of American Chemical Society*, 1995, 117, 8982-8987.
- [21] X. Ge, L. Tolosa, G. Rao, Dual-Labeled Glucose Binding Protein for Ratiometric Measurements of Glucose, *Analytical Chemistry*, 2004, 76,1403-1410.
- [22] S. Mansouri, J. S. Schultz, A miniature optical glucose sensor based on affinity binding, *Biotechnology*, 1984, 885-890.
- [23] S. D’Auria, P. Herman, M. Rossi, J. R. Lakowicz, The fluorescence emission of the apo-glucose oxidase from *Aspergillus niger* as probe to estimate glucose concentrations, *Biochemical Biophysical Research Communications*, 1999, 263, 550–553.
- [24] M. J. McShane, S. Rastegar, M.V. Pishko, G. L. Cote, R. J. Russel, Monte Carlo modeling for implantable fluorescent analyte sensors, *IEEE Transactions in Biomedical Engineering*, 2000, 47, 624-632.
- [25] M. J. McShane, R. J. Russel, M. V. Pishko, G. L. Cote, Towards Minimally-Invasive Glucose Monitoring Using Implanted Fluorescent Microspheres, *IEEE-EMBS Magazine* , 2000, 19, 36-45.

- [26] B. L. Ibey, M. A. Meledeo, V. A. Gant, V. Yadavalli, M. V. Pishko, G. L. Cote, Implantable fluorescence-based glucose sensor development, *Proceedings of SPIE*, 2003, 4965, 1-6.
- [27] R. J. Russel, M. V. Pishko, C. C. Gefrides, M. J. McShane, G. L. Cote', A Fluorescence-Based Glucose Biosensor Using Concanavalin A and Dextran Encapsulated in a Poly(ethylene glycol) Hydrogel, *Analytical Chemistry*, 1999, 71, 3126-3132.
- [28] M. J. McShane, Microcapsules as 'Smart Tattoo' Glucose Sensors: Engineering Systems with Enzymes and Glucose-Binding Elements, in *Topics in Fluorescence*, Plenum Press, 2005.
- [29] E. Wilkins, P. Atanasov, Glucose monitoring: state of the art and future possibilities, *Medicine Engineering Physics*, 1996, 18 (4), 273-288.
- [30] W. Kerner, Implantable glucose sensors: present status and future developments, *Experimental and Clinical Endocrinology Diabetes*, 2001, 109, S341-S346.
- [31] M. Gerritsen, J.A. Jansen, J.A. Lutterman, Performance of subcutaneously implanted glucose sensors for continuous monitoring, *The Netherlands Journal of Medicine*, 1994, 1999, 54, 167-179.
- [32] M. J. McShane, Potential for Glucose Monitoring with Nanoengineered Fluorescent Biosensors, *Diabetes Technology and Therapeutics*, 2002, 4, 533-538.
- [33] C. A. Royer, Approaches to teaching fluorescence spectroscopy, *Biophysical Journal*, 1995, 68 (3), 1191-1195.
- [34] R. A. Mathies, K. Peck, L. Stryer, Optimization of high-sensitivity fluorescence detection, *Analytical Chemistry*, 1990, 62, 1786-1791.
- [35] http://www.pti-nj.com/tech_3.html, accessed on 9/10/2005.
- [36] H. J. Hecht, D. Schomburg, H. Kalisz, R. D. Schmid, The 3D structure of glucose oxidase from *Aspergillus niger*. Implications for the use of GOD as a biosensor enzyme, *Biosensors and Bioelectronics*, 1993, 8(3-4), 197-203.
- [37] R. Wilson, A. P. F. Turner, Glucose oxidase: an ideal enzyme, *Biosensors and Bioelectronics*, 1992, 7, 165-185.
- [38] H. J. Hecht, H. M. Kalisz, J. Hendle, R. D. Schmid, D. Schomburg, Crystal structure of glucose oxidase from *Aspergillus niger* refined at 2.3 Å resolution, *Journal of Molecular Biology*, 1993, 229(1), 153-72.

- [39] M. Meyer, G. Wohlfahrt, J. Knablein, D. Schomburg, Aspects of the mechanism of catalysis of glucose oxidase: a docking, molecular mechanics and quantum chemical study, *Journal of Computer Aided Molecular Design*, 1998, 12(5), 425-40.
- [40] H. Xu, J. W. Aylott, R. Kopelman, Fluorescent nano-PEBBLE sensors designed for intracellular glucose imaging, *Analytst*, 2002, 127(11), 1471-7.
- [41] Y. Cao, Y-E.L. Koo, R. Kopelman, Poly(decyl methacrylate)-based fluorescent PEBBLE swarm nanosensors for measuring dissolved oxygen in biosamples, *Analytst*, 2004, 129, 745-750.
- [42] S. M. Buck, H. Xu, M. Brasuel, M. A. Philbert, R. Kopelman, Nanoscale probes encapsulated by biologically localized embedding (PEBBLEs) for ion sensing and imaging in live cells, *Talanta*, 2004, 63, 41-59.
- [43] H. A. Clark, R. Kopelman, R. Tjalkens, M.A. Philbert, Optical nanosensors for chemical analysis inside single living cells. 2. Sensors for pH and calcium and the intracellular application of PEBBLE sensors, *Analytical Chemistry*, 1999, 71, 4837-4843.
- [44] H. Xu, J. W. Aylott, R. Kopelman, T. J. Miller, M. A. Philbert, A real-time ratiometric method for the determination of molecular oxygen inside living cells using sol-gel-based spherical optical nanosensors with applications to rat C6 glioma, *Analytical Chemistry*, 2001, 73, 4124-4133.
- [45] Y-E. L. Koo, Y. Cao, R. Kopelman, S. M. Koo, M. Brasuel, M. A. Philbert, Real-time measurements of dissolved oxygen inside live cells by organically modified silicate fluorescent nanosensors, *Analytical Chemistry*, 76, 2498-2505.
- [46] M. Brasuel, R. Kopelman, T. J. Miller, R. Tjalkens, M. A. Philbert, Fluorescent nanosensors for intracellular chemical analysis: decyl methacrylate liquid polymer matrix and ion-exchange-based potassium PEBBLE sensors with real-time application to viable rat C6 glioma cells, *Analytical Chemistry*, 2001, 73, 2221-2228.
- [47] E. J. Park, M. Brasuel, C. Behrend, M. A. Philbert, R. Kopelman, Ratiometric optical PEBBLE nanosensors for real-time magnesium ion concentration inside viable cells, *Analytical Chemistry*, 2003, 75, 3784-3791.
- [48] J. P. Sumner, J. W. Aylott, E. Monson, R. Kopelman. A fluorescent PEBBLE nanosensor for intracellular free zinc, *The Analyst*, 2001, 127, 11-16.
- [49] M. G. Brasuel, T. J. Miller, R. Kopelman, M. A. Philbert, Liquid polymer nano-PEBBLEs for Cl₂ analysis and biological applications, *The Analyst*, 2003, 128, 1262-1267.

- [50] J. P. Sumner, R. Kopelman, Alexa Fluor 488 as an iron sensing molecule and its application in PEBBLE nanosensors, *The Analyst*, 2005, 130, 528-533.
- [51] J. Q. Brown, R. Srivastava, M. J. McShane, Encapsulation of Glucose Oxidase an an Oxygen-Quenched Fluorophore in Polyelectrolyte-Coated Calcium Alginate Microspheres: Potential for Implantable Optical Glucose Sensor Systems, *Biosensors and Bioelectronics*, 2005, 22, 212-216.
- [52] M. J. McShane, J. Q. Brown, K. B. Guice, Y. M. Lvov, Polyelectrolyte microshells as carriers for fluorescent sensors: Loading and sensing properties of a Ruthenium-based oxygen sensor, *Journal of Nanoscience and Nanotechnology*, 2002, 2, 1-6.
- [53] Rohit Srivastava, Michael J McShane, Application of Self-Assembled Ultrathin Film Coatings to Stabilize Macromolecule Encapsulation in Alginate Microspheres, *Journal of Microencapsulation*, 2005, 22 (4), 397-411.
- [54] Rohit Srivastava, J Quincy Brown, Huiguang Zhu, Michael J McShane, Stabilization of Glucose Oxidase in Alginate Microspheres with Photoreactive Diazo-resin Nanofilm Coatings, *Biotechnology and Bioengineering*, 2005, 91 (1), 124-131.
- [55] Rohit Srivastava, J Quincy Brown, Huiguang Zhu, Michael J. McShane, Stable Encapsulation of Active Enzyme by Application of Multilayer Nanofilm Coatings to Alginate Microspheres, *Macromolecular Bioscience*, 2005, 5, 717-727.
- [56] Huiguang Zhu, Rohit Srivastava, Jonathan Q. Brown, Michael J. McShane, Spontaneous loading of positively charged macromolecules into alginate templated polyelectrolyte multilayer capsules, Accepted in *Biomacromolecules*. May 2005.
- [57] E. Katz, I. Willner, Biomolecule-Functionalized Carbon Nanotubes: Applications in Nanobioelectronics, *Chemical Physics and Physical Chemistry*, 2004, 5 (8), 1084-04.
- [58] L. Dai, P. He, S. Li, Functionalized surfaces based on polymers and carbon nanotubes for some biomedical and optoelectronic applications, *Nanotechnology*, 2003, 14, 1081-1097.
- [59] B. Gary, Carbon nanotubes serve as near-infrared optical sensors, *Biophotonics International*, 2005, 12 (3), 57-59.
- [60] J-S. Ye, Y. Wen, W. D. Zhang, L. M. Gan, G. Q. Xu, F-S. Sheu, Nonenzymatic glucose detection using multi-walled carbon nanotube electrodes, *Electrochemistry Communications*, 2004, 6 (1), p 66-70.

- [61] P. W. Barone, S. Baik, D. A. Heller, M. S. Strano, Near-infrared optical sensors based on single-walled carbon nanotubes, *Nature Materials*, 2005, 4, 86-92.
- [62] K. J. Ziegler, Developing implantable optical biosensors, *Trends in Biotechnology*, 2005, 23 (9), 440-444.
- [63] F. Hussain, D. J. S. Birch, J. C. Pickup, Glucose sensing based on the intrinsic fluorescence of sol-gel immobilized yeast hexokinase, *Analytical Biochemistry*, 2005, 339 (1), 137-143.
- [64] H. Bittiger, H. P. Schnebli, Concanavalin A as a Tool, John Wiley & Sons Ltd., London, 1976.
- [65] A. E. Clarke, M. A. Denborough, The interaction of concanavalin A with blood-group-substance glycoproteins from human secretions, *Biochemistry Journal*, 1971, 121(5), 811-816.
- [66] R. Ballerstadt, R. Ehwald, Suitability of aqueous dispersions of dextran and concanavalin A for glucose sensing in different variants of the affinity sensor, *Biosensors and Bioelectronics*, 1994, 9, 557-567.
- [67] R. Ehwald, R. Ballerstadt, H. Dautzenberg, Viscosimetric Affinity Assay, *Analytical Biochemistry*, 1996, 234, 1-8.
- [68] U. Beyer, R. Ehwald, L-G. Fleischer, Post-Stress Thickening of Dextran /Concanavalin A Solutions Used as Sensitive Fluids in a Viscosimetric Affinity Assay for Glucose, *Biotechnology Progress*, 1997, 13, 722-726.
- [69] C. Barnes, C. D'Silva, J. P. Jones, T. J. Lewis, A concanavalin A-coated piezoelectric crystal biosensor, *Sensors and Actuators B: Chemical*, 1991, B3, 295-304.
- [70] Y. M. Lvov, Thin Film Nanofabrication by Alternate Adsorption of Polyions, Nanoparticles, and Proteins, in *Handbook of Surfaces and Interfaces of Materials*, edited by H. S. Nalwa, Academic Press, 2003.
- [71] Y. Ebara, Y. Okahata, A Kinetic Study of Concanavalin A Binding to Glycolipid Monolayers by Using a Quartz-Crystal Microbalance, *Journal of American Chemical Society*, 1994, 116 (25), 11209-11212.
- [72] Y. M. Lvov, J. K. Ariga, I. Ichinose, T. Kunitake, Layer-by-layer Architectures of Concanavalin A by means of Electrostatic and Biospecific Interactions, *Journal of Chemical Society Chemical Communications*, 1995, 2313-2314.
- [73] J-I. Anzai, Y. Kobayashi, Construction of Multilayer Thin Films of Enzymes By Means of Sugar-Lectin Interactions, *Langmuir*, 2000, 16, 2851-2856.

- [74] T. Hoshi, S. Akase, and J-I. Anzai, Preparation of Multilayer Thin Films Containing Avidin through Sugar-Lectin Interactions and Their Binding Properties, *Langmuir*, 2002, 18, 7024-7028.
- [75] K. Sato, Y. Imoto, J. Sugama, S. Seki, H. Inoue, T. Odagiri, T. Hoshi, and J-I. Anzai, Sugar-Induced Disintegration of Layer-by-Layer Assemblies Composed of Concanavalin A and Glycogen, *Langmuir*, 2005, 21, 797-799.
- [76] J. Svitel, A. Dzgoev, K. Ramanathan, B. Danielsson, Surface plasmon resonance based pesticide assay on a renewable biosensing surface using the reversible concanavalin A monosaccharide interaction, *Biosensors and Bioelectronics*, 2000, 15, 411-415.
- [77] K. Aslan, J. Zhang, J. R. Lakowicz, C. D. Geddes, Saccharide Sensing Using Gold and Silver Nanoparticles-A Review, *Journal of Fluorescence*, 2004, 14 (4), 391-400.
- [78] R. Ballerstadt, J. S. Schultz, Kinetics of dissolution of Concanavalin A:Dextran sols in response to glucose measured by surface plasmon resonance, *Sensors and Actuators*, B46, 1998, 50-55.
- [79] S. Goto, H. Terada, Analysis of binding affinity of sugars to concanavalin A by surface plasmon resonance sensor Biacore, *Spectroscopy: An International Journal*, 2002, 16 (34), 285-288.
- [80] S. Goto, K. Masuda, M. Miura, K. Kanazawa, M. Sasaki, M. Masui, M. Shiramiz, H. Terada, H. Chuman, Quantitative Estimation Of Interaction Between Carbohydrates And Concanavalin A By Surface Plasmon Resonance Biosensor, *Chemical and Pharmaceutical Bulletin*, 2002, 50(4), 445.
- [81] K. Aslan, J. R. Lakowicz, C. D. Geddes, Nanogold-plasmon-resonance-based glucose sensing, *Analytical Biochemistry*, 2004, 330, 145-155.
- [82] K. Aslan, J. R. Lakowicz, C. D. Geddes, Tunable plasmonic glucose sensing based on the dissociation of Con A-aggregated dextran-coated gold colloids, *Analytica Chimica Acta*, 2004, 517, 139-144.
- [83] J. Zhang, D. Roll, C. D. Geddes, J. R. Lakowicz, Aggregation of Silver Nanoparticle Dextran Adducts with Concanavalin A and Competitive Complexation with Glucose, *Journal of Physical Chemistry B*, 2004, 108, 12210-12214.
- [84] J. S. Schultz, G. Sims, Affinity Sensors for Individual Metabolites, *Biotechnology and Bioengineering Symposium*, 1979, No. 9, 65-71.

- [85] J. S. Schultz, S. Mansouri, I. J. Goldstein, Affinity sensor: A new technique for developing implantable sensors for glucose and other metabolites, *Diabetes care*, 1982, 5(3), 245-253.
- [86] D. L. Meadows, J. S. Schultz, Fiber Optic biosensors based on changes in fluorescence energy transfer, *Talanta*, 1988, 35 (2), 145-150.
- [87] D. L. Meadows, J. S. Schultz, Miniature fiber optic sensor based on fluorescence energy transfer, *Proceeding of SPIE*, 1992, 1648, 202-211.
- [88] D. L. Meadows, J. S. Schultz, Design, manufacture and characterization of an optical fiber glucose affinity sensor based on an homogeneous fluorescence energy transfer assay system, *Analytica Chimica Acta*, 1993, 280, 21-30.
- [89] R. Ballerstadt, J. S. Schultz, Competitive-binding assay method based on fluorescence quenching of ligands held in close proximity by a multivalent receptor, *Analytica Chimica Acta*, 1997, 345 (1-3), 203.
- [90] L. Tolosa, H. Szmackinski, G. Rao, J. R. Lakowicz, Lifetime-Based Sensing of Glucose Using Energy Transfer with a Long Lifetime Donor, *Analytical Biochemistry*, 1997, 250, 102-108.
- [91] L. Tolosa, H. Malak, G. Rao, J. R. Lakowicz, Optical assay for glucose based on the luminescence decay time of the long wavelength dye Cy5™, *Sensors and Actuators*, 1997, B 45, 93-99.
- [92] N. DiCesare, J. R. Lakowicz, Wavelength Ratiometric Fluorescent Probes for Glucose, *Proceedings of SPIE*, 2002, 4625, 152-159.
- [93] L. Tolosa, I. Gryczynski, L. R. Eichhorn, J. D. Dattelbaum, F. N. Castellano, G. Rao, J. R. Lakowicz, Glucose Sensor for Low-Cost Lifetime-Based Sensing Using a Genetically Engineered Protein, *Analytical Biochemistry*, 1999, 267, 114-120.
- [94] J. R. Lakowicz, I. Gryczynski, Z. Gryczynski, J. D. Dattelbaum, L. Tolosa, G. Rao, Novel Methods for Fluorescence Sensing, *Proceedings of SPIE*, 1999, 3602, 234-243.
- [95] F. Liang, T. Pan, E. M. Sevick-Muraca, Measurements of fluorescence resonance energy transfer in the concanavalin A-dextran affinity system using frequency-domain lifetime spectroscopy, *Proceedings of SPIE*, 2005, 5702, 7-14.
- [96] L. J. McCartney, J. C. Pickup, O. J. Rolinski, D. J. S. Birch, Near-Infrared Fluorescence Lifetime Assay for Serum Glucose Based on Allophycocyanin-Labeled Concanavalin A, *Analytical Biochemistry*, 2001, 292, 216-221.

- [97] R. Ballerstadt, J. S. Schultz, A Fluorescence Affinity Hollow Fiber Sensor for Continuous Transdermal Glucose Monitoring, *Analytical Chemistry*, 2000, 72, 4185-92.
- [98] R. Ballerstadt, A. Polak, A. Beuhler, J. Frye, In vitro long-term performance study of a near-infrared fluorescence affinity sensor for glucose monitoring, *Biosensors and Bioelectronics*, 2004, 19, 905–914.
- [99] R. Ballerstadt, A. Gowda, R. McNichols, Fluorescence Resonance Energy Transfer Based Near-Infrared Fluorescence Sensor For Glucose Monitoring, *Diabetes Technology and Therapeutics*, 2004, 6 (2), 191-200.
- [100] J. C. Pickup, F. Hussain, N. D. Evans, O. J. Rolinski, D. J. S. Birch, Fluorescence-based glucose sensors, *Biosensors and Bioelectronics*, 2005, 20 (12), 2555-2565.
- [101] V. Scognamiglio, M. Staiano, M. Rossi, S. D'Auria, Protein-based biosensors for diabetic patients, *Journal of Fluorescence*, 2004, 14, 491-498.
- [102] S. D'Auria, R. Barone, M. Rossi, R. Nucci, G. Barone, D. Fessas, E. Bertoli, F. Tanfani, Effects of temperature and SDS on the structure of b-glycosidase from the thermophilic archaeon *Sulfolobus solfataricus*, *Biochemistry Journal*, 1997, 323, 833–840.
- [103] S. D'Auria, N. Di Cesare, Z. Gryczynski, I. Gryczynski, M. Rossi, J. R. Lakowicz, A thermophilic apoglucosehydrogenase as nonconsuming glucose sensor, *Biochemical Biophysical Research Communications*, 2000, 274, 727–731.
- [104] S. D'Auria, N. Di Cesare, M. Staiano, Z. Gryczynski, M. Rossi, J. R. Lakowicz, A Novel Fluorescence Competitive Assay for Glucose Determinations by Using a Thermostable Glucokinase from the Thermophilic Microorganism *Bacillus stearothermophilus*, *Analytical Biochemistry*, 2002, 303, 138–144.
- [105] J. S. Marvin, H.W. Hellings, Engineering Biosensors by Introducing Fluorescent Allosteric Signal Transducers: Construction of a Novel Glucose Sensor, *Journal of American Chemical Society*, 1998, 120, 7–11.
- [106] H. W. Hellings, J. S. Marvin, Protein Engineering and the development of generic Biosensors, *Trends in Biotechnology*, 1998, 16, 183-189.
- [107] K. Ye, J. S. Schultz, Genetic Engineering of an Allosterically Based Glucose Indicator Protein for Continuous Glucose Monitoring by Fluorescence Resonance Energy Transfer, *Analytical Chemistry*, 2003, 75, 3451-3459.
- [108] R. Badugu, J. R. Lakowicz, C. D. Geddes, A Glucose Sensing Contact Lens: A Non-Invasive Technique for Continuous Physiological Glucose Monitoring, *Journal of Fluorescence*, 2003, 13 (5), 371-375.

- [109] R. Badugu, J. R. Lakowicz, C. D. Geddes, Noninvasive Continuous Monitoring of Physiological Glucose Using a Monosaccharide-Sensing Contact Lens, *Analytical Chemistry*, 2004, 76, 610-618.
- [110] R. Badugu, J. R. Lakowicz, C. D. Geddes, Wavelength-Ratiometric Probes for the Selective Detection of Fluoride Based on the 6-Aminoquinolinium Nucleus and Boronic Acid Moiety, *Journal of Fluorescence*, 14 (6), 693-703.
- [111] R. Badugu, J. R. Lakowicz, C. D. Geddes, Ophthalmic Glucose Monitoring Using Disposable Contact Lenses—A Review, *Journal of Fluorescence*, 2004, 14 (5), 617-633.
- [112] R. Badugu, J. R. Lakowicz, C. D. Geddes, Spectroscopic and Photophysical Characterization of Fluorescent Chemosensors for Monosaccharides Based on N-Phenylboronic Acid Derivatives of 1,8-Naphthalimide, *Journal of Fluorescence*, 2002, 12 (2), 147-154.
- [113] N. DiCesare, J. R. Lakowicz, Evaluation of Two Synthetic Glucose Probes for Fluorescence-Lifetime-Based Sensing, *Analytical Chemistry*, 2001, 73, 154-160.
- [114] H. Cao, D. I. Diaz, N. DiCesare, J. R. Lakowicz, M. D. Heagy, Monoboronic Acid Sensor That Displays Anomalous Fluorescence Sensitivity to Glucose, *Organic Letters*, 2002, 4 (9), 1503-1505.
- [115] H. Fang, G. Kaur, B. Wang, Progress in Boronic Acid-Based Fluorescent Glucose Sensors, *Journal of Fluorescence*, 2004, 14, 481-489.
- [116] J. R. Lakowicz, Principles of Fluorescence Spectroscopy, 2nd edition, Kluwer Academic/Plenum Press, New York, 1999.
- [117] C. G. Dos Remedios, P. D. J. Moens, Fluorescence resonance energy transfer spectroscopy is a reliable “ruler” for measuring structural changes in proteins - Dispelling the problem of the unknown orientation factor, *Journal of Structural Biology*, 1995, 115, 175-185.
- [118] J. N. Miller, Fluorescence resonance energy transfer methods in bioanalysis, *Analyst*, 2005, 130, 265-270.
- [119] <http://www.cyto.purdue.edu/flowcyt/educate/confocal/524Lec3/38>, accessed this site on 9/10/2005.
- [120] R. M. Clegg, in Fluorescence Imaging Spectroscopy and Microscopy, edited by X. F. Wang, B. Herman, Wiley, NY, 1996.
- [121] P. Wu, L. Brand, Resonance energy transfer: Methods and application, *Analytical Biochemistry*, 1994, 218, 1-13.

- [122] D. J. S. Birch, O. J. Rolinski, Fluorescence resonance energy transfer sensors, *Research on Chemical Intermediates*, 2001, 27 (4,5), 425-446.
- [123] M. Chantal, C. Lebrun, M. Prats, Fluorescence resonance energy transfer (FRET): Theory and experiments, *Biochemical Education*, 1998, 26(4), 320-323.
- [124] I. Rasnik, S.A. McKinney, T. Ha, Surfaces and orientations: much to FRET about?, *Accounts of Chemical Research*, 2005, 38 (7), 542-548.
- [125] Y. Goto, Y. Hagihara, Mechanism of the conformational transition of melittin, *Biochemistry*, 1992, 31, 732-738.
- [126] K. Cai, V. Schicht, Structural studies of folding intermediates of serine hydroxylmethyltransferase using fluorescence resonance energy transfer, *Journal of Biological Chemistry*, 1996, 271, 2711-27320
- [127] E. R. Chapman, K. Alexander, T. Vorherr, E. Carofoli, D. R. Storm, Fluorescence energy transfer analysis of calmodulin-peptide complexes, *Biochemistry*, 1992, 31, 12819-12825.
- [128] I. L. Medintz¹, A. R. Clapp, H. Mattoussi, E. R. Goldman¹, B. Fisher, J. M. Mauro, Self-assembled nanoscale biosensors based on quantum dot FRET donors, *Nature materials*, 2003, 2, 630-638.
- [129] D. M. Willard, A. Orden, Resonance energy transfer sensor, *Nature materials*, 2003, 2, 575-576.
- [130] J-P. Chen, M-S. Hsu, Mathematical Analysis of Sensors Based On Affinity Interactions Between Competitive Receptor-Protein Pairs, *Journal Chemical Technology Biotechnology*, 1996, 66, 389-397.
- [131] J-P. Chen, Performance Of Affinity Biosensors With Competitive Displacement Mechanism, *Journal Chemical Technology Biotechnology*, 1993, 56, 273-277.
- [132] B. L. Liu, J. S. Schultz, Equilibrium Binding in Immunosensors, *IEEE Transactions on Biomedical Engineering*, 1986, 33 (2), 133-138.
- [133] D. L. Meadows, J. S. Schultz, A Molecular Model For Singlet/Singlet Energy Transfer Of Monovalent Ligand/Receptor Interactions, *Biotechnology and Bioengineering*, 1991, 37, 1066-1075.
- [134] J. S. Schultz, Sensitivity and dynamics of bioreceptor-based biosensors, *Annals of New York Academic Sciences*, 1987, 506, 406-414.
- [135] H. R. Clark, T. A. Barbari, G. Rao, Modeling the Response Time of An In Vivo Glucose Affinity Sensor, *Biotechnology Progress*, 1999, 15, 259-266.

- [136] H. P. Svensson, J. F. Kadow, V. M. Vrudhula, P. M. Wallace, P. D. Senter, Monoclonal Antibody-b-Lactamase Conjugates for the Activation of a Cephalosporin Mustard Prodrug, *Bioconjugate Chemistry*, 1992, 3(2), 176-181.
- [137] G. Sauerbrey, Verwendung von Schwingquarzen zur Wägung dünner Schichten und zur Mikrowägung, *Z. Physics*, 1959, 155, 206.
- [138] G. B. Sukhorukov, L. Dähne, J. Hartmann, E. Donath, H. Möhwald, Controlled Precipitation of Dyes into Hollow Polyelectrolyte Capsules based on Colloids and Biocolloids, *Advanced Materials*, 2000, 12, 112-115.
- [139] G. Ibarz, L. Dähne, E. Donath, H. Möhwald, Smart Micro- and Nanocontainers for Storage, Transport, and Release, *Langmuir*, 2001, 9(2), 481-486.
- [140] I. Willner, V. Heleg-Shabtai, R. Blonder, E. Katz, G. Tao, A. F. Bückmann, A. Heller, Electrical Wiring of Glucose Oxidase by Reconstitution of FAD-Modified Monolayers Assembled on Au-Electrodes, *Journal of American Chemical Society*, 1996, 118, 10321.
- [141] Y. Xiao, F. Patolsky, E. Katz, J. F. Hainfeld, I. Willner, 'Plugging into enzymes': Nanowiring of redox-enzymes by a gold nanoparticle, *Science*, 2003, 299, 1877.
- [142] H. Zhu, E. W. Stein, Z. Lu, Y. M. Lvov, M. J. McShane, Synthesis of Size-Controlled Monodisperse Manganese Carbonate Microparticles as Templates for Uniform Polyelectrolyte Microcapsule Formation, *Chemistry of Materials*, 2005, 17, 2323-2328.
- [143] M. J. McShane, Y. M. Lvov, in *Dekker Encyclopedia of Nanoscience & Nanotechnology*, edited by J. A. Schwartz, C. I. Contescu, K. Putyera, Marcel Dekker, NY, 2005.
- [144] H. Zhu, M. J. McShane, Macromolecule Encapsulation in Diazo-resin (DAR) Based Hollow Polyelectrolyte Microcapsules, *Langmuir*, 2005, 21, 424-430.
- [145] B. E. P. Swoboda, V. J. Massay, *Biological Chemistry*, 1965, 240, 2209-15.
- [146] D. L. Meadows, J. S. Schultz, A molecular model for singlet/singlet energy transfer of monovalent ligand/receptor interactions, *Biotechnology Bioengineering*, 1991, 37(11), 1066-1075.
- [147] G. Wohlfahrt, S. Witt, J. Hendle, D. Schomburg, H. M. Kalisz, H. J. Hecht, 1.8 and 1.9 resolution structures of the *Penicillium amagasakiense* and *Aspergillus niger* glucose oxidases as a basis for modelling substrate complexes, *Acta Crystallographica*, 1999, D55, 969-77.

- [148] D.C. Labaree, T. Y. Reynolds, R. B. Hochberg, Estradiol-16 α -carboxylic Acid Esters as Locally Active Estrogens, *Journal Medicinal Chemistry*, 2001, 44, 1802-1814.
- [149] S. Tanna, M. J. Taylor, G. J. Adams, Insulin delivery governed by covalently modified lectin-glycogen gels sensitive to glucose, *Journal Pharmacy and Pharmacology*, 1999, 51, 1093-1098.
- [150] H. Zhu, E. W. Stein, Z. Lu, Y. M. Lvov, M. J. McShane, Synthesis of Size-Controlled Monodisperse Manganese Carbonate Microparticles as Templates for Uniform Polyelectrolyte Microcapsule Formation, *Chemistry of Materials*, 2005, 17, 2323-2328.
- [151] S. Chinnayelka, H. Zhu, M. J. McShane, Fabrication of Hybrid Organo/Inorgano Polyelectrolyte Microcapsules and their Application in Biomaterial Encapsulation, *Advanced Materials*, to be submitted.
- [152] Y. Shirosaki, K. Tsuru, S. Hayakawa, A. Osaka, M. A. Lopes, J. D. Santos, M. Helena, *In vitro* cytocompatibility of MG63 cells on chitosan-organosiloxane hybrid membranes, *Biomaterials*, 2005, 26 (5), 485-493.